

**3rd Generation Partnership Project;
Technical Specification Group Radio Access Network;
Study on radiated metrics and test methodology for the
verification of multi-antenna reception performance
of NR User Equipment (UE);
(Release 16)**



Keywords

NR, radio

3GPP

Postal address

3GPP support office address

650 Route des Lucioles - Sophia Antipolis
Valbonne - FRANCE
Tel.: +33 4 92 94 42 00 Fax: +33 4 93 65 47 16

Internet

<http://www.3gpp.org>

Copyright Notification

No part may be reproduced except as authorized by written permission.
The copyright and the foregoing restriction extend to reproduction in all media.

© 2020, 3GPP Organizational Partners (ARIB, ATIS, CCSA, ETSI, TSDSI, TTA, TTC).
All rights reserved.

UMTS™ is a Trade Mark of ETSI registered for the benefit of its members

3GPP™ is a Trade Mark of ETSI registered for the benefit of its Members and of the 3GPP Organizational Partners

LTE™ is a Trade Mark of ETSI registered for the benefit of its Members and of the 3GPP Organizational Partners

GSM® and the GSM logo are registered and owned by the GSM Association

Contents

Foreword.....	6
1 Scope	7
2 References	7
3 Definitions, symbols and abbreviations	7
3.1 Definitions	7
3.2 Symbols	8
3.3 Abbreviations.....	8
4 General	8
4.1 Device types.....	8
4.2 Testing configuration.....	9
4.3 Testing Bands	9
5 Performance metrics.....	10
5.1 Figure of Merits	10
5.2 Averaging of throughput curves	11
6 Measurement methodologies.....	11
6.1 Environmental conditions	11
6.2 Measurement setup	12
6.2.1 Multi-Probe Anechoic Chamber (MPAC) for FR1	12
6.2.1.1 Calibration procedure	12
6.2.1.2 Test procedure	13
6.2.2 Radiated Two Stage (RTS) for FR1	13
6.2.2.1 RTS system setup	13
6.2.2.2 Test procedure	14
6.2.3 3D Multi-Probe Anechoic Chamber (MPAC) for FR2	16
6.2.3.1 Calibration procedure	18
6.2.3.2 Test procedure	18
6.3 Test methodology verification	19
6.4 Test method applicability.....	19
6.5 EUT positioning in the chamber	19
6.6 Minimum Range Length for FR1 MIMO OTA Systems.....	20
6.6.1 MPAC.....	21
6.6.2 RTS.....	21
7 Channel Models.....	21
7.1 General.....	21
7.2 Channel Models	22
7.2.1 Channel Models for FR1	27
7.2.2 Channel Models for FR2	34
7.3 Channel Model emulation of the Base Station beamforming configuration	39
7.4 Verification of Channel Model implementation	39
7.4.1 Channel Models validation.....	39
7.4.1.1 Power Delay Profile (PDP).....	40
7.4.1.2 Doppler/Temporal correlation	43
7.4.1.3 Spatial correlation.....	45
7.4.1.4 Cross-polarization.....	51
7.4.1.5 Power validation	53
7.4.1.6 PAS similarity percentage (PSP)	55
7.4.2 Pass/Fail Criteria	58
8 Base station configuration.....	58
8.1 General.....	58
8.2 gNodeB emulator settings.....	58

Annex A:	UE coordinate system	67
A.1	Reference coordinate system.....	67
A.2	Test conditions and angle definitions.....	68
A.3	DUT positioning guidelines	68
A.4	Test Zone dimensions.....	72
Annex B:	Measurement uncertainty	72
B.1	Measurement uncertainty budget for FR1	73
B.1.1	Measurement Uncertainty assessment for MPAC	73
B.1.2	Measurement error contribution descriptions for MPAC	73
B.1.2.1	Mismatch for measurement process	73
B.1.2.2	Measure distance uncertainty	73
B.1.2.3	Quality of quiet zone	73
B.1.2.4	Base Station simulator	74
B.1.2.5	Channel Emulator	74
B.1.2.6	Amplifier uncertainties	74
B.1.2.7	Random uncertainty.....	75
B.1.2.8	Throughput measurement: output level step resolution.....	75
B.1.2.9	DUT sensitivity drift.....	75
B.1.2.10	Signal flatness.....	75
B.1.2.11	Mismatch for calibration process.....	75
B.1.2.12	Reference antenna positioning misalignment	75
B.1.2.13	Total Uncertainty of the Network Analyzer	75
B.1.2.14	Uncertainty of an absolute gain of the calibration antenna.....	76
B.1.2.15	Offset of the Phase Center of the Reference Antenna	76
B.2	Measurement uncertainty budget for FR2.....	76
B.2.1	Measurement Uncertainty assessment	76
B.2.2	Measurement error contribution descriptions	76
B.2.2.1	Mismatch for measurement process	76
B.2.2.2	Measure distance uncertainty	77
B.2.2.3	Quality of quiet zone	77
B.2.2.4	Base Station simulator	77
B.2.2.5	Channel Emulator	77
B.2.2.6	Amplifier uncertainties	77
B.2.2.7	Random uncertainty.....	78
B.2.2.8	Throughput measurement: output level step resolution.....	78
B.2.2.9	DUT sensitivity drift.....	78
B.2.2.10	Signal flatness.....	78
B.2.2.11	Mismatch for calibration process.....	78
B.2.2.12	Reference antenna positioning misalignment	78
B.2.2.13	Total Uncertainty of the Network Analyzer	79
B.2.2.14	Uncertainty of an absolute gain of the calibration antenna.....	79
B.2.2.15	Offset of the Phase Center of the Reference Antenna	79
Annex C:	Environmental requirements	79
C.1	Scope	79
C.2	Ambient temperature.....	79
C.3	Operating voltage	79
Annex D:	Procedure to characterize the quality of the quiet zone	79
D.1	FR1 quality of the quiet zone	79
D.2	FR2 quality of the quiet zone	81
Annex E:	Change history	83

Foreword

This Technical Report has been produced by the 3rd Generation Partnership Project (3GPP).

The contents of the present document are subject to continuing work within the TSG and may change following formal TSG approval. Should the TSG modify the contents of the present document, it will be re-released by the TSG with an identifying change of release date and an increase in version number as follows:

Version x.y.z

where:

- x the first digit:
 - 1 presented to TSG for information;
 - 2 presented to TSG for approval;
 - 3 or greater indicates TSG approved document under change control.
- y the second digit is incremented for all changes of substance, i.e. technical enhancements, corrections, updates, etc.
- z the third digit is incremented when editorial only changes have been incorporated in the document.

1 Scope

The present document is the technical report for the study item on NR MIMO OTA, which was approved at TSG RAN#80 [2]. The scope of the SI is to define the radiated metrics and end-to-end test methodology for the verification of multi-antenna reception performance of NR UEs in FR1 and FR2 and the associated preliminary measurement uncertainty budgets.

2 References

The following documents contain provisions which, through reference in this text, constitute provisions of the present document.

- References are either specific (identified by date of publication, edition number, version number, etc.) or non-specific.
- For a specific reference, subsequent revisions do not apply.
- For a non-specific reference, the latest version applies. In the case of a reference to a 3GPP document (including a GSM document), a non-specific reference implicitly refers to the latest version of that document *in the same Release as the present document*.

- [1] 3GPP TR 21.905: "Vocabulary for 3GPP Specifications".
- [2] RP-182691, "Revised SID: Study on radiated metrics and test methodology for the verification of multi-antenna reception performance of NR UEs," CAICT, OPPO, Samsung, 3GPP RAN #82, December 2018.
- [3] 3GPP TR 37.977: "Universal Terrestrial Radio Access (UTRA) and Evolved Universal Terrestrial Radio Access (E-UTRA); Verification of radiated multi-antenna reception performance of User Equipment (UE)".
- [4] 3GPP TR 38.810: "Study on test methods for New Radio".
- [5] IEEE Std 149: "IEEE Standard Test Procedures for Antennas", IEEE.
- [6] 3GPP TS 38.508-1: "User Equipment (UE) conformance specification; Part 1: Common test environment".
- [7] 3GPP TR 25.914: "Measurement of Radio Performances for UMTS terminals in speech mode".
- [8] 3GPP TS 34.114: "User Equipment (UE) / Mobile Station (MS) Over The Air (OTA) antenna performance; Conformance testing".
- [9] 3GPP TS 38.521-2: "User Equipment (UE) conformance specification; Radio transmission and reception; Part 2: Range 2 Standalone".

3 Definitions, symbols and abbreviations

3.1 Definitions

For the purposes of the present document, the terms and definitions given in 3GPP TR 21.905 [1] and the following apply. A term defined in the present document takes precedence over the definition of the same term, if any, in 3GPP TR 21.905 [1].

PSP (PAS Similarity Percentage): The similarity of the PAS produced by the OTA system and the reference PAS, which is presented by the Total Variation Distance (TVD) of power angular spectrum (PAS). PSP is defined as $(1 - \text{TVD}) * 100\%$. PSP=100% denotes full similarity and PSP=0% denotes full dissimilarity.

3.2 Symbols

For the purposes of the present document, the following symbols apply:

D_{rad}	The diameter of the effective radiating aperture
R_{TZ}	The radius of the test zone

3.3 Abbreviations

For the purposes of the present document, the abbreviations given in 3GPP TR 21.905 [1] and the following apply. An abbreviation defined in the present document takes precedence over the definition of the same abbreviation, if any, in 3GPP TR 21.905 [1].

3D	three-dimensional
AOA	Azimuth angle Of Arrival
AOD	Azimuth angle Of Departure
AS	Angular Spread
ASA	Azimuth angle Spread of Arrival
ASD	Azimuth angle Spread of Departure
BS	Base Station
CDL	Clustered Delay Line
D2D	Device-to-Device
DML	Data Mode Landscape
DMP	Data Mode Portrait
DMSU	Data Mode Screen Up
DS	Delay Spread
EUT	Equipment Under Test
FR1	Frequency Range 1
FR2	Frequency Range 2
FS	Free Space
FWA	Fixed wireless access
InO	Indoor Office
LOS	Line Of Sight
MIMO	Multiple Input Multiple Output
MPAC	Multi-Probe Anechoic Chamber
NLOS	Non-LOS
OTA	Over The Air
PAS	Power Angular Spectrum
PDP	Power Delay Profile
PSP	PAS Similarity Percentage
RMS	Root Mean Square
RTS	Radiated Two Stage
TVD	Total Variation Distance
UE	User Equipment
UMa	Urban Macro
UMi	Urban Micro
XPR	Cross-Polarization Ratio
ZOA	Zenith angle Of Arrival
ZOD	Zenith angle Of Departure
ZSA	Zenith angle Spread of Arrival
ZSD	Zenith angle Spread of Departure

4 General

4.1 Device types

The following device types are in the scope of this study:

- Smartphone

- Tablet
- Wearable device
- Fixed wireless access (FWA) terminal
- Other UE types are not precluded for discussion as a second priority

The development of test methodology aspects shall initially focus on the smartphone device type.

4.2 Testing configuration

Utilizing the free space (FS) testing configuration is the first priority. A second priority is the study of head/hand/body blocking and its impact on test methods – this will be in collaboration with CTIA who plan to study these aspects.

4.3 Testing Bands

The present technical report covers both FR1 and FR2 operating bands.

Table 4.3-1: Definition of frequency ranges

Frequency range designation	Corresponding frequency range
FR1	7125 MHz
FR2	24250 MHz – 52600 MHz

Table 4.3-2: NR operating bands in FR1

NR operating band	Uplink (UL) operating band BS receive / UE transmit $F_{UL_low} - F_{UL_high}$	Downlink (DL) operating band BS transmit / UE receive $F_{DL_low} - F_{DL_high}$	Duplex Mode
n1	1920 MHz – 1980 MHz	2110 MHz – 2170 MHz	FDD
n2	1850 MHz – 1910 MHz	1930 MHz – 1990 MHz	FDD
n3	1710 MHz – 1785 MHz	1805 MHz – 1880 MHz	FDD
n5	824 MHz – 849 MHz	869 MHz – 894 MHz	FDD
n7	2500 MHz – 2570 MHz	2620 MHz – 2690 MHz	FDD
n8	880 MHz – 915 MHz	925 MHz – 960 MHz	FDD
n12	699 MHz – 716 MHz	729 MHz – 746 MHz	FDD
n20	832 MHz – 862 MHz	791 MHz – 821 MHz	FDD
n25	1850 MHz – 1915 MHz	1930 MHz – 1995 MHz	FDD
n28	703 MHz – 748 MHz	758 MHz – 803 MHz	FDD
n34	2010 MHz – 2025 MHz	2010 MHz – 2025 MHz	TDD
n38	2570 MHz – 2620 MHz	2570 MHz – 2620 MHz	TDD
n39	1880 MHz – 1920 MHz	1880 MHz – 1920 MHz	TDD
n40	2300 MHz – 2400 MHz	2300 MHz – 2400 MHz	TDD
n41	2496 MHz – 2690 MHz	2496 MHz – 2690 MHz	TDD
n50	1432 MHz – 1517 MHz	1432 MHz – 1517 MHz	TDD ¹
n51	1427 MHz – 1432 MHz	1427 MHz – 1432 MHz	TDD
n66	1710 MHz – 1780 MHz	2110 MHz – 2200 MHz	FDD
n70	1695 MHz – 1710 MHz	1995 MHz – 2020 MHz	FDD
n71	663 MHz – 698 MHz	617 MHz – 652 MHz	FDD
n74	1427 MHz – 1470 MHz	1475 MHz – 1518 MHz	FDD
n75	N/A	1432 MHz – 1517 MHz	SDL
n76	N/A	1427 MHz – 1432 MHz	SDL
n77	3300 MHz – 4200 MHz	3300 MHz – 4200 MHz	TDD
n78	3300 MHz – 3800 MHz	3300 MHz – 3800 MHz	TDD
n79	4400 MHz – 5000 MHz	4400 MHz – 5000 MHz	TDD
n80	1710 MHz – 1785 MHz	N/A	SUL
n81	880 MHz – 915 MHz	N/A	SUL
n82	832 MHz – 862 MHz	N/A	SUL
n83	703 MHz – 748 MHz	N/A	SUL
n84	1920 MHz – 1980 MHz	N/A	SUL
n86	1710 MHz – 1780MHz	N/A	SUL

Table 4.3-3: NR operating bands in FR2

Operating Band	Uplink (UL) operating band BS receive UE transmit	Downlink (DL) operating band BS transmit UE receive	Duplex Mode
	$F_{UL_low} - F_{UL_high}$	$F_{DL_low} - F_{DL_high}$	
n257	26500 MHz – 29500 MHz	26500 MHz – 29500 MHz	TDD
n258	24250 MHz – 27500 MHz	24250 MHz – 27500 MHz	TDD
n260	37000 MHz – 40000 MHz	37000 MHz – 40000 MHz	TDD
n261	27500 MHz – 28350 MHz	27500 MHz – 28350 MHz	TDD

5 Performance metrics

5.1 Figure of Merits

5.1.1 Definition of MIMO throughput

MIMO throughput is defined here as the time-averaged number of correctly received transport blocks in a communication system running an application, where a Transport Block is defined in the reference measurement channel. From OTA perspective, this is also called MIMO OTA throughput. It will be used as the baseline figure of merit for FR1 and also FR2 static testing.

The MIMO OTA throughput is measured at the top of physical layer of NR system under the use of FRC, the SS transmit fixed-size payload bits to the DUT. The DUT signals back either ACK or NACK to the SS. The SS then records the following:

- Number of ACKs,
- Number of NACKs, and
- Number of DTX slots

Hence the MIMO (OTA) throughput can be calculated as

$$\text{MIMO (OTA) Throughput} = \frac{\text{Transmitted TBS} \times \text{Num of ACKs}}{\text{MeasurementTime}}$$

Where Transmitted TBS is the Transport Block Size transmitted by the SS, which is fixed for a FRC during the measurement period. MeasurementTime is the total composed of successful slots (ACK), unsuccessful slots (NACK) and DTX-symbols.

The time-averaging is to be taken over a time period sufficiently long to average out the variations due to the fading channel. Therefore, this is also called the average MIMO OTA throughput. The throughput should be measured at a time when eventual start-up transients in the system have evanesced.

5.2 Averaging of throughput curves

For FR1 MIMO OTA measurement, the throughput curves shall be averaged by:

The average TRMS of free space data mode portrait (FS DMP), free space data mode landscape (FSDML), and free space data mode screen up (FS DMSU), as defined in Annex A.3. The averaging shall be done in linear scale for the TRMS results at these DUT positions.

$$TRMS_{\text{average},x} = 10 \log \left[3 / \left(\frac{1}{10^{S_{\text{FS_DMP},x}/10}} + \frac{1}{10^{S_{\text{FS_DML},x}/10}} + \frac{1}{10^{S_{\text{FS_DMSU},x}/10}} \right) \right]$$

where

$$S_{\text{MODE},x} = 10 \log \left[12 / \left(\frac{1}{10^{P_{\text{MODE},x,0}/10}} + \frac{1}{10^{P_{\text{MODE},x,1}/10}} + \dots + \frac{1}{10^{P_{\text{MODE},x,11}/10}} \right) \right]$$

Such that *MODE* is one of {*FS_DMP*, *FS_DML*, *FS_DMSU*}, *x* is one of throughput outage (for example {[70%, 95%]}), and {*P_{MODE,x,0}*, ..., *P_{MODE,x,11}*} are the measured sensitivity values at each azimuth position.

How to process FR2 throughput data is FFS.

6 Measurement methodologies

6.1 Environmental conditions

UE-noise limited environmental condition is adopted for both FR1 and FR2 MIMO OTA testing, i.e., UE throughput characterized as a function of signal power incident to the DUT antennas.

6.2 Measurement setup

6.2.1 Multi-Probe Anechoic Chamber (MPAC) for FR1

MPAC test method is the reference methodology for FR NR MIMO OTA testing. By arranging an array of antennas around the Equipment Under Test (EUT), a spatial distribution of angles of arrival in MPAC system may be simulated to expose the EUT to a near field environment that appears to have originated from a complex multipath far field environment.

As illustrated schematically in Figure 6.2.1-1, signals propagate from the base station/communication tester to the EUT through a simulated multipath environment known as a spatial channel model, where appropriate channel impairments such as Doppler and fading are applied to each path prior to injecting all of the directional signals into the chamber simultaneously through the antenna array. The resulting field distribution in the test zone is then integrated by the EUT antenna(s) and processed by the receiver(s) just as it would do so in any non-simulated multipath environment. MPAC system with 16 uniformly-spaced dual-polarized probes is permitted for NR FR1 MIMO OTA testing.

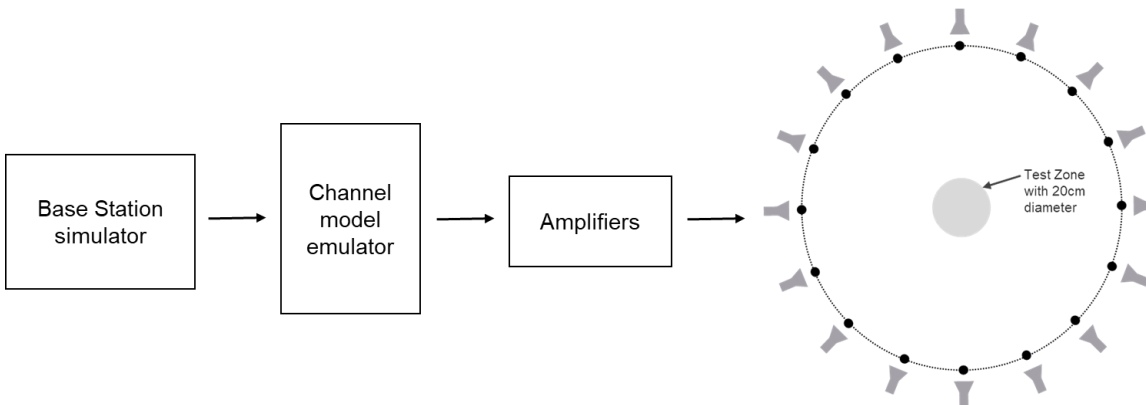


Figure 6.2.1-1: MPAC system layout for NR FR1 MIMO OTA testing

6.2.1.1 Calibration procedure

The system needs to be calibrated by using a reference calibration antenna with known gain values in order to ensure that the downlink signal power is correct. In non-standalone (NSA) mode, the LTE link antenna provides a stable LTE signal without precise path loss or polarization control.

Unlike traditional TRP/TRS testing where the path loss corrections can all be applied as a post processing step to the measured data, the path loss for each probe in the MPAC system must be balanced at test time in order to generate the desired channel model environment within the test zone of the chamber. The imbalance of each path during testing would result in an alteration of the angular dependence of the channel model (i.e. varied characteristics of generated channel model) within the test zone of the chamber.

1. Place a vertical reference dipole in the center of the test zone, connected to a VNA port, with the other VNA port connected to the input of the channel emulator unit – Figure 7.4.1.1-1.
 2. Configure the channel emulator for bypass mode.
 3. Measure the response of each path from each vertical polarization probe to the reference antenna in the center of test zone.
 4. Adjust the power on all vertical polarization branches of the channel emulator so that the powers received at the center are equal.
 5. Repeat the steps 1 to 4 with the magnetic loop and horizontally polarized probes instead, and adjust the horizontal polarization branches of the channel emulator.
 6. The worst-case path loss becomes the reference path loss of the entire system, this loss is used to compute the power in the center of the test zone relative to the output power of the Base Station simulator. Besides, based on the reference path loss, the relative offset of each path loss shall be corrected.

Note: calibration based on other antennas, e.g., horn antennas is not precluded.

6.2.1.2 Test procedure

Before throughput testing, the initial conditions shall be confirmed to reach the correct measurement state for each test case.

1. Ensure environmental requirements of Annex C are met.
2. Configure the test system according to Clauses 8.2 and 7.2 for the applicable test case.
3. Verify the implementation of the channel model as specified in Clause 7.4.1.
4. Position the UE in the chamber according to Annex A.
5. Power on the UE.
6. Set up the connection.

Note: For step 3, the verification of the channel model implementation is usually performed once for each channel model as part of the laboratory accreditation process, and will remain valid as long as the setup and instruments remain unchanged. Otherwise the channel model validation may need to be performed prior to starting each throughput test.

For throughput testing, the following steps shall be followed in order to evaluate NR MIMO OTA performance of the DUT:

1. Measure MIMO OTA throughput from one measurement point, the maximum downlink power is TBD. MIMO OTA throughput is the minimum downlink signal power resulting in a pre-defined throughput value ([70% and 95%]) of the maximum theoretical throughput. The downlink signal power step size shall be no more than 0.5 dB when RF power level is near the NR MIMO sensitivity level.
2. Rotate the UE around vertical axis of the test system by 30 degrees and repeat from step 1 until one complete rotation has been measured i.e. 12 different UE azimuth rotations.
3. Repeat the test from step 1 for each specified device orientation. A list of orientations is given in Annex A.3.
4. The postprocessing method to calculate the average MIMO Throughput is defined in 5.2.

6.2.2 Radiated Two Stage (RTS) for FR1

RTS test method is the harmonized methodology for FR1 NR MIMO OTA testing, according to the applicability criteria.

6.2.2.1 RTS system setup

One example RTS system layout suitable for 4x4 testing is shown in Figure 6.2.2.1-1 while Figure 6.2.2.1-2 illustrates the coordinate system and one example dual-probe antenna configuration. The Base Station emulator sends the downlink signals to the channel emulator, which could be integrated within the base station emulator or be external. The specified channel models are implemented in the channel emulator and the output signals from the channel emulator are fed to the probe antennas. The DUT is placed in the centre of the anechoic chamber and a separate communication antenna is used for the uplink connection with the Base Station emulator. Depending on chamber size and path losses, amplifiers may be needed for downlink and uplink.

To support the channel model scenarios in Clause 7.1, at least two cross-polarized probe antennas located at different positions are required for the 4x4 MIMO OTA RTS test methodology. The probe antennas can be placed on a circular arc around the DUT in the x-y plane as shown in Figure 6.2.2.1-1 or the y-z plane as shown in Figure 6.2.2.1-2 with each dual-polarized probe antenna placed arbitrarily on the arc. If more than two dual-polarized probe antennas are placed on the arc, electric switching could be used to select the required probe antenna.

The DUT is placed in the centre of the arc in the desired test condition and can be rotated in the x-y plane. The distributed axis system can perform 3D or 2D antenna pattern measurements which can then be used to determine the transmission paths between the probe antennas/polarizations and the DUT antennas. The transmission matrix, H , is then described by a 4 x 4 or 2 x 2 matrix depending on whether 4x4 or 2x2 MIMO OTA is tested. Changing the probe antenna positions and/or rotating the DUT alters the transmission matrix. To perform the second stage RTS test, it is only necessary to find

one transmission matrix which can achieve sufficient isolation after applying an inverted channel matrix using the channel emulator. The minimum isolation level sufficient for the 2nd stage throughput is FFS.

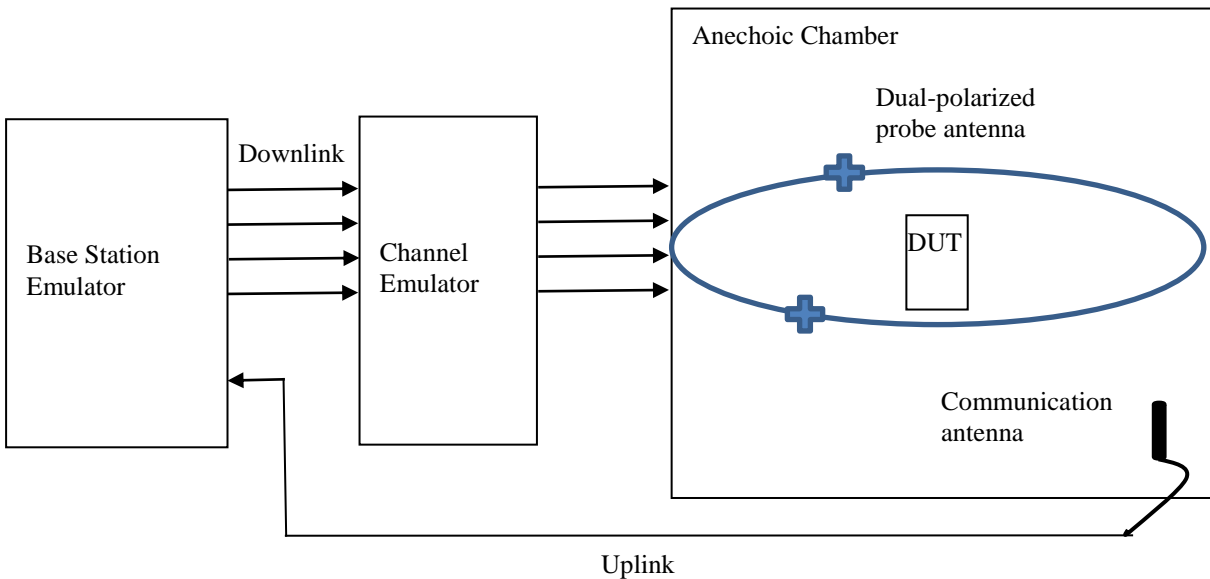


Figure 6.2.2.1-1: Example RTS system layout for 2x2 or 4x4 NR FR1 MIMO OTA testing

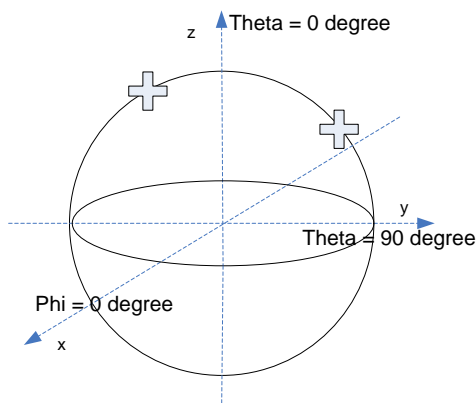


Figure 6.2.2.1-2: Coordination system and one probe antenna layout example for RTS NR FR1 MIMO OTA testing

6.2.2.2 Test procedure

The RTS test method divides the test procedure into two stages: The First stage is to acquire the DUT's antenna pattern, and the second stage is to calibrate the transmission matrix between probe antennas and the DUT's receiver prior to performing the throughput tests.

First stage: Antenna pattern measurement

The first stage is to acquire the DUT's antenna pattern. For this to be a non-intrusive antenna measurement, the DUT needs to have the capability of measuring the amplitude and relative phase of known signals incident at the DUT antennas. This functionality is commonly referred to as the Antenna Test Function (ATF) using the SS Reference Signal Received Power per Branch (SS-RSRPB) and SS Reference Signal Antenna Relative Phase (SS-RSARP) measurements. This capability is implemented as part of a test mode in the device. By rotating the DUT relative to the known incident signal it is possible to construct the 3D or 2D antenna patterns from the DUT amplitude measurements and relative phase measurements between the antennas. To fully characterize the antennas, measurements are made at two orthogonal probe antenna orientations, typically vertical and horizontal. This can be done by switching between two separate probe antennas or by rotating a single probe antenna polarization direction.

The absolute accuracy of the resulting antenna patterns is not primarily a function of the accuracy of the DUT measurements but is referenced to the calibration of the known incident signals in the anechoic chamber. The linearity of the DUT measurements for amplitude and relative phase can also be calibrated out if necessary. The measured amplitude and phase information should be transmitted over the uplink air interface which is active during the pattern measurements. This may take the form of an IP data connection with associated client application (depends on the support of chip vendors) or using a layer 3 signalling connection.

Second stage: Wireless channel calibration and throughput measurements

The second stage of the RTS MIMO OTA test method is illustrated in Figure 6.2.2.2-1 using a 2 x 2 MIMO configuration as an example. The specified base station antenna pattern from Table 7.2-7 is loaded into the channel emulator as the Tx antenna pattern, while the measured DUT's antenna pattern obtained in the 1st stage is loaded into the channel emulator as the Rx antenna pattern and both are then convolved with the spatial channel model chosen to evaluate the DUT performance. This process generates the signals at the DUT receiver that would have been received by the DUT had it been placed in the chosen 2D or 3D spatial field.

Prior to the throughput test, a “wireless cable” connection needs to be established between the probe antennas and DUT’s receivers. The purpose of the wireless cable connection is to enable the signals generated by the channel emulator, which are already conditioned to include the effect of the device antennas, to be directly connected to the device receiver as if through a lossless cable connection. However, this can only be done by calibrating out the impact of the signal propagation in the anechoic chamber and the impact of the receive antennas in the device. To achieve this calibration, it is necessary to measure the propagation matrix inside the anechoic chamber (dotted lines in Figure 6.2.2.2-1) and modify the transmitted signals by multiplying by the inverse matrix of the propagation matrix. This approach will make the DUT receive signals equivalent to cable conducted conditions at the receiver but with radiated self-interference included.

The isolation between branches in the second stage can be measured by establishing a connection and measuring the difference in dB between the SS-RSRPB reported for each DUT receiver. For a DUT to be usable with the RTS method a minimum isolation of FFS has to be achieved averaged over sufficient number of SS-RSRPB measurements.

The choice of DUT orientation for the radiated second stage can be chosen from the measured antenna pattern to avoid any nulls in either antenna which would otherwise reduce the achievable isolation.

After the isolation has been confirmed, the throughput tests are performed for each rotation angle. During this second stage it is not necessary to alter the device orientation physically relative to the probe antennas since the rotation of the DUT relative to the chosen channel model is performed electrically within the channel emulator by rotating the measured DUT’s antenna pattern measured in the first stage.

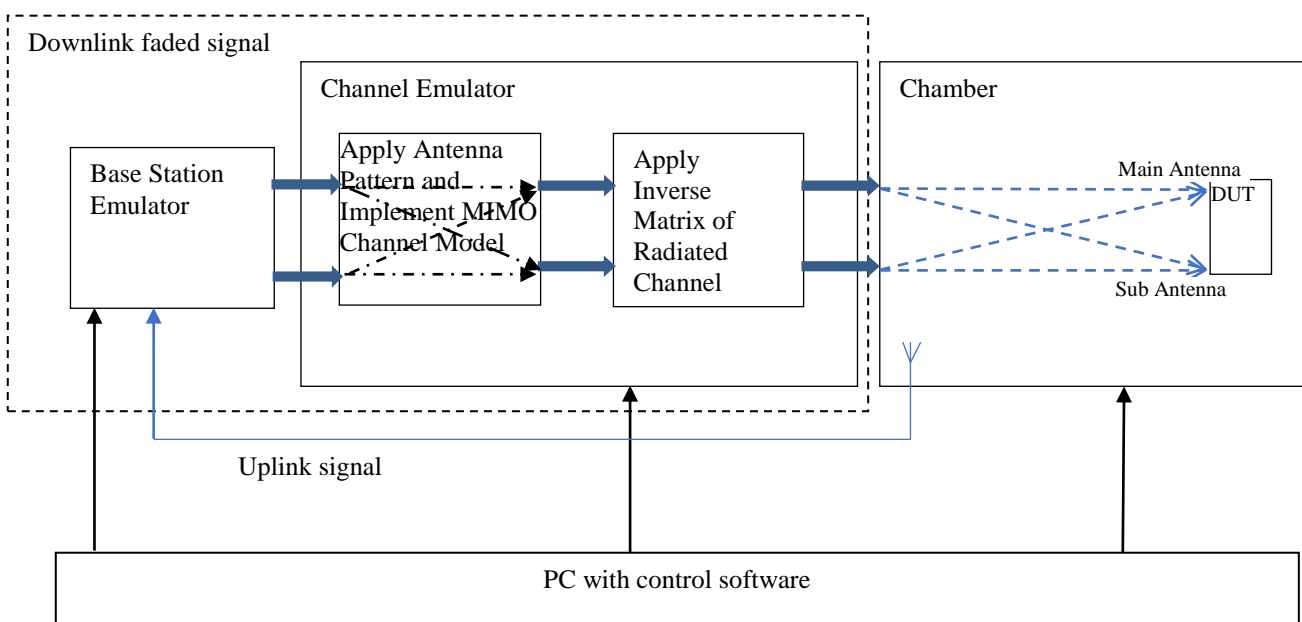


Figure 6.2.2.2-1: Illustration of the 2x2 RTS Second Stage

The applicability criteria of RTS MIMO OTA test method are:

- The RTS method requires device support for the antenna test function (ATF)
- The RTS method is only applicable to devices which do not change their antenna pattern or configuration in response to the radio environment
- The RTS method can only be used if the isolation between channels is above FFS dB. Separate values might be required for 2x2 and 4x4.

6.2.3 3D Multi-Probe Anechoic Chamber (MPAC) for FR2

The 3D MPAC test method is the reference methodology for FR2 NR MIMO OTA testing. By arranging an array of antennas around the Equipment Under Test (EUT), a spatial distribution of angles of arrival in the 3D MPAC system may be simulated to expose the EUT to a near field environment that appears to have originated from a complex multipath far field environment.

As illustrated schematically in Figure 6.2.3-1, signals propagate from the base station/communication tester to the EUT through a simulated multipath environment known as a spatial channel model, where appropriate channel impairments such as Doppler and fading are applied to each path prior to injecting all of the directional signals into the chamber simultaneously through the probe array. The resulting field distribution in the test zone is then integrated by the EUT antenna(s) and processed by the receiver(s) just as it would do so in any non-simulated multipath environment. The 3D MPAC system with 6 dual-polarized probes (illustrated with black dots in Figure 6.2.3-1) placed on a sector with minimum radius of 0.75m from the centre of the test zone is permitted for NR FR2 MIMO OTA testing.

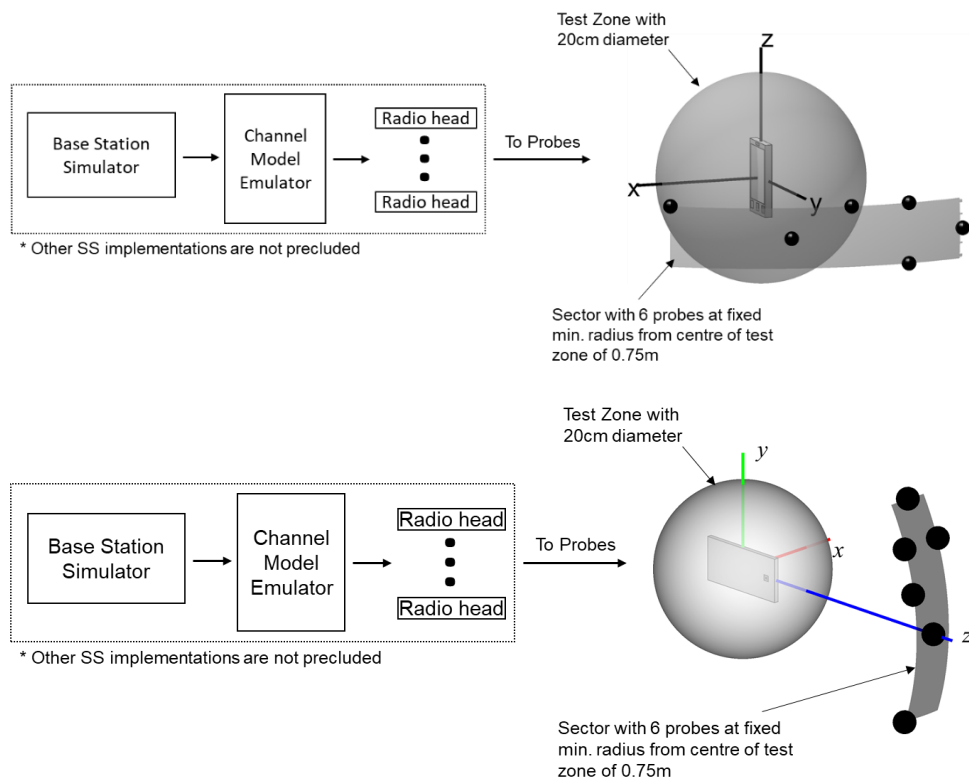


Figure 6.2.3-1: 3D MPAC system layout for NR FR2 MIMO OTA testing

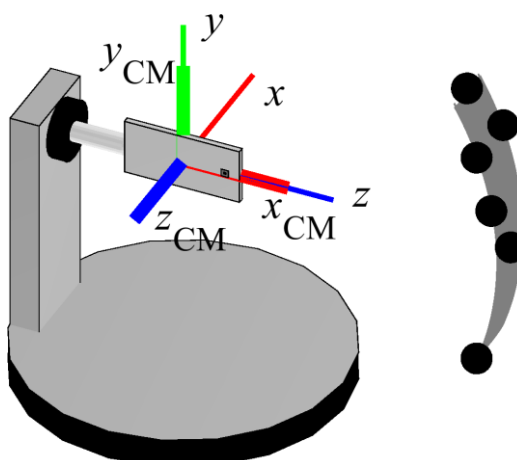
The exact probe locations with respect to the OTA test system coordinate system are tabulated in Table 6.2.3-1.

Table 6.2.3-1. FR2 3D MPAC Probe Locations in OTA test system coordinate system

Probe Number	Theta [deg]	Phi [deg]
1	0.090	0.075
2	11.285	116.785
3	20.685	-104.355
4	20.685	104.395
5	20.695	75.795
6	30.090	90.0105

The 3D MPAC probes in Table 6.2.3-1 can be implemented using conventional millimetre-wave probes as well as IFF-based probes as long as the same probe configuration and same number of probes is used.

The channel model parameters and probe locations for channel model implementation are defined in a channel model coordinate system, which is illustrated in figure 6.2.3-2. The channel model coordinate axes x_{CM} , y_{CM} , and z_{CM} correspond to the OTA test system coordinate axes z , y , and $-x$, respectively.

**Figure 6.2.3-2: Channel Model Coordinate Axes**

The probe locations with respect to channel model coordinate axes are tabulated in table 6.2.3-2.

Table 6.2.3-2. FR2 3D MPAC Probe Locations in Channel Model Coordinate System

Probe Number	Theta [deg]	Phi [deg]
1	90	0
2	85	10
3	85	-20
4	85	20
5	95	20
6	90	30

The channel model rotations assumed for this probe configuration are tabulated in Table 6.2.3-3.

Table 6.2.3-3. Channel Model Rotations

InO CDL-A		UMi CDL-C	
Phi [deg]	Theta [deg]	Phi [deg]	Theta [deg]
70.0-5	-2.0	107.032	15.0

6.2.3.1 Calibration procedure

The system needs to be calibrated by using a reference calibration antenna with known gain values in order to ensure that the downlink signal power is correct. In non-standalone (NSA) mode, the LTE link antenna provides a stable LTE signal without precise path loss or polarization control.

The path loss for each probe in the 3D MPAC system must be calibrated at test time in order to generate the desired channel model environment within the test zone of the chamber. The imbalance of each path during testing would result in an alteration of the angular dependence of the channel model (i.e. varied characteristics of generated channel model) within the test zone of the chamber.

For the calibration measurement, the reference antenna is placed in the centre of the quiet zone, connected to a VNA port, with the other VNA port connected to the input of the channel emulator unit as illustrated schematically in Figure 7.4.1.1-1. For each probe antenna, the reference antenna needs to be aligned in polarization, i.e., θ or ϕ , and direction with the probe antenna that corresponds to the respective path to be calibrated. For each calibration measurement, the channel emulator needs to be configured in bypass mode. The calibration process determines the composite loss, $L_{\text{path,pol}}$, of the entire receiver chain path gains (measurement antenna, amplification) and losses (switches, combiners, cables, path loss, etc.). The calibration measurement is repeated for each measurement path (two orthogonal polarizations and each signal path).

6.2.3.2 Test procedure

Before throughput testing, the initial conditions shall be confirmed to reach the correct measurement state for each test case.

1. Ensure environmental requirements of Annex C are met.
2. Configure the test system according to Clauses 8.2 and 7.2 for the applicable test case.
3. Verify the implementation of the channel model as specified in Clause 7.4.1.
4. Position the UE in the chamber according to Annex D.3.
5. Power on the UE.
6. Set up the connection.

Note: For step 3, the verification of the channel model implementation is usually performed once for each channel model as part of the laboratory accreditation process, and will remain valid as long as the setup and instruments remain unchanged. Otherwise the channel model validation may need to be performed prior to starting each throughput test.

For throughput testing, the following steps shall be followed in order to evaluate NR MIMO OTA performance of the DUT:

1. Position the DUT in the default P0 alignment option (Orientation 1), as defined in Section D.3
2. Measure MIMO OTA throughput, the maximum downlink power is TBD. MIMO OTA throughput is the minimum downlink signal power resulting in a pre-defined throughput value ([FFS]) of the maximum theoretical throughput. The downlink signal power step size shall be no more than 0.5 dB when RF power level is near the NR MIMO sensitivity level.
3. Rotate the UE to the next test point. Table 6.2.3.2-1 lists 36 evenly spaced test points determined using the charged particle approach and with test point #1 centred at (0,0).
4. Repeat the test from step 2 for each specified test point. If the re-positioning concept is applied, the device needs to be positioned in P0 Orientation 2 (either option 1 or option 2).
5. The postprocessing method and the performance metric are FFS.

Table 6.2.3.2-1. Evenly spaced FR2 test points with a constant density

Test Point Number	Theta [deg]	Phi [deg]
1	0.0	0.0
2	33.5	139.7
3	33.9	49.7
4	35.5	-142.9
5	35.5	-76.9
6	37.6	-17.2
7	52.3	94.7
8	56.9	175.7
9	62.5	20.4
10	63.7	-99.8
11	67.1	-55.0
12	69.3	-139.5
13	69.5	130.1
14	70.3	60.8
15	72.1	-16.2
16	88.7	-167.5
17	88.7	98.5
18	89.3	157.0
19	93.9	-78.9
20	94.6	31.6
21	95.3	-115.6
22	99.6	-38.3
23	103.8	-1.1
24	104.4	66.3
25	110.1	127.5
26	115.1	-145.6
27	120.8	171.9
28	125.3	-60.7
29	128.2	-104.1
30	128.8	91.3
31	129.9	35.8
32	136.0	-13.4
33	145.8	138.1
34	150.2	-153.3
35	160.6	-67.4
36	161.7	59.1

6.3 Test methodology verification

For FR1 MPAC and FR2 3D-MPAC MIMO OTA system, the power verification is defined in subclause 7.4.1.5.

6.4 Test method applicability

For FR1 MIMO OTA, the MPAC system is applicable for up to 4x4 MIMO with device within 20cm. For FR2 MIMO OTA, the 3D-MPAC system is applicable for up to 2x2 MIMO with device within 20cm.

6.5 EUT positioning in the chamber

6.5.1 Minimum test zone size

The minimum test zone size for NR MIMO OTA test methods, both FR1 and FR2, is 20cm. Another test zone size larger than 20cm is FFS. “Black-box” testing approach is adopted for NR MIMO OTA testing, the physical center of the EUT shall be placed in the centre of the test zone, the EUT shall be completely contained within the test zone size defined by respective operation band. The detailed test zone size for each band is listed in Annex A.4.

6.5.2 EUT orientation within the test zone

In order to minimize measurement uncertainty, it's important that test house ensure the EUT is oriented within the chamber's test zone in a standardized manner. Annex A.3 provides a preliminary set of normative EUT orientation conditions.

For FR1 MIMO OTA, the DUT shall be tested under Free Space Data Mode Portrait (FS DMP), Free Space Data Mode Landscape (FS DML), and Free Space Data Mode Screen Up flat (FS DMSU), the DUT azimuthal rotation shall be performed over 360 degrees per orientation in 30 degree steps (12 total positions). Fine angular steps at FR1 high frequency for rotation is FFS.

For FR2 MIMO OTA, the DUT shall be tested using a 3D scan. With the DUT positioned in the default P0 alignment option, as defined in Section A.3, measurements on 36 evenly spaced test points with a constant density shall be performed.

6.6 Minimum Range Length for FR1 MIMO OTA Systems

This sub-section specifies the minimum range lengths for NR FR1 MIMO OTA systems. The range length is defined as the distance from the centre of the test zone to the aperture of the measurement probes/antennas, as illustrated in Figure 6.6-1 for MPAC and Figure 6.6-2 for RTS.

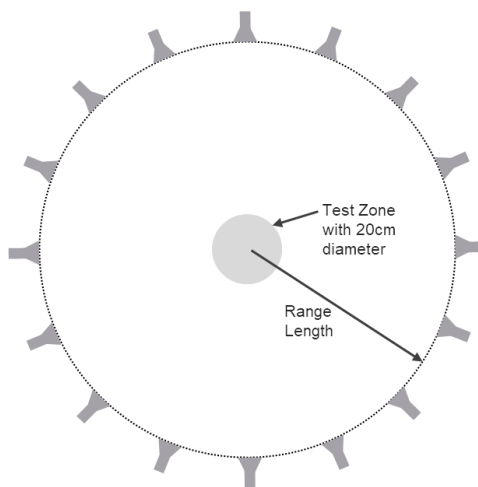


Figure 6.6-1: Illustration of range length definition of MPAC

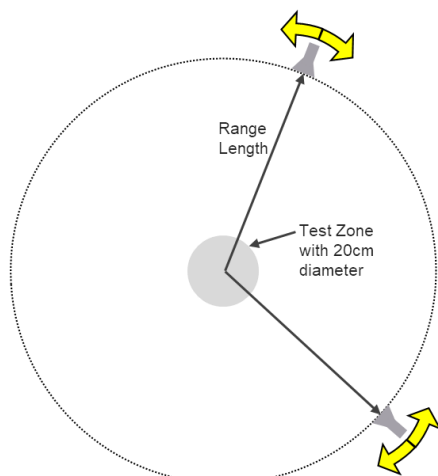


Figure 6.6-2: Illustration of range length definition of RTS

6.6.1 MPAC

The minimum range length for NR FR1 MPAC OTA systems with 20cm test zone size is 1.2m. While for MPAC systems, the far-field requirements do not have to apply, it was shown that the spatial correlation can be impacted significantly for distances below 1.2m.

6.6.2 RTS

For RTS NR FR1 MIMO OTA systems, far-field conditions have to apply due to the pattern measurements in the first stage. The minimum range length shall be the maximum of the following three limits

- The phase uncertainty limit: $R_{TZ}+2D_{rad}^2/\lambda$
- The amplitude uncertainty limit: $3D$
- The reactive Near-Field limit: $R_{TZ}+2\lambda$

where R_{TZ} is defined as the radius of the test zone, i.e., $R_{TZ}=D/2$, and D_{rad} is the diameter of the effective radiating aperture. The minimum range length calculations for $D=20$ cm test zone size RTS systems shall assume that D_{rad} is 20cm below 1.5GHz and decrease linearly from 20cm to 5cm from 1.5GHz to 7.125GHz, respectively. The last column of Table 6.6.2-1 shall be considered the minimum range length for NR FR1 RTS MIMO systems with 20cm test zone size.

Table 6.6.2-1. Minimum Range Length for RTS Systems with 20cm test zone size.

f [GHz]	D_{rad} [m]	R_{TZ}+2D_{rad}²/λ	3D = 6R_{TZ}	R_{TZ}+2λ	max(R_{TZ}+2λ, 3D, R_{TZ}+2D²/λ)
0.41	0.20	0.21	0.60	1.56	1.56
0.60	0.20	0.26	0.60	1.10	1.10
0.70	0.20	0.29	0.60	0.96	0.96
0.80	0.20	0.31	0.60	0.85	0.85
1.00	0.20	0.37	0.60	0.70	0.70
1.20	0.20	0.42	0.60	0.60	0.60
1.40	0.20	0.47	0.60	0.53	0.60
1.60	0.20	0.53	0.60	0.47	0.60
1.80	0.20	0.58	0.60	0.43	0.60
2.00	0.20	0.63	0.60	0.40	0.63
2.20	0.20	0.69	0.60	0.37	0.69
2.40	0.18	0.60	0.60	0.35	0.60
2.60	0.17	0.61	0.60	0.33	0.61
2.80	0.17	0.61	0.60	0.31	0.61
3.00	0.16	0.62	0.60	0.30	0.62
4.00	0.13	0.58	0.60	0.25	0.60
5.00	0.11	0.48	0.60	0.22	0.60
6.00	0.08	0.36	0.60	0.20	0.60
7.00	0.05	0.24	0.60	0.19	0.60
7.13	0.05	0.22	0.60	0.18	0.60

7 Channel Models

7.1 General

The different channel models are defined to create corresponding complex multipath radio propagation conditions for FR1 and FR2. The following scenarios are selected for NR MIMO OTA:

FR1 scenarios:

- For 2x2 MIMO: Urban Macro
- For 4x4 MIMO: Urban Micro

FR2 static testing scenarios:

- Urban Micro street canyon and Indoor

In order to describe unambiguously the procedure of generating realizations CDL channel models, various aspects need to be clarified, e.g., details of scaling procedure, inclusion of BS antenna arrays and beams to the model output, and removing unwanted randomness of model realizations.

The concept of angular scaling is based on rotating AoDs/ZoDs and scaling CDL model using the methods in TR 38.901 (section 7.7.5.1) to make them fit the median values in TR 38.901 Table 7.5-6 for the accepted scenarios.

For NR MIMO OTA testing, the following channel models are required to be measured: FR1 UMi CDL-A in table 7.2.1-1, FR1 UMa CDL-C in table 7.2.1-8; FR2 InO CDL-A in table 7.2.2-6, FR2 UMi CDL-C in table 7.2.2-3.

For NR FR1 and FR2 MIMO OTA testing, the number of samples for sequence length at each testing point is FFS.

7.2 Channel Models

This section describes amendments to the step-wise procedure of the CDL subclause 7.7.1 in TR 38.901 for generating fast fading radio channel realizations. This channel model methodology considers non-Jakes spectrum with the multi-path fading propagation conditions between the gNB emulator and test chamber probe modelled based on Clustered Delay Line (CDL) methodology.

First, the RMS delay spread values of CDL models are normalized first and they must be scaled in delay so that a desired RMS delay spread can be achieved. The scaled delays can be obtained according to the following equation:

$$\tau_{n,\text{scaled}} = \tau_{n,\text{model}} \cdot DS_{\text{desired}}, \quad (7.2-1)$$

in which

- $\tau_{n,\text{model}}$ is the normalized delay value of the n th cluster in a CDL in Tables 7.7.1.1 – 7.7.1.5 of [2]
- $\tau_{n,\text{scaled}}$ is the new delay value (in [ns]) of the n th cluster
- DS_{desired} is the target delay spread (in [ns]).

Values of DS_{desired} for FR1/FR2 and for different model scenarios are specified in Table 7.2-1. Target delay spread values. Table 7.2-1.

Table 7.2-1. Target delay spread values.

Frequency	Scenario	DS _{desired}
FR1	UMi	100 ns
FR1	UMa	365 ns
FR2	UMi	60 ns
FR2	InO	30 ns

Subsequently, the departure and arrival angles (based on subclause 7.7.1 step 1 in TR38.901 are generated by combining 7.7-5 and part of step 7 in subclause 7.5. The arrival angles of azimuth using are generated using the following equation

$$\phi_{n,m,\text{AOAscaled}} = \frac{AS_{\text{desired}}}{AS_{\text{model}}} (\phi_{n,\text{AOA}} + c_{\text{ASA}} \alpha_m - \mu_{\phi,\text{model}}) + \mu_{\phi,\text{model}}, \quad (7.2-2)$$

where

- $\phi_{n,\text{AOA}}$ and c_{ASA} are the cluster AOA and the cluster-wise rms azimuth spread of arrival angles (cluster ASA), respectively, in Tables 7.7.1.1 – 7.7.1.5 of TR38.901
- α_m denotes the ray offset angles within a cluster given by Table 7.5-3,
- $\mu_{\phi,\text{model}} = \arg \left\{ \sum_{n=1}^N \sum_{m=1}^M \exp(j\phi_{n,m}) P_{n,m}^{\text{linear}} \right\}$ is the mean angle of the original channel model table in NLOS case (equation is specified in Annex A.2 of TR38.901) and the LOS angle $\mu_{\phi,\text{model}} = \phi_{1,\text{AOA}}$ in LOS case,

- Tables 7.2-2 and 7.2-3 contain the non-circular angle spread values of the original CDL models of TR38.901 before any angular scaling, AS_{model} are the angular spreads derived from the original CDL Tables 7.7.1.1 – 7.7.1.5 of TR38.901. TR25.996 describes μ_θ :

$$\mu_\theta = \frac{\sum_{n=1}^N \sum_{m=1}^M \theta_{n,m} \cdot P_{n,m}}{\sum_{n=1}^N \sum_{m=1}^M P_{n,m}}, \quad (7.2-3)$$

The values are calculated for the AOD, AOA, ZOD, and ZOA angles after removing the mean angle following the definition of rms angular spread in TR25.996, without finding the minimum over circular shifts. Here, the calculation is performed after removing the mean angle first and subsequently equation A-2 from Annex A of TR38.901

$$\mu_{\phi,\text{model}} = \arg \left\{ \sum_{n=1}^N \sum_{m=1}^M \exp(j\phi_{n,m}) P_{n,m}^{\text{linear}} \right\}, \quad (7.2-4)$$

is used to rotate μ_θ to zero (and also wrap AOAs within +/-180). Equations A-3

$$\mu_\theta = \frac{\sum_{n=1}^N \sum_{m=1}^M \theta_{n,m} \cdot P_{n,m}}{\sum_{n=1}^N \sum_{m=1}^M P_{n,m}}, \quad (7.2-5)$$

and A-1 of TR 25.996

$$\sigma_{AS} = \sqrt{\frac{\sum_{n=1}^N \sum_{m=1}^M (\theta_{n,m,\mu})^2 \cdot P_{n,m}}{\sum_{n=1}^N \sum_{m=1}^M P_{n,m}}}, \quad (7.2-6)$$

are used to calculate the AS_{model}. Note that equation A-2 of TR 25.996 is not applied to AS_{model} calculations, the following equation is used instead $\theta_{n,m,\mu} = \theta_{n,m} - \mu_\theta$

AS_{desired} is the target angular spread. Table 7.2-4 specifies AS_{desired} values for CDL-A,B,C,D,E UMi and UMa at FR1 and Table 7.2-5 specifies the corresponding AS_{desired} values at FR2. These target values are obtained by determining median angular spreads of Table 7.5-6 of TR38.901.

The angular scaling is applied to the ray angles and no further scaling is performed. The generation of AOD ($\phi_{n,m,\text{AOD}}$), ZOA ($\theta_{n,m,\text{ZOA}}$), and ZOD ($\theta_{n,m,\text{ZOD}}$) follows a procedure similar to AOA as described above. Here, the azimuth angles may need to be wrapped around to be within [0, 360] degrees, while the zenith angles may need to be clipped to be within [0, 180] degrees.

Each CDL parameter table contains two sets of three rows, i.e., three clusters, with exactly same angular parameters. This is harmful for the statistical properties of the models as they become non-WSS across the ensemble of model realizations. Instead of making the angular parameters non-equal by introducing small offsets to angles of the three rows, the problematic clusters are treated as midpaths as intended when the CDLs were drawn from statistical distributions which works across all frequency ranges. For the clusters that look like midpaths, e.g., Cluster 2-4 and 5-7 for CDL-A and Cluster 2-4 and 6-8 for CDL-C, the powers for each of the three clusters are added and using the regular midpath power distribution of 0.5, 0.3, and 0.2 specified in Table 7.5-5 of TR38.901, the powers for each of the midpaths are calculated. Notice that the intra cluster delay spread in Table 7.5-5 of TR38.901 is not followed, and the same delays as the original CDL are followed for the midpaths (aka Sub-Cluster). This helps keeping the rms DS of the modified CDL to 1s.

Table 7.2-2: Original (non-circular) angle spreads of CDL models UMi and UMa (K-factor 9 dB)

Model	AS _{model} [deg]			
	ASD	ASA	ZSD	ZSA
CDL-A	73.6985	85.2676	28.5575	21.0831
CDL-B	41.5917	59.3326	5.9633	10.3818
CDL-C	39.0949	71.1175	4.0666	10.4245
CDL-D	15.6771	17.3604	2.4462	1.5362
CDL-E	13.1544	37.5640	1.4577	2.4601

Table 7.2-3: Original (non-circular) angle spreads of CDL-D and CDL-E models InO (K-factor 7 dB)

Model	AS _{model} [deg]			
	ASD	ASA	ZSD	ZSA
CDL-D	18.9859	21.0747	2.9629	1.8735
CDL-E	15.7784	45.3434	1.7692	2.9982

Table 7.2-4: Desired AS for UMi and UMa at 3.5 GHz (FR1)

Model	AS _{desired} [deg]			
	ASD	ASA	ZSD	ZSA
UMi NLOS (CDL-A, B, C)	23.9751	57.2457	0.7762	7.8320
UMi LOS (CDL-D, E)	15.0432	47.6149	0.6166	4.6204
UMa NLOS (CDL-A, B, C)	25.7620	74.1138	4.8978	18.2050
UMa LOS (CDL-D, E)	14.0180	64.5654	3.4674	8.9125

Note: For UMa frequency fc = 6 as stated in **Error! Reference source not found.**, and other parameters hUMa = 25, hUMi = 10, hUT = 1.5, and D2D = 100.

Table 7.2-5: Desired AS for UMi and InO at 28 GHz (FR2)

Model	AS _{desired} [deg]			
	ASD	ASA	ZSD	ZSA
UMi NLOS (CDL-A, B, C)	15.6188	49.3183	0.7762	7.2695
UMi LOS (CDL-D, E)	13.7050	41.0212	0.6166	3.8350
InO NLOS (CDL-A, B, C)	41.6869	50.3659	12.0226	14.7109
InO LOS (CDL-D, E)	39.8107	31.8526	1.3702	11.4756

Subsequently, the AOD angles are coupled to AOA angles within a cluster n . Instead of random procedure, the coupling is performed using the fixed coupling pattern specified in Table 7.2-6. The same fixed coupling pattern is applied for all clusters n .

Table 7.2-6: Fixed coupling pattern of ray angles to be applied for each cluster

	m																			
$\phi_{n,m,AOD}$	6	12	5	10	8	11	16	14	18	9	20	4	2	15	7	13	19	17	3	1
$\phi_{n,m,AOA}$	20	9	12	1	13	18	10	4	8	2	6	14	11	19	7	3	17	5	15	16
$\theta_{n,m,ZOD}$	2	16	3	11	18	9	5	17	4	19	15	20	13	7	10	1	8	12	6	14
$\theta_{n,m,ZOA}$	15	18	13	1	12	9	6	7	5	3	2	8	14	17	19	16	11	20	10	4

In the next steps, the linear cross polarization power ratios (XPR) κ are calculated for each ray m of each cluster n as

$$\kappa_{n,m} = 10^{X/10}, \quad (7.2-7)$$

where X is the per-cluster XPR in dB from Tables 7.7.1.1 – 7.7.1.5 of TR38.901.

The gNB beam pattern including the assumptions for gNB antenna for definitions and symbols of subclause 7.3 of TR38.901 for FR1 and FR2 are summarized in Table 7.2-7.

Table 7.2-7: BS Antenna Parameters

Parameter description	Symbol	Parameter value		
		FR1 ≤ 2.5GHz	FR1 > 2.5GHz	FR2
Antenna panels in vertical dimension	M_g	1	1	1
Antenna panels in horizontal dimension	N_g	1	1	1
Elements per panel in vertical dimension	M_e	4	8	8
Elements per panel in horizontal dimension	N_e	8	8	16
Number of polarizations per panel	P	2	2	2
Element spacing in horizontal dimension (λ)	d_H	0.5	0.5	0.5
Element spacing in vertical dimension (λ)	d_V	0.5	0.5	0.5

Antenna element radiation patterns, including orientation of the element main polarization components as well as orientation of the antenna array for both FR1 and FR2 are as in the example pattern in Table 7.3-1 of TR38.901. The antenna element parameters are $\theta_{3dB} = 65^\circ$, $\phi_{3dB} = 65^\circ$, $A_{max} = 30\text{dB}$, $SLAv = 30\text{dB}$, $G_{E,max} = 8\text{ dBi}$.

It is assumed the co-polarized elements of the array are combined to a single RF port, i.e. they compose an antenna array that can form beams by setting certain weights per element. Weight vector for the first polarization and for the second polarization is

$$[\alpha_{1,1} \quad \dots \quad \alpha_{M_e, N_e}] = \left\{ \frac{1}{M_e N_e} \exp \left(-j 2\pi \frac{\hat{r}_{tx,max}^T \cdot \bar{d}_{tx,m_e,n_e}}{\lambda_0} \right) \right\} \in \mathbb{C}^{1 \times M_e N_e}, \quad (7.2-8)$$

where \bar{d}_{tx,m_e,n_e} is the location vector of transmit antenna element $m_e = 1, \dots, M_e$ and $n_e = 1, \dots, N_e$, and $\hat{r}_{tx,max}$ is a spherical unit vector denoting the target beam direction. Determination of beam directions $\hat{r}_{tx,max}$ is

described in section 7.3..

Random initial phase $\{\Phi_{n,m}^{\theta\theta}, \Phi_{n,m}^{\theta\phi}, \Phi_{n,m}^{\phi\theta}, \Phi_{n,m}^{\phi\phi}\}$ are not used for the different polarization combinations ($\theta\theta, \theta\phi, \phi\theta, \phi\phi$). Instead, a fixed and pre-defined set of initial phases $\{\Phi_m^{\theta\theta}, \Phi_m^{\theta\phi}, \Phi_m^{\phi\theta}, \Phi_m^{\phi\phi}\}$ of Table 7.2-8 and a scalar random initial phase term $\Phi_{n,m} \sim \text{Uni}(-\pi, \pi)$ is used for each ray m of each cluster n .

The set of fixed initial phases can be same for all clusters, i.e. $\Phi_{n,m}^{\theta\theta} = \Phi_m^{\theta\theta} \forall n = 1, \dots, N$ etc. for all four polarization combinations. These 20×4 initial phase values can be specified either by a table of values or by setting a random number generator and a fixed seed number. The distribution of scalar initial phases $\Phi_{n,m}$ is uniform within $[-\pi, \pi]$. Its purpose is to enable generation of different fading sequences on different uses of the model, but still maintaining the power angular distribution of the model. The scalar initial phases can be fixed (or removed) if completely deterministic process, i.e. exactly same fading sequences at each model use, is aimed at.

Table 7.2-8: Fixed initial phases for 2x2 polarization matrices. These values are drawn from uniform distribution

<i>m</i>	$\Phi_m^{\theta\theta}$ [rad]	$\Phi_m^{\phi\theta}$ [rad]	$\Phi_m^{\theta\phi}$ [rad]	$\Phi_m^{\phi\phi}$ [rad]
1	1.7609	-0.6928	-1.6230	-0.6037
2	-2.5356	-2.3124	2.7775	2.8660
3	0.4725	-2.7660	-1.6664	-0.9226
4	2.0181	-3.0448	-2.8713	-2.0798
5	0.9369	1.4560	0.9283	-0.3084
6	0.2954	-1.2798	1.5375	-1.9544
7	1.1735	-1.9886	-0.8263	0.7893
8	1.7607	-2.6319	2.6979	1.7324
9	-0.0830	-0.4030	-0.3344	-1.2167
10	0.0535	0.0677	1.9957	1.8525
11	0.9068	-0.7627	1.9577	0.2062
12	-0.9379	2.7583	2.3621	0.3151
13	0.7695	0.5469	-1.8363	-1.2488
14	-0.1827	-1.6934	2.1634	-1.9179
15	-1.7221	-2.0690	-1.7111	-0.4040
16	-1.1869	2.6602	-0.4385	-1.9804
17	2.5439	3.0143	-0.3841	-2.4434
18	-1.5201	-0.5735	0.5962	-1.4941
19	0.6462	1.3271	-1.7483	-2.4038
20	-1.2775	-1.1386	-0.4765	0.0494

To determine the channel all clusters are treated as "weaker cluster", i.e., no further sub-clusters in delay should be generated. The BS beamforming weights defined in Equation 7.2-8 for antenna elements are used and the BS antenna signals are summed for BS beamforming. The BS transmits downlink signals with S beams. Index $s = 1, \dots, S$ denotes the formed beam index. Each beam may have different and thus the beamforming weight of eq. (7.2-8) becomes specific for index s as α_{s,m_e,n_e} ; it should be noted though that there are always two orthogonally polarized beams to the same direction. Here, the random initial phases $\Phi_{n,m}$ are used for sub-paths, but not for the different polarization combinations ($\theta\theta$, $\theta\phi$, $\phi\theta$, $\phi\phi$). The channel coefficient for time instant t , Rx antenna/beam u , Tx beam s , and cluster n is defined by the following equations. They apply for the NLOS clusters and the LOS path, respectively:

$$\begin{aligned}
 H_{u,s,n}^{\text{NLOS}}(t) = & \sqrt{\frac{P_n}{M}} \sum_{m=1}^M \sum_{n_e=1}^{N_e} \sum_{m_e=1}^{M_e} \left[F_{rx,u,\theta}(\theta_{n,m,ZOA}, \varphi_{n,m,AOA}) \right]^T \begin{bmatrix} \exp(j\Phi_m^{\theta\theta}) & \sqrt{\kappa_{n,m}^{-1}} \exp(j\Phi_m^{\theta\phi}) \\ \sqrt{\kappa_{n,m}^{-1}} \exp(j\Phi_m^{\phi\theta}) & \exp(j\Phi_m^{\phi\phi}) \end{bmatrix} \begin{bmatrix} F_{tx,s,m_e,n_e,\theta}(\theta_{n,m,ZOD}, \varphi_{n,m,AOD}) \\ F_{tx,s,m_e,n_e,\phi}(\theta_{n,m,ZOD}, \varphi_{n,m,AOD}) \end{bmatrix} \\
 & \alpha_{s,m_e,n_e} \exp(j\Phi_{n,m}) \exp\left(\frac{j2\pi(\hat{r}_{rx,n,m}^T \bar{d}_{rx,u})}{\lambda_0}\right) \exp\left(\frac{j2\pi(\hat{r}_{tx,n,m}^T \bar{d}_{tx,s,m_e,n_e})}{\lambda_0}\right) \exp\left(j2\pi \frac{\hat{r}_{rx,n,m}^T \bar{v}}{\lambda_0} t\right), \tag{7.2-9}
 \end{aligned}$$

$$\begin{aligned}
 H_{u,s,n}^{\text{LOS}}(t) = & \sum_{n_e=1}^{N_e} \sum_{m_e=1}^{M_e} \left[F_{rx,u,\theta}(\theta_{LOS,ZOA}, \varphi_{LOS,AOA}) \right]^T \begin{bmatrix} 1 & 0 \\ 0 & -1 \end{bmatrix} \begin{bmatrix} F_{tx,s,\theta}(\theta_{LOS,ZOD}, \varphi_{LOS,AOD}) \\ F_{tx,s,\phi}(\theta_{LOS,ZOD}, \varphi_{LOS,AOD}) \end{bmatrix} \alpha_{s,m_e,n_e} \\
 & \exp\left(j2\pi \frac{(\hat{r}_{rx,LOS}^T \bar{d}_{rx,u})}{\lambda_0}\right) \exp\left(j2\pi \frac{(\hat{r}_{tx,LOS}^T \bar{d}_{tx,s,m_e,n_e})}{\lambda_0}\right) \exp\left(j2\pi \frac{\hat{r}_{rx,LOS}^T \bar{v}}{\lambda_0} t\right), \tag{7.2-10}
 \end{aligned}$$

where $F_{tx,s,m_e,n_e,\theta}$, $F_{tx,s,m_e,n_e,\phi}$, and \bar{d}_{tx,s,m_e,n_e} are the theta and phi polarized radiation patterns and the position vector of the BS antenna element m_e , n_e of sub-array s , respectively. Symbols $F_{rx,u,\theta}$, $F_{rx,u,\phi}$, $\hat{r}_{rx,n,m}$, $\hat{r}_{tx,n,m}$, and $\bar{d}_{rx,u}$, are determined as in TR 38.901. UE velocity vector \bar{v} is determined as

$$v_{n,m} = \frac{\hat{r}_{rx,n,m}^T \bar{v}}{\lambda_0}, \text{ where } \bar{v} = v \begin{bmatrix} \sin \theta_v \cos \phi_v & \sin \theta_v \sin \phi_v & \cos \theta_v \end{bmatrix}^T. \quad (7.2-11)$$

UE velocity v is defined as follows: 30km/h for FR1 vs 3 km/h (Indoor Office) and 12 km/h (UMi) for FR2. The UE travelling direction (ϕ_v, θ_v) are as follows for FR1:

- (135°,90°) for UMi CDL A channel model
- ([127.0455°],90°) for UMi CDL C channel model
- ([182.1659°],90°) for UMa CDL A channel model
- (65°,90°) for UMa CDL C channel model

The UE travelling direction (ϕ_v, θ_v) are as follows for FR2:

- (112.51°,90°) for InO CDL-A channel model
- (74.11°,90°) for UMi CDL-C channel model

7.2.1 Channel Models for FR1

The Channel model parameter tables for CDL-A, B, C, D, and E for UMa and UMi at 3.5 GHz are presented in this subclause without the effect of base station antenna filtering.

For FR1, the baseline emulated propagation environment for FR1 MIMO OTA is 2D without elevation modelling, i.e., all ZOA are set 90° and ZSA is 0° in the following tables.

Tables 7.2.1-1**Error! Reference source not found.**—7.2.1-5 show the model parameters, UMi CDL-A—CDL-E models, respectively. For the determination of desired zenith spread of departure (ZSD_{desired}) from table 7.5-8 of TR38.901, the following parameters are used h_{BS} = 10 m, h_{UT} = 1.5 m, and d2d = 100 m.

Table 7.2.1-1: Channel model parameters for UMi CDL-A at 3.5 GHz

Cluster #	Absolute Delay [ns]	Power in [dB]	AOD in [°]	AOA in [°]	ZOD in [°]	ZOA in [°]
1	0	-13.4014	-59.324	98.721	95.9936	90
2	38.19	0	-2.752	-156.546	97.1624	90
3	40.25	-2.2185	-2.752	-156.546	97.1624	90
4	58.68	-3.9794	-2.752	-156.546	97.1624	90
5	46.1	-5.9799	27.9576	115.7066	97.9452	90
6	53.75	-8.1984	27.9576	115.7066	97.9452	90
7	67.08	-9.9593	27.9576	115.7066	97.9452	90
8	57.5	-10.5014	38.1399	-55.2369	98.7118	90
9	76.18	-7.5014	-27.9638	-82.1587	96.1295	90
10	153.75	-15.9014	50.144	127.5226	95.3467	90
11	189.78	-6.6014	-28.3867	99.1238	98.0648	90
12	222.42	-16.7014	42.4666	-131.84	99.2935	90
13	217.18	-12.4014	-51.1586	82.1383	98.7444	90
14	249.42	-15.2014	-57.3396	115.7066	98.902	90
15	251.19	-10.8014	-43.6439	-58.728	95.912	90
16	305.82	-11.3014	-45.6283	-69.4699	95.7272	90
17	408.1	-12.7014	52.4212	-85.7169	95.806	90
18	445.79	-16.2014	46.8909	138.3987	99.0271	90
19	456.95	-18.3014	41.7835	161.2923	94.9226	90
20	479.66	-18.9014	-39.9679	168.543	95.083	90
21	500.66	-16.6014	-51.5165	132.7593	99.2962	90
22	530.43	-19.9014	39.7665	-155.942	95.2461	90
23	965.86	-29.7014	-19.6683	101.3393	98.5677	90
Per-Cluster Parameters						
Parameter	C _{ASD} in [°]	C _{ASA} in [°]	C _{zSD} in [°]	C _{zSA} in [°]	XPR in [dB]	
Value	1.6266	7.385	0.0815	0	10	

Table 7.2.1-2: Channel model parameters for UMi CDL-B at 3.5 GHz

Cluster #	Absolute Delay [ns]	Power in [dB]	AOD in [°]	AOA in [°]	ZOD in [°]	ZOA in [°]
1	0	0	3.2594	-173.655	105.6621	90
2	10.72	-2.2185	3.2594	-173.655	105.6621	90
3	21.55	-3.9794	3.2594	-173.655	105.6621	90
4	20.95	-3.2014	-21.7581	127.2975	106.8987	90
5	28.7	-9.8014	-39.8007	-91.3552	107.4194	90
6	29.86	-1.2	-8.6729	155.8564	105.3237	90
7	37.52	-3.4185	-8.6729	155.8564	105.3237	90
8	50.55	-5.1794	-8.6729	155.8564	105.3237	90
9	36.81	-7.6014	-40.8383	-93.0919	107.2762	90
10	36.97	-3.0014	28.1617	133.6653	105.1674	90
11	57	-8.9014	-43.6052	-87.11	104.9592	90
12	52.83	-9.0014	40.7281	98.1597	104.6858	90
13	110.21	-4.8014	-32.1917	106.2642	105.3497	90
14	127.56	-5.7014	-31.2117	-91.1623	105.2325	90
15	154.74	-7.5014	33.292	-95.697	105.0893	90
16	178.42	-1.9014	15.5376	-140.658	105.2976	90
17	201.69	-7.6014	-43.8934	-93.8638	104.9071	90
18	282.94	-12.2014	-54.327	62.7505	106.8857	90
19	302.19	-9.8014	-46.8333	-82.6718	104.9722	90
20	361.87	-11.4014	-49.7155	69.6972	107.4584	90
21	410.67	-14.9014	-61.8207	57.058	107.3413	90
22	427.9	-9.2014	41.4774	91.7918	107.2241	90
23	478.34	-11.3014	-46.8333	-64.726	106.9508	90
Per-Cluster Parameters						
Parameter	C _{ASD} in [°]	C _{ASA} in [°]	C _{zSD} in [°]	C _{zSA} in [°]	XPR in [dB]	
Value	5.7644	21.2262	0.3905	0	8	

Table 7.2.1-3: Channel model parameters for UMi CDL-C at 3.5 GHz

Cluster #	Absolute Delay [ns]	Power in [dB]	AOD in [°]	AOA in [°]	ZOD in [°]	ZOA in [°]
1	0	-4.4215	-36.1891	-122.2815	98.9242	90
2	20.99	-1.25	-21.5937	125.831	99.1915	90
3	22.19	-3.4684	-21.5937	125.831	99.1915	90
4	23.29	-5.2294	-21.5937	125.831	99.1915	90
5	21.76	-2.5215	-32.5709	-143.6126	99.5732	90
6	63.66	0	-7.4275	166.4003	99.306	90
7	64.48	-2.2185	-7.4275	166.4003	99.306	90
8	65.6	-3.9794	-7.4275	166.4003	99.306	90
9	65.84	-7.4215	37.2175	73.8315	100.4513	90
10	79.35	-7.1215	-47.1664	82.7664	98.5616	90
11	82.13	-10.7215	41.5716	-79.6999	100.6231	90
12	93.36	-11.1215	-67.1585	66.9895	98.218	90
13	122.85	-5.1215	-41.5244	84.0543	100.165	90
14	130.83	-6.8215	-47.0437	-96.2818	100.2604	90
15	217.04	-8.7215	-55.7519	94.8406	98.1225	90
16	271.05	-13.2215	55.3698	53.9494	100.2604	90
17	425.89	-13.9215	53.2234	16.0364	98.4852	90
18	460.03	-13.9215	46.8456	32.2963	98.1416	90
19	549.02	-15.8215	-70.1021	18.2098	97.9698	90
20	560.77	-17.1215	48.9306	37.0455	100.7376	90
21	630.65	-16.0215	49.6052	33.7452	98.1225	90

22	663.74	-15.7215	57.7615	29.801	98.1034	90
23	704.27	-21.6215	65.6725	11.6092	100.4513	90
24	865.23	-22.8215	-83.5324	56.2837	100.9476	90
Per-Cluster Parameters						
Parameter	CASD in [°]	CASA in [°]	CZSD in [°]	CZSA in [°]	XPR in [dB]	
Value	1.2265	12.0742	0.5726	0	7	

Table 7.2.1-4: Channel model parameters for UMi CDL-D at 3.5 GHz

Cluster #	Cluster PAS	Absolute Delay [ns]	Power in [dB]	AOD in [°]	AOA in [°]	ZOD in [°]	ZOA in [°]
1	Specular (LOS path)	0	-0.2	0	180	98.5	90
	Laplacian	0	-13.8303	0	-180	98.5	90
2	Laplacian	3.5275	-19.1289	85.5931	-69.0402	95.2232	90
3	Laplacian	61.6807	-21.3474	85.5931	-69.0402	95.2232	90
4	Laplacian	137.3705	-23.1083	85.5931	-69.0402	95.2232	90
5	Laplacian	141.6035	-18.2289	12.4743	133.3735	98.2479	90
6	Laplacian	181.8169	-20.4474	12.4743	133.3735	98.2479	90
7	Laplacian	261.6389	-22.2083	12.4743	133.3735	98.2479	90
8	Laplacian	178.8941	-23.2303	33.2009	-62.0624	98.5	90
9	Laplacian	407.3746	-28.1303	-61.8919	-109.358	95.9542	90
10	Laplacian	799.9337	-23.9303	-31.5697	36.555	96.6852	90
11	Laplacian	949.8016	-25.1303	50.4731	-14.3389	99.8359	90
12	Laplacian	978.4246	-30.3303	-126.759	-71.2668	93.9125	90
13	Laplacian	1262.337	-28.0303	74.0784	83.851	95.4753	90
Per-Cluster Parameters							
Parameter		CASD in [°]	CASA in [°]	CZSD in [°]	CZSA in [°]	XPR in [dB]	
Value		4.7978	21.9419	0.7562	0	11	

Table 7.2.1-5: Channel model parameters for UMi CDL-E at 3.5 GHz

Cluster #	Cluster PAS	Absolute Delay [ns]	Power in [dB]	AOD in [°]	AOA in [°]	ZOD in [°]	ZOA in [°]
1	Specular (LOS path)	0	-0.03	0	180	99.6	90
	Laplacian	0	-22.2442	0	-180	99.6	90
2	Laplacian	49.9706	-16.0427	65.756	-25.0925	101.5457	90
3	Laplacian	52.9593	-18.2612	65.756	-25.0925	101.5457	90
4	Laplacian	54.8089	-20.0221	65.756	-25.0925	101.5457	90
5	Laplacian	52.9593	-23.1142	-22.986	80.8762	99.5154	90
6	Laplacian	69.2365	-22.6142	18.526	94.9462	100.1076	90
7	Laplacian	185.8637	-18.8128	10.6353	-148.945	99.2616	90
8	Laplacian	187.8204	-21.0313	10.6353	-148.945	99.2616	90
9	Laplacian	190.702	-22.7922	10.6353	-148.945	99.2616	90
10	Laplacian	257.2613	-22.5142	21.7281	-133.48	100.1076	90
11	Laplacian	361.5249	-25.8142	37.3951	-71.8765	98.2465	90
12	Laplacian	530.7998	-20.4142	0.5718	138.1703	99.3039	90
13	Laplacian	1168.55	-30.0142	63.9262	2.2763	97.9081	90
14	Laplacian	2009.522	-29.4142	65.8703	15.2055	101.7149	90
Per-Cluster Parameters							
Parameter		CASD in [°]	CASA in [°]	CZSD in [°]	CZSA in [°]	XPR in [dB]	
Value		5.7179	13.9432	1.2689	0	8	

Tables 7.2.1-6—7.2.1-10 tabulate channel model parameters for UMa CDL-A—CDL-E models at 3.5 GHz, respectively.

In the determination of desired angle spreads ($\text{AS}_{\text{desired}}$), frequency is set 6 GHz as stated in Table 7.5-6 Part-1 of TR38.901.

For the determination of desired zenith spread of departure ($\text{ZSD}_{\text{desired}}$) from table 7.5-7 of TR38.901, the following parameters are used $h_{\text{UT}} = 1.5 \text{ m}$, and $d_{2d} = 100 \text{ m}$.

Table 7.2.1-6: Channel model parameters for UMa CDL-A at 3.5 GHz

Cluster #	Absolute Delay [ns]	Power in [dB]	AOD in [°]	AOA in [°]	ZOD in [°]	ZOA in [°]
1	0	-13.4014	-63.5923	70.1754	89.1998	90
2	139.3935	0	-2.804	-154.231	96.5746	90
3	146.9125	-2.2185	-2.804	-154.231	96.5746	90
4	214.182	-3.9794	-2.804	-154.231	96.5746	90
5	168.265	-5.9799	30.1944	92.1659	101.5139	90
6	196.1875	-8.1984	30.1944	92.1659	101.5139	90
7	244.842	-9.9593	30.1944	92.1659	101.5139	90
8	209.875	-10.5014	41.1356	-23.0699	106.3504	90
9	278.057	-7.5014	-29.8948	-57.9245	90.0573	90
10	561.1875	-15.9014	54.0343	107.4637	85.1179	90
11	692.697	-6.6014	-30.3493	70.6969	102.2686	90
12	811.833	-16.7014	45.7847	-122.245	110.0206	90
13	792.707	-12.4014	-54.8184	48.7064	106.5562	90
14	910.383	-15.2014	-61.46	92.1659	107.551	90
15	916.8435	-10.8014	-46.7436	-27.5897	88.6853	90
16	1116.243	-11.3014	-48.8759	-41.4968	87.519	90
17	1489.565	-12.7014	56.4812	-62.5312	88.0164	90
18	1627.1335	-16.2014	50.5387	121.5446	108.3399	90
19	1667.8675	-18.3014	45.0506	151.184	82.4424	90
20	1750.759	-18.9014	-42.7936	160.5712	83.4543	90
21	1827.409	-16.6014	-55.2029	114.2434	110.0378	90
22	1936.0695	-19.9014	42.8834	-153.449	84.4834	90
23	3525.389	-29.7014	-20.9811	73.5652	105.4414	90
Per-Cluster Parameters						
Parameter	C _{ASD} in [°]	C _{ASA} in [°]	C _{ZSD} in [°]	C _{ZSA} in [°]	XPR in [dB]	
Value	1.7478	9.5611	0.5145	0	10	

Table 7.2.1-7: Channel model parameters for UMa CDL-B at 3.5 GHz

Cluster #	Absolute Delay [ns]	Power in [dB]	AOD in [°]	AOA in [°]	ZOD in [°]	ZOA in [°]
1	0	0	3.8721	-170.785	105.7717	90
2	39.128	-2.2185	3.8721	-170.785	105.7717	90
3	78.6575	-3.9794	3.8721	-170.785	105.7717	90
4	76.4675	-3.2014	-23.0099	112.7684	113.5742	90
5	104.755	-9.8014	-42.3972	-64.2347	116.8595	90
6	108.989	-1.2	-8.9495	149.7425	103.6362	90
7	136.948	-3.4185	-8.9495	149.7425	103.6362	90
8	184.5075	-5.1794	-8.9495	149.7425	103.6362	90
9	134.3565	-7.6014	-43.5122	-66.4831	115.956	90
10	134.9405	-3.0014	30.6303	121.0127	102.6507	90
11	208.05	-8.9014	-46.4853	-58.7386	101.3365	90
12	192.8295	-9.0014	44.1333	75.0448	99.6118	90
13	402.2665	-4.8014	-34.2211	85.5375	103.8005	90
14	465.594	-5.7014	-33.1681	-63.9849	103.0613	90
15	564.801	-7.5014	36.143	-69.8558	102.1579	90
16	651.233	-1.9014	17.0654	-128.065	103.472	90
17	736.1685	-7.6014	-46.795	-67.4824	101.008	90
18	1032.731	-12.2014	-58.0062	29.2019	113.4921	90
19	1102.994	-9.8014	-49.9539	-52.9926	101.4187	90
20	1320.826	-11.4014	-53.051	38.1956	117.1059	90
21	1498.946	-14.9014	-66.0584	21.8321	116.3667	90
22	1561.835	-9.2014	44.9385	66.8006	115.6275	90
23	1745.941	-11.3014	-49.9539	-29.7588	113.9027	90
Per-Cluster Parameters						
Parameter	C _{ASD} in [°]	C _{ASA} in [°]	C _{zSD} in [°]	C _{zSA} in [°]	XPR in [dB]	
Value	6.194	27.4808	2.464	0	8	

Table 7.2.1-8: Channel model parameters for UMa CDL-C at 3.5 GHz

Cluster #	Absolute Delay [ns]	Power in [dB]	AOD in [°]	AOA in [°]	ZOD in [°]	ZOA in [°]
1	0	-4.4215	-37.4195	-96.4031	96.7645	90
2	76.6135	-1.25	-21.7362	118.7405	98.4506	90
3	80.9935	-3.4684	-21.7362	118.7405	98.4506	90
4	85.0085	-5.2294	-21.7362	118.7405	98.4506	90
5	79.424	-2.5215	-33.5316	-124.0196	100.8594	90
6	232.359	0	-6.5142	171.2639	99.1732	90
7	235.352	-2.2185	-6.5142	171.2639	99.1732	90
8	239.44	-3.9794	-6.5142	171.2639	99.1732	90
9	240.316	-7.4215	41.4581	51.4188	106.3995	90
10	289.6275	-7.1215	-49.2149	62.9864	94.4761	90
11	299.7745	-10.7215	46.1367	-41.2744	107.4834	90
12	340.764	-11.1215	-70.697	42.5606	92.3083	90
13	448.4025	-5.1215	-43.1524	64.6538	104.5929	90
14	477.5295	-6.8215	-49.0831	-62.7423	105.1951	90
15	792.196	-8.7215	-58.4403	78.6184	91.7061	90
16	989.3325	-13.2215	60.9633	25.6781	105.1951	90
17	1554.4985	-13.9215	58.6569	-23.4063	93.9944	90
18	1679.1095	-13.9215	51.8037	-2.3553	91.8265	90
19	2003.923	-15.8215	-73.86	-20.5926	90.7426	90
20	2046.8105	-17.1215	54.0442	3.7933	108.2061	90
21	2301.8725	-16.0215	54.7691	-0.4794	91.7061	90

22	2422.651	-15.7215	63.5332	-5.5859	91.5856	90
23	2570.5855	-21.6215	72.0338	-29.1381	106.3995	90
24	3158.0895	-22.8215	-88.2912	28.7003	109.5309	90
Per-Cluster Parameters						
Parameter	CASD in [°]	CASA in [°]	CZSD in [°]	CZSA in [°]	XPR in [dB]	
Value	1.3179	15.632	3.6131	0	7	

Table 7.2.1-9: Channel model parameters for UMa CDL-D at 3.5 GHz

Cluster #	Cluster PAS	Absolute Delay [ns]	Power in [dB]	AOD in [°]	AOA in [°]	ZOD in [°]	ZOA in [°]
1	Specular (LOS path)	0	-0.2	0	180	98.5	90
	Laplacian	0	-13.8303	0	-180	98.5	90
2	Laplacian	12.8753	-19.1289	79.7601	-157.697	80.0732	90
3	Laplacian	225.1344	-21.3474	79.7601	-157.697	80.0732	90
4	Laplacian	501.4023	-23.1083	79.7601	-157.697	80.0732	90
5	Laplacian	516.8527	-18.2289	11.6242	116.7749	97.0826	90
6	Laplacian	663.6315	-20.4474	11.6242	116.7749	97.0826	90
7	Laplacian	954.9819	-22.2083	11.6242	116.7749	97.0826	90
8	Laplacian	652.9634	-23.2303	30.9383	-20.0777	98.5	90
9	Laplacian	1486.917	-28.1303	-57.6741	147.6324	84.1838	90
10	Laplacian	2919.758	-23.9303	-29.4182	-14.5102	88.2944	90
11	Laplacian	3466.776	-25.1303	47.0334	44.6351	106.0125	90
12	Laplacian	3571.25	-30.3303	-118.12	95.5983	72.7025	90
13	Laplacian	4607.53	-28.0303	69.03	177.7798	81.4907	90
Per-Cluster Parameters							
Parameter		CASD in [°]	CASA in [°]	CZSD in [°]	CZSA in [°]	XPR in [dB]	
Value		4.4709	29.753	4.2523	0	11	

Table 7.2.1-10: Channel model parameters for UMa CDL-E at 3.5 GHz

Cluster #	Cluster PAS	Absolute Delay [ns]	Power in [dB]	AOD in [°]	AOA in [°]	ZOD in [°]	ZOA in [°]
1	Specular (LOS path)	0	-0.03	0	180	99.6	90
	Laplacian	0	-22.2442	0	-180	99.6	90
2	Laplacian	182.3926	-16.0427	61.2748	-98.1037	110.5415	90
3	Laplacian	193.3013	-18.2612	61.2748	-98.1037	110.5415	90
4	Laplacian	200.0527	-20.0221	61.2748	-98.1037	110.5415	90
5	Laplacian	193.3013	-23.1142	-21.4195	45.5889	99.1243	90
6	Laplacian	252.7131	-22.6142	17.2635	64.6678	102.4543	90
7	Laplacian	678.4024	-18.8128	9.9105	-137.889	97.6971	90
8	Laplacian	685.5446	-21.0313	9.9105	-137.889	97.6971	90
9	Laplacian	696.0624	-22.7922	9.9105	-137.889	97.6971	90
10	Laplacian	939.0038	-22.5142	20.2473	-116.92	102.4543	90
11	Laplacian	1319.566	-25.8142	34.8467	-33.3854	91.9885	90
12	Laplacian	1937.419	-20.4142	0.5328	123.2792	97.935	90
13	Laplacian	4265.208	-30.0142	59.5698	67.1651	90.0856	90
14	Laplacian	7334.755	-29.4142	61.3814	84.697	111.493	90
Per-Cluster Parameters							
Parameter		CASD in [°]	CASA in [°]	CZSD in [°]	CZSA in [°]	XPR in [dB]	
Value		5.3282	18.9069	7.1358	0	8	

7.2.2 Channel Models for FR2

Channel model parameter tables for CDL-A and C for UMi and InO at 28 GHz are presented in this subclause. The channel model tables presented here are only the propagation parameters, i.e., without the effect of base station antenna filtering.

Tables 7.2.2.1—7.2.2.5 show the model parameters, UMi CDL-A—CDL-E models, respectively. For the determination of desired zenith spread of departure ($ZSD_{desired}$) from table 7.5-8 of TR38.901, the following parameters are used $h_{BS} = 10$ m, $h_{UT} = 1.5$ m, and $d2d = 100$ m.

Table 7.2.2-1: Channel model parameters for UMi CDL-A at 28 GHz

Cluster #	Absolute Delay [ns]	Power in [dB]	AOD in [°]	AOA in [°]	ZOD in [°]	ZOA in [°]
1	0	-13.4014	-39.363	112.1365	95.9936	100.6889
2	22.914	0	-2.5086	-157.634	97.1624	88.9311
3	24.15	-2.2185	-2.5086	-157.634	97.1624	88.9311
4	35.208	-3.9794	-2.5086	-157.634	97.1624	88.9311
5	27.66	-5.9799	17.4974	126.7698	97.9452	89.8621
6	32.25	-8.1984	17.4974	126.7698	97.9452	89.8621
7	40.248	-9.9593	17.4974	126.7698	97.9452	89.8621
8	34.5	-10.5014	24.1308	-70.3543	98.7118	73.6909
9	45.708	-7.5014	-18.9331	-93.5479	96.1295	76.7596
10	92.25	-15.9014	31.951	136.9496	95.3467	67.8293
11	113.868	-6.6014	-19.2086	112.4835	98.0648	77.7251
12	133.452	-16.7014	26.9494	-136.349	99.2935	66.4156
13	130.308	-12.4014	-34.0436	97.8501	98.7444	74.415
14	149.652	-15.2014	-38.0703	126.7698	98.902	106.7919
15	150.714	-10.8014	-29.1481	-73.3619	95.912	97.9305
16	183.492	-11.3014	-30.4408	-82.6162	95.7272	99.7579
17	244.86	-12.7014	33.4345	-96.6134	95.806	99.9303
18	267.474	-16.2014	29.8317	146.3196	99.0271	68.6913
19	274.17	-18.3014	26.5044	166.0428	94.9226	66.8293
20	287.796	-18.9014	-26.7533	172.2895	95.083	62.6917
21	300.396	-16.6014	-34.2767	141.4611	99.2962	107.7918
22	318.258	-19.9014	25.1904	-157.113	95.2461	109.4124
23	579.516	-29.7014	-13.5289	114.3922	98.5677	111.2743
Per-Cluster Parameters						
Parameter	C _{ASD} in [°]	C _{ASA} in [°]	C _{zSD} in [°]	C _{zSA} in [°]	XPR in [dB]	
Value	1.0596	6.3623	0.0815	1.0344	10	

Table 7.2.2-2: Channel model parameters for UMi CDL-B at 28 GHz

Cluster #	Absolute Delay [ns]	Power in [dB]	AOD in [°]	AOA in [°]	ZOD in [°]	ZOA in [°]
1	0	0	0.3941	-175.004	105.6621	76.7603
2	6.432	-2.2185	0.3941	-175.004	105.6621	76.7603
3	12.93	-3.9794	0.3941	-175.004	105.6621	76.7603
4	12.57	-3.2014	-15.9038	134.1256	106.8987	65.837
5	17.22	-9.8014	-27.6578	-104.101	107.4194	63.4563
6	17.916	-1.2	-7.3793	158.7297	105.3237	68.7779
7	22.512	-3.4185	-7.3793	158.7297	105.3237	68.7779
8	30.33	-5.1794	-7.3793	158.7297	105.3237	68.7779
9	22.086	-7.6014	-28.3337	-105.597	107.2762	79.3511
10	22.182	-3.0014	16.6169	139.6116	105.1674	67.9377
11	34.2	-8.9014	-30.1363	-100.444	104.9592	64.6467
12	31.698	-9.0014	24.8034	109.0228	104.6858	62.1259
13	66.126	-4.8014	-22.7008	116.0051	105.3497	76.2702
14	76.536	-5.7014	-22.0624	-103.935	105.2325	78.931
15	92.844	-7.5014	19.9591	-107.841	105.0893	65.2068
16	107.052	-1.9014	8.3929	-146.576	105.2976	76.1301
17	121.014	-7.6014	-30.324	-106.262	104.9071	64.1565
18	169.764	-12.2014	-37.1211	78.5171	106.8857	79.5612
19	181.314	-9.8014	-32.2392	-96.62	104.9722	64.0865
20	217.122	-11.4014	-34.1169	84.5019	107.4584	61.6358
21	246.402	-14.9014	-42.0029	73.6129	107.3413	63.4563
22	256.74	-9.2014	25.2916	103.5368	107.2241	63.5964
23	287.004	-11.3014	-32.2392	-81.1593	106.9508	65.1368
Per-Cluster Parameters						
Parameter	C _{ASD} in [°]	C _{ASA} in [°]	C _{zSD} in [°]	C _{zSA} in [°]	XPR in [dB]	
Value	3.7533	18.2868	0.3905	4.9015	8	

Table 7.2.2-3: Channel model parameters for UMi CDL-C at 28 GHz

Cluster #	Absolute Delay [ns]	Power in [dB]	AOD in [°]	AOA in [°]	ZOD in [°]	ZOA in [°]
1	0	-4.4215	-30.4353	-134.4434	98.9242	83.3318
2	12.594	-1.25	-20.9269	129.1633	99.1915	72.5229
3	13.314	-3.4684	-20.9269	129.1633	99.1915	72.5229
4	13.974	-5.2294	-20.9269	129.1633	99.1915	72.5229
5	13.056	-2.5215	-28.0782	-152.8206	99.5732	71.1282
6	38.196	0	-11.6982	164.1145	99.306	74.7544
7	38.688	-2.2185	-11.6982	164.1145	99.306	74.7544
8	39.36	-3.9794	-11.6982	164.1145	99.306	74.7544
9	39.504	-7.4215	17.3861	84.3647	100.4513	69.2454
10	47.61	-7.1215	-37.5865	92.0623	98.5616	66.7349
11	49.278	-10.7215	20.2226	-97.7585	100.6231	72.0348
12	56.016	-11.1215	-50.6106	78.4702	98.218	64.4337
13	73.71	-5.1215	-33.911	93.1719	100.165	85.4238
14	78.498	-6.8215	-37.5066	-112.0441	100.2604	64.1548
15	130.224	-8.7215	-43.1797	102.4645	98.1225	64.7824
16	162.63	-13.2215	29.2116	67.2359	100.2604	92.467
17	255.534	-13.9215	27.8133	34.5731	98.4852	65.6889
18	276.018	-13.9215	23.6584	48.5813	98.1416	68.7572
19	329.412	-15.8215	-52.5282	36.4455	97.9698	59.1339
20	336.462	-17.1215	25.0168	52.6729	100.7376	65.3402
21	378.39	-16.0215	25.4562	49.8296	98.1225	58.4365

22	398.244	-15.7215	30.7697	46.4316	98.1034	65.2705
23	422.562	-21.6215	35.9234	30.759	100.4513	62.6903
24	519.138	-22.8215	-61.2775	69.2469	100.9476	61.993
Per-Cluster Parameters						
Parameter	CASD in [°]	CASA in [°]	CZSD in [°]	CZSA in [°]	XPR in [dB]	
Value	0.799	10.4021	0.5726	4.8814	7	

Table 7.2.2-4: Channel model parameters for UMi CDL-D at 28 GHz

Cluster #	Cluster PAS	Absolute Delay [ns]	Power in [dB]	AOD in [°]	AOA in [°]	ZOD in [°]	ZOA in [°]
1	Specular (LOS path)	0	-0.2	0	180	98.5	81.5
	Laplacian	0	-13.8303	0	-180	98.5	81.5
2	Laplacian	2.1165	-19.1289	77.9794	-34.5531	95.2232	94.9807
3	Laplacian	37.0084	-21.3474	77.9794	-34.5531	95.2232	94.9807
4	Laplacian	82.4223	-23.1083	77.9794	-34.5531	95.2232	94.9807
5	Laplacian	84.9621	-18.2289	11.3647	139.8304	98.2479	76.2575
6	Laplacian	109.0901	-20.4474	11.3647	139.8304	98.2479	76.2575
7	Laplacian	156.9833	-22.2083	11.3647	139.8304	98.2479	76.2575
8	Laplacian	107.3364	-23.2303	30.2476	-78.3945	98.5	73.2618
9	Laplacian	244.4247	-28.1303	-56.3864	-69.288	95.9542	61.7782
10	Laplacian	479.9602	-23.9303	-28.7614	56.4193	96.6852	73.5114
11	Laplacian	569.8809	-25.1303	45.9833	-37.2797	99.8359	95.2304
12	Laplacian	587.0548	-30.3303	-115.483	-136.177	93.9125	54.2889
13	Laplacian	757.4022	-28.0303	67.4889	47.3128	95.4753	60.0307
Per-Cluster Parameters							
Parameter		CASD in [°]	CASA in [°]	CZSD in [°]	CZSA in [°]	XPR in [dB]	
Value		4.371	18.9034	0.7562	7.4893	11	

Table 7.2.2-5: Channel model parameters for UMi CDL-E at 28 GHz

Cluster #	Cluster PAS	Absolute Delay [ns]	Power in [dB]	AOD in [°]	AOA in [°]	ZOD in [°]	ZOA in [°]
1	Specular (LOS path)	0	-0.03	0	180	99.6	80.4
	Laplacian	0	-22.2442	0	-180	99.6	80.4
2	Laplacian	29.9823	-16.0427	59.9068	3.3088	101.5457	80.4
3	Laplacian	31.7756	-18.2612	59.9068	3.3088	101.5457	80.4
4	Laplacian	32.8854	-20.0221	59.9068	3.3088	101.5457	80.4
5	Laplacian	31.7756	-23.1142	-20.9413	94.6029	99.5154	81.0235
6	Laplacian	41.5419	-22.6142	16.8781	106.7245	100.1076	89.5973
7	Laplacian	111.5182	-18.8128	9.6893	-153.245	99.2616	83.9854
8	Laplacian	112.6923	-21.0313	9.6893	-153.245	99.2616	83.9854
9	Laplacian	114.4212	-22.7922	9.6893	-153.245	99.2616	83.9854
10	Laplacian	154.3568	-22.5142	19.7953	-139.922	100.1076	84.2971
11	Laplacian	216.9149	-25.8142	34.0687	-86.8495	98.2465	92.2473
12	Laplacian	318.4799	-20.4142	0.5209	143.9629	99.3039	81.3353
13	Laplacian	701.1301	-30.0142	58.2398	-22.9654	97.9081	93.1826
14	Laplacian	1205.713	-29.4142	60.011	-11.8267	101.7149	77.1264
Per-Cluster Parameters							
Parameter		CASD in [°]	CASA in [°]	CZSD in [°]	CZSA in [°]	XPR in [dB]	
Value		5.2093	12.0124	1.2689	10.912	8	

Tables 7.2.2-6—7.2.2.10 tabulate channel model parameters for InO CDL-A—CDL-E models at 28 GHz, respectively.

Table 7.2.2-6: Channel model parameters for InO CDL-A at 28 GHz

Cluster #	Absolute Delay [ns]	Power in [dB]	AOD in [°]	AOA in [°]	ZOD in [°]	ZOA in [°]
1	0	-13.4014	-101.633	110.3637	77.4554	114.0008
2	11.457	0	-3.2678	-157.49	95.5583	90.2073
3	12.075	-2.2185	-3.2678	-157.49	95.5583	90.2073
4	17.604	-3.9794	-3.2678	-157.49	95.5583	90.2073
5	13.83	-5.9799	50.1288	125.3079	107.6831	92.0912
6	16.125	-8.1984	50.1288	125.3079	107.6831	92.0912
7	20.124	-9.9593	50.1288	125.3079	107.6831	92.0912
8	17.25	-10.5014	67.8333	-68.3566	119.5552	59.3663
9	22.854	-7.5014	-47.105	-92.0429	79.5604	65.5763
10	46.125	-15.9014	88.7055	135.7039	67.4357	47.5044
11	56.934	-6.6014	-47.8403	110.7181	109.5355	67.5301
12	66.726	-16.7014	75.3564	-135.753	128.5646	44.6436
13	65.154	-12.4014	-87.4352	95.7739	120.0604	60.8316
14	74.826	-15.2014	-98.1824	125.3079	122.5022	126.3512
15	75.357	-10.8014	-74.3689	-71.4282	76.1924	108.4188
16	91.746	-11.3014	-77.8193	-80.879	73.3297	112.1169
17	122.43	-12.7014	92.665	-95.1735	74.5505	112.4658
18	133.737	-16.2014	83.0491	145.2729	124.4388	49.2488
19	137.085	-18.3014	74.1685	165.4151	60.8681	45.4809
20	143.898	-18.9014	-67.9771	171.7944	63.352	37.1078
21	150.198	-16.6014	-88.0574	140.3112	128.6067	128.3747
22	159.129	-19.9014	70.6615	-156.959	65.878	131.6542
23	289.758	-29.7014	-32.6811	112.6674	117.3239	135.4221
Per-Cluster Parameters						
Parameter	C _{ASD} in [°]	C _{AZA} in [°]	C _{ZSD} in [°]	C _{ZSA} in [°]	XPR in [dB]	
Value	2.8282	6.4975	1.263	2.0933	10	

Table 7.2.2-7: Channel model parameters for InO CDL-B at 28 GHz

Cluster #	Absolute Delay [ns]	Power in [dB]	AOD in [°]	AOA in [°]	ZOD in [°]	ZOA in [°]
1	0	0	9.3327	-174.826	105.9611	81.8761
2	3.216	-2.2185	9.3327	-174.826	105.9611	81.8761
3	6.465	-3.9794	9.3327	-174.826	105.9611	81.8761
4	6.285	-3.2014	-34.1667	133.2233	125.1141	59.7711
5	8.61	-9.8014	-65.5384	-102.417	133.1785	54.9534
6	8.958	-1.2	-11.4147	158.35	100.7192	65.7225
7	11.256	-3.4185	-11.4147	158.35	100.7192	65.7225
8	15.165	-5.1794	-11.4147	158.35	100.7192	65.7225
9	11.043	-7.6014	-67.3425	-103.945	130.9608	87.119
10	11.091	-3.0014	52.6316	138.8259	98.2999	64.0221
11	17.1	-8.9014	-72.1535	-98.6816	95.0741	57.3623
12	15.849	-9.0014	74.4815	107.5873	90.8403	52.2611
13	33.063	-4.8014	-52.3082	114.7179	101.1224	80.8842
14	38.268	-5.7014	-50.6043	-102.247	99.308	86.2688
15	46.422	-7.5014	61.552	-106.237	97.0902	58.4959
16	53.526	-1.9014	30.6814	-145.794	100.316	80.6008
17	60.507	-7.6014	-72.6547	-104.624	94.2677	56.3704
18	84.882	-12.2014	-90.7961	76.4337	124.9125	87.5441
19	90.657	-9.8014	-77.7663	-94.7768	95.2758	56.2287
20	108.561	-11.4014	-82.7778	82.5456	133.7833	51.2692

21	123.201	-14.9014	-103.826	71.4253	131.9688	54.9534
22	128.37	-9.2014	75.7845	101.9848	130.1543	55.2368
23	143.502	-11.3014	-77.7663	-78.9878	125.9205	58.3542
Per-Cluster Parameters						
Parameter	CASD in [°]	CASA in [°]	CZSD in [°]	CZSA in [°]	XPR in [dB]	
Value	10.0229	18.6752	6.0483	9.9189	8	

Table 7.2.2-8: Channel model parameters for InO CDL-C at 28 GHz

Cluster #	Absolute Delay [ns]	Power in [dB]	AOD in [°]	AOA in [°]	ZOD in [°]	ZOA in [°]
1	0	-4.4215	-48.3848	-132.8363	93.0309	93.3988
2	6.297	-1.25	-23.0068	128.723	97.1699	71.5254
3	6.657	-3.4684	-23.0068	128.723	97.1699	71.5254
4	6.987	-5.2294	-23.0068	128.723	97.1699	71.5254
5	6.528	-2.5215	-42.0936	-151.6038	103.0827	68.703
6	19.098	0	1.6247	164.4166	98.9437	76.0412
7	19.344	-2.2185	1.6247	164.4166	98.9437	76.0412
8	19.68	-3.9794	1.6247	164.4166	98.9437	76.0412
9	19.752	-7.4215	79.2514	82.9728	116.6821	64.8928
10	23.805	-7.1215	-67.4716	90.8339	87.4138	59.8126
11	24.639	-10.7215	86.8222	-95.3722	119.3429	70.5376
12	28.008	-11.1215	-102.233	76.9531	82.0922	55.1556
13	36.855	-5.1215	-57.6616	91.9671	112.2475	97.6324
14	39.249	-6.8215	-67.2583	-109.9613	113.7257	54.5912
15	65.112	-8.7215	-82.3998	101.457	80.614	55.8612
16	81.315	-13.2215	110.8139	65.4801	113.7257	111.8854
17	127.767	-13.9215	107.0819	32.1236	86.2312	57.6958
18	138.009	-13.9215	95.9924	46.4294	80.9097	63.905
19	164.706	-15.8215	-107.3512	34.0358	78.2489	44.4306
20	168.231	-17.1215	99.6178	50.6078	121.1167	56.9902
21	189.195	-16.0215	100.7907	47.7042	80.614	43.0194
22	199.122	-15.7215	114.9725	44.234	80.3184	56.8491
23	211.281	-21.6215	128.7278	28.2285	116.6821	51.6277
24	259.569	-22.8215	-130.7032	67.5339	124.3688	50.2165
Per-Cluster Parameters						
Parameter	CASD in [°]	CASA in [°]	CZSD in [°]	CZSA in [°]	XPR in [dB]	
Value	2.1326	10.6231	8.8692	9.8783	7	

Table 7.2.2-9: Channel model parameters for InO CDL-D at 28 GHz

Cluster #	Cluster PAS	Absolute Delay [ns]	Power in [dB]	AOD in [°]	AOA in [°]	ZOD in [°]	ZOA in [°]
1	Specular (LOS path)	0	-0.2	0	180	98.5	81.5
	Laplacian	0	-12.1055	0	-180	98.5	81.5
2	Laplacian	0.8738	-17.404	-172.96	42.7638	92.4883	114.5755
3	Laplacian	15.2798	-19.6225	-172.96	42.7638	92.4883	114.5755
4	Laplacian	34.0301	-21.3834	-172.96	42.7638	92.4883	114.5755
5	Laplacian	35.0787	-16.504	27.2592	154.306	98.0376	68.6373
6	Laplacian	45.0405	-18.7225	27.2592	154.306	98.0376	68.6373
7	Laplacian	64.8144	-20.4834	27.2592	154.306	98.0376	68.6373
8	Laplacian	44.3165	-21.5055	72.5514	-115.009	98.5	61.2872
9	Laplacian	100.9167	-26.4055	-135.248	20.546	93.8293	33.1118
10	Laplacian	198.1633	-22.2055	-68.9868	100.9531	95.1704	61.8997
11	Laplacian	235.2893	-23.4055	110.295	-88.7107	100.9509	115.188

12	Laplacian	242.3799	-28.6055	83.0045	78.3003	90.0836	14.7365
13	Laplacian	312.7121	-26.3055	161.8778	-34.6022	92.9507	28.8242
Per-Cluster Parameters							
Parameter		C _{ASD} in [°]	C _A S _A in [°]	C _{ZSD} in [°]	C _{ZSA} in [°]	XPR in [dB]	
Value		10.4843	12.0913	1.3873	18.3753	11	

Table 7.2.2-10: Channel model parameters for InO CDL-E at 28 GHz

Cluster #	Cluster PAS	Absolute Delay [ns]	Power in [dB]	AOD in [°]	AOA in [°]	ZOD in [°]	ZOA in [°]
1	Specular (LOS path)	0	-0.03	0	180	99.6	80.4
	Laplacian	0	-20.5194	0	-180	99.6	80.4
2	Laplacian	12.3987	-14.3178	145.0787	66.3397	103.1625	80.4
3	Laplacian	13.1402	-16.5363	145.0787	66.3397	103.1625	80.4
4	Laplacian	13.5992	-18.2972	145.0787	66.3397	103.1625	80.4
5	Laplacian	13.1402	-21.3894	-50.7145	125.0665	99.4451	81.931
6	Laplacian	17.1789	-20.8894	40.8743	132.864	100.5293	102.9826
7	Laplacian	46.1165	-17.0879	23.4649	-162.789	98.9804	89.2034
8	Laplacian	46.602	-19.3064	23.4649	-162.789	98.9804	89.2034
9	Laplacian	47.317	-21.0673	23.4649	-162.789	98.9804	89.2034
10	Laplacian	63.8316	-20.7894	47.939	-154.219	100.5293	89.9689
11	Laplacian	89.7015	-24.0894	82.5056	-120.079	97.1217	109.4894
12	Laplacian	131.7019	-18.6894	1.2616	156.8183	99.0579	82.6965
13	Laplacian	289.9404	-28.2894	141.0417	-78.9842	96.5022	111.7859
14	Laplacian	498.6022	-27.6894	145.331	-71.819	103.4723	72.3621
Per-Cluster Parameters							
Parameter		C _{ASD} in [°]	C _A S _A in [°]	C _{ZSD} in [°]	C _{ZSA} in [°]	XPR in [dB]	
Value		12.6155	7.7272	2.3234	26.7929	8	

7.3 Channel Model emulation of the Base Station beamforming configuration

The basic parameters of NR BS antenna is specified in table 7.2-7. The propagation environment generated in the test zone is channel model defined in section 7.2 with base station antenna filtering effect. For the channel model emulation in the chamber, the beamforming characteristic of the BS pattern is defined as follow:

- For FR1: A code book of 60 fixed beams is constructed to a grid of five elevation angles from -20° to +20° with 10° steps and 12 azimuth angles from -80° to +80° with ~15° steps;
- For FR2: A code book of 128 fixed beams is constructed to a grid of eight elevation angles from -25° to +25° with ~7.1° step size and 16° azimuth angles from -60° to +60° with 8° step size;

For NR FR1 MIMO OTA, 2 strongest transmitting beams are selected from the pre-defined beam grid based on their proximity to the strong clusters of each FR1 channel model.

For NR FR2 MIMO OTA, 1 strongest transmitting beam is generated from BS, the direction of this beam towards the strongest cluster of each FR2 channel model.

7.4 Verification of Channel Model implementation

7.4.1 Channel Models validation

This clause describe the MIMO OTA validation measurements, in order to ensure that the channel models are correctly implemented and hence capable of generating the propagation environment, as described by the model, within the test zone.

The following measurements shall be done for FR1 channel model validation:

- Power Delay Profile (PDP)
- Doppler/Temporal correlation
- Spatial correlation
- Cross-polarization
- Power validation

The following measurements shall be done for FR2 channel model validation:

- Power Delay Profile (PDP)
- Doppler/Temporal correlation
- PAS similarity percentage (PSP)
- Cross-polarization
- Power validation

Frequencies to be used to test for channel model validation and quality of quiet zone validation:

Table 7.4.1-1: Channel model validation and Quality of Quiet Zone validation frequencies

NR FR1 Bands	Range	Test frequency (MHz)
n71	Low	617MHz
n12, n17, n29, n14, n28, [n29]		722MHz
n5, n8, n18, n20		836.5MHz
n50, n51, n74	Mid	1575.42MHz
n3, n2, n25, n39		1880MHz
n1, n34, n65		2132.5MHz
n7, n30, n41, n40, n38, [n90]		2450MHz
n77, n78	High	3600MHz
n79		[4700MHz]

Table 7.4.1-2: Channel model validation and Quality of Quiet Zone validation frequencies

NR FR2 Bands	Range	Test Frequency (MHz)
n257	Low	27750
n260	High	38500
n258	Low	25875
n261	Low	27925

7.4.1.1 Power Delay Profile (PDP)

This measurement checks that the resulting power delay profile (PDP) is in-line with the PDP defined for the channel model. For PDP validation measurement, only Vertical validation is required.

FR1 PDP validation procedure for MPAC system:

The PDP measurement is performed with a Vector Network Analyzer (VNA). An example setup for PDP measurement is shown in Figure 7.4.1.1-1. VNA transmits frequency sweep signals thorough the NR MIMO OTA test system. A reference antenna (i.e dipole antenna), within the center of the test zone, receives the signal and VNA analyses the frequency response of the system. A number of traces (frequency responses) are measured and recorded by VNA and analyzed by a post processing SW, e.g., Matlab. Special care has to be taken into account to keep the fading conditions unchanged, i.e. frozen, during the short period of time of a single trace measurement. The fading may proceed only in between traces.

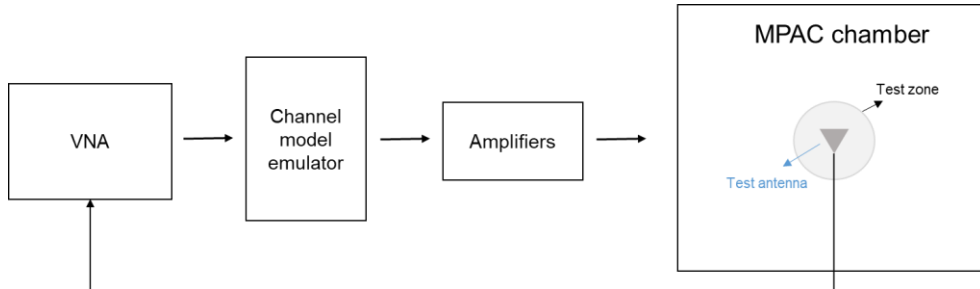


Figure 7.4.1.1-1: Setup for PDP measurements

Step the emulation and store traces from VNA. I.e. run the emulation to CIR number 1, pause, measure VNA trace, run the emulation to CIR number 10, pause, measure VNA trace. Continue until 1000 VNA traces are measured.

VNA settings:

Table 7.4.1.1-1: VNA settings for PDP measurements

Item	Unit	Value
Center frequency	MHz	Downlink center frequency in Table 7.4.1-1
Span	MHz	200
Number of traces		1000
Number of points		1101
Averaging		1

Channel model specification:

Table 7.4.1.1-2: Channel model specification for PDP measurements

Item	Unit	Value
Center frequency	MHz	Downlink center frequency in Table 7.4.1-1
Distance between traces in channel model	wavelength (Note)	> 2
Channel model		As specified in Clause 7.2
NOTE: Time [s] = distance [λ] / MS speed [λ/s] MS speed [λ/s] = MS speed [m/s] / Speed of light [m/s] * Center frequency [Hz]		

Method of measurement result analysis:

Measured VNA traces (frequency responses $H(t,f)$) are saved into a hard drive. The data is read into, e.g., Matlab. The analysis is performed by taking the Fourier transform of each FR. The resulting impulse responses $h(t,\tau)$ are averaged in power over time:

$$P(\tau) = \frac{1}{T} \sum_{t=1}^T |h(t, \tau)|^2$$

Finally the resulting PDP is shifted in delay, such that the first tap is on delay zero.

FR2 PDP validation procedure for 3D-MPAC system:

The PDP measurement is performed with a Vector Network Analyzer (VNA). An example setup for PDP measurement is shown in Figure 7.4.1.1-2. VNA transmits frequency sweep signals thorough the NR MIMO OTA test system. A reference antenna, within the centre of the test zone, receives the signal and VNA analyses the frequency response of the system. A number of traces (frequency responses) are measured and recorded by VNA and analyzed by a post processing SW, e.g., Matlab. Special care has to be taken into account to keep the fading conditions unchanged, i.e. frozen, during the short period of time of a single trace measurement. The fading may proceed only in between traces.

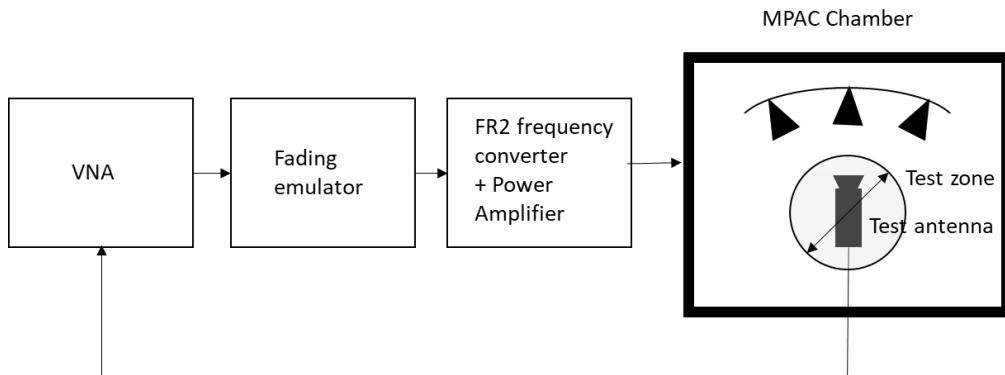


Figure 7.4.1.1-2: Setup for PDP measurements (FR2)

Step the emulation and store traces from VNA. I.e. run the emulation to CIR number 1, pause, measure VNA trace, run the emulation to CIR number 10, pause, measure VNA trace. Continue until 1000 VNA traces are measured.

VNA settings:

Table 7.4.1.1-1: VNA settings for PDP measurements

Item	Unit	Value
Center frequency	MHz	Downlink center frequency in Table 7.4.1-2
Span	MHz	200
Number of traces		1000
Number of points		1101
Averaging		1

Channel model specification:

Table 7.4.1.1-3: Channel model specification for FR2 PDP measurements

Item	Unit	Value
Center frequency	MHz	Downlink center frequency in Table 7.4.1-2
Distance between traces in channel model	wavelength (Note)	> 2
Channel model		As specified in Clause 7.2
NOTE: Time [s] = distance [λ] / MS speed [λ/s] MS speed [λ/s] = MS speed [m/s] / Speed of light [m/s] * Center frequency [Hz]		

Method of measurement result analysis:

Measured VNA traces (frequency responses $H(t,f)$) are saved into a hard drive. The data is read into, e.g., Matlab. The analysis is performed by taking the Inverse Fourier transform of each trace. The resulting impulse responses $h(t,\tau)$ are averaged in power over time:

$$P(\tau) = \frac{1}{T} \sum_{t=1}^T |h(t, \tau)|^2$$

Finally, the resulting PDP is shifted in delay, such that the first tap is on delay zero.

7.4.1.2 Doppler/Temporal correlation

This measurement checks the Doppler/temporal correlation. For Doppler/Temporal correlation validation measurement, only Vertical validation is required.

FR1 Doppler/Temporal correlation validation procedure for MPAC system:

The Doppler spectrum is measured with a spectrum analyzer as shown in Figure 7.4.1.2-1. In this case a signal generator transmits CW signal through the NR MIMO OTA test system. The signal is received by a test antenna within the test area. Finally the signal is analyzed by a spectrum analyzer and the measured spectrum is compared to the target spectrum. This setup can be used to measure Doppler Spectrum of the Channel models defined in Clause 7.2.

Method of measurement:

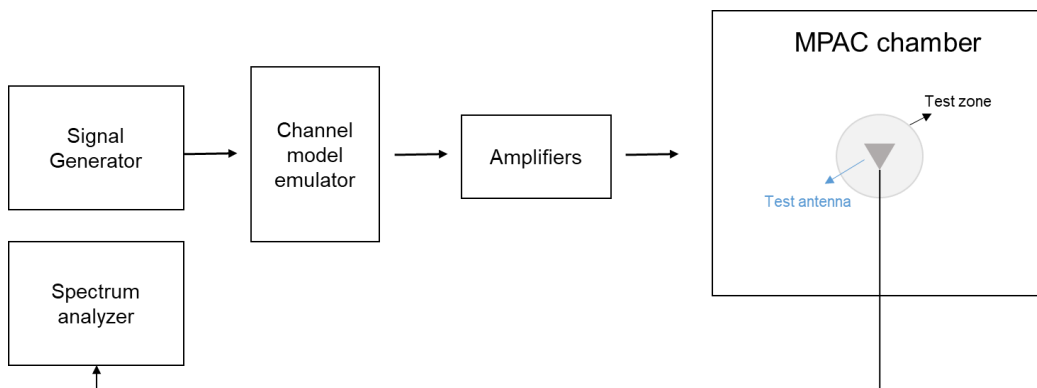


Figure 7.4.1.2-1: Setup for Doppler measurements

Sine wave (CW, carrier wave) signal is transmitted from the signal generator. The signal is connected from the signal generator to fading emulator via cables. The fading emulator output signals are connected to power amplifier boxes via cables. The amplified signals are then transferred via cables to the probe antennas. The probe antennas radiate the signals over the air to the test antenna. The Doppler spectrum is measured by the spectrum analyzer and the trace is saved.

Signal generator settings:

Table 7.4.1.2-1: Signal generator settings for Doppler/Temporal correlation measurements

Item	Unit	Value
Center frequency	MHz	Downlink center frequency in Table 7.4.1-1
Modulation		OFF

Spectrum analyzer settings:

Table 7.4.1.2-2: Spectrum analyzer settings for Doppler/Temporal correlation measurements

Item	Unit	Value
Center frequency	MHz	Downlink center frequency in Table 7.4.1-1
Minimum Span	Hz	4 kHz
RBW	Hz	1
VBW	Hz	1
Number of points		16002
Averaging		100

Channel model specification:

Table 7.4.1.2-3: Channel model specification for Doppler/Temporal correlation measurements

Item	Unit	Value
Center frequency	MHz	Downlink center frequency in Table 7.4.1-1
Channel model		As specified in Clause 7.2
Mobile speed	km/h	100

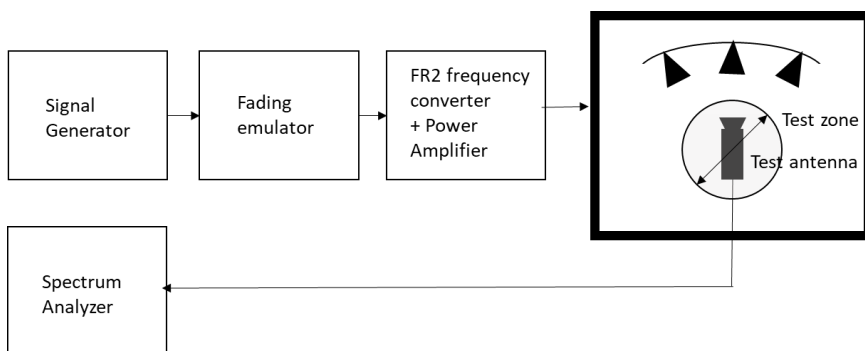
Method of measurement result analysis: Measurement data file (Doppler power spectrum) is saved into hard drive. The data is read into, e.g., Matlab. The analysis is performed by taking the Fourier transformation of the Doppler spectrum.

The resulting temporal correlation function $R_t(\Delta t)$ is normalized such that $\max(\operatorname{Re}(R_t(\Delta t))) = 1$. Then the function values left from the maximum is cut out. Further on the function values after, e.g. seven periods is cut out.

FR2 Doppler/Temporal correlation validation procedure for 3D-MPAC system:

The Doppler spectrum is measured with a spectrum analyzer as shown in Figure 7.4.1.2-2. In this case a signal generator transmits CW signal through the NR MIMO OTA test system. The signal is received by a test antenna within the test area. Finally, the signal is analysed by a spectrum analyser and the measured spectrum is compared to the target spectrum. This setup can be used to measure Doppler Spectrum of the Channel models defined in Clause 7.2.

Method of measurement:

**Figure 7.4.1.2-2: Setup for Doppler measurements**

Sine wave (CW, carrier wave) signal is transmitted from the signal generator. The signal is connected from the signal generator to fading emulator via cables. The fading emulator output signals are connected to frequency converter and power amplifier boxes via cables. The amplified signals are then transferred via cables to the probe antennas. The probe antennas radiate the signals over the air to the test antenna. The Doppler spectrum is measured by the spectrum analyzer and the trace is saved.

Signal generator settings:

Table 7.4.1.2-2: Signal generator settings for Doppler/Temporal correlation measurements

Item	Unit	Value
Center frequency	MHz	Downlink center frequency in Table 7.4.1-2
Modulation		OFF

Spectrum analyzer settings:

Table 7.4.1.2-2: Spectrum analyzer settings for Doppler/Temporal correlation measurements

Item	Unit	Value
Center frequency	MHz	Downlink center frequency in Table 7.4.1-2
Minimum Span	Hz	4 kHz
RBW	Hz	1
VBW	Hz	1
Number of points		16002
Averaging		100

Channel model specification:

Table 7.4.1.2-3: Channel model specification for Doppler/Temporal correlation measurements

Item	Unit	Value
Center frequency	MHz	Downlink center frequency in Table 7.4.1-2
Channel model		As specified in Clause 7.2
Mobile speed	km/h	3

Method of measurement result analysis: Measurement data file (Doppler power spectrum) is saved into hard drive. The data is read into, e.g., Matlab. The analysis is performed by taking the Fourier transformation of the Doppler spectrum.

The resulting temporal correlation function $R_t(\Delta t)$ is normalized such that $\max(\text{Re}(R_t(\Delta t))) = 1$. Then the function values left from the maximum is cut out. Further on the function values after, e.g. seven periods is cut out.

7.4.1.3 Spatial correlation

This measurement checks whether the measured correlation curve follows the theoretical curve. For spatial correlation validation measurement, both Vertical and Horizontal validation are required. Spatial correlation validation is only adopted for FR1 MIMO OTA.

The spatial correlation validation measurement setup is illustrated in Figure 7.4.1.3-1. The network analyser transmits signals through the fading emulator and probes. The 16 probes radiate the signals within the anechoic chamber and a receiving test antenna is placed within the test zone. The test antenna is attached to a positioner that can move the antenna to pre-defined spatial locations on a fixed radius from the centre of the quiet zone. The received signal is measured with the network analyser.

The measurement and analysis procedure is as follows:

1. Set the target channel model to fading emulator.
2. For each position of the test antenna in the test zone, step & pause the emulator to different time instances. Measure the frequency responses $H(f, t) = H(m\Delta f, n\Delta T)$, $m = 0, \dots, M - 1$ for all stepped channel snapshots $n = 0, \dots, N - 1$, where the interval between frequency and time samples is Δf and ΔT , respectively. The number of channel snapshots N and frequency samples M should be sufficiently high so that the matrix can be estimated reliably.

3. Move the measurement antenna with a positioner to another location k and repeat step 2 to record frequency responses $H_k(m\Delta f, n\Delta T)$ of all stepped channel snapshots.
4. Repeat step 3 to record frequency responses at all $k = 1, \dots, K$ spatial sample points.
5. Stack measured time and frequency samples to a vector and calculate correlation between the first spatial sample point (i.e. $k = 1$) and other spatial points $k = 1, \dots, K$
6. $\rho_k = \text{corr}[\text{vec}(H_1(m\Delta f, n\Delta T)), \text{vec}(H_k(m\Delta f, n\Delta T))]$
7. Take the theoretical reference spatial correlation of the corresponding spatial sample points. Plot both the measured and theoretical curves.
8. Calculate the weighted RMS correlation error between the measured and the reference.

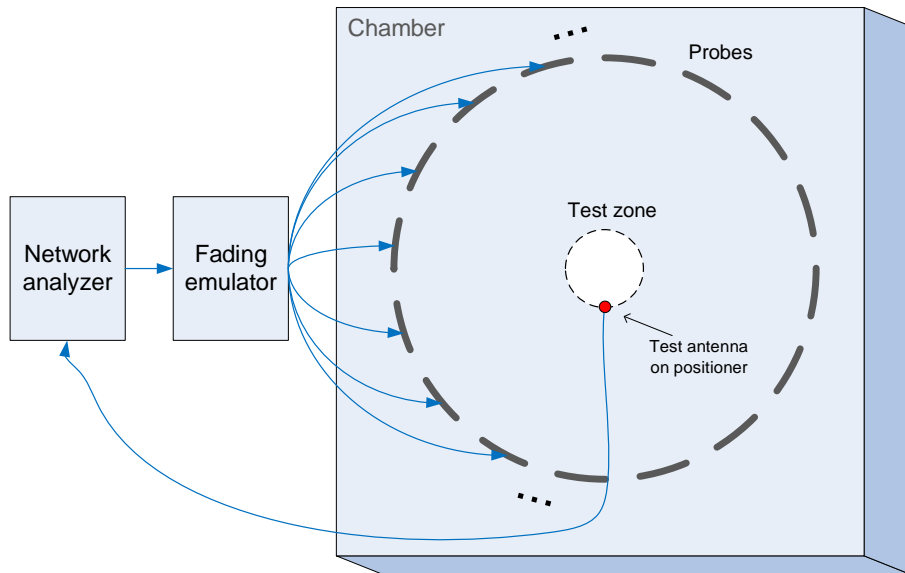


Figure 7.4.1.3-1: Configuration for spatial correlation validation

Time and frequency samples

The number of temporal snapshots N and frequency samples M is TBD. They must be chosen to minimize the validation measurement time, but sufficiently high to keep an adequate correlation estimation accuracy. It is beneficial to choose the time sampling interval ΔT larger than the coherence time of the channel model, such that the recorded time samples represent independent fading occasions. The same principle applies also to frequency sampling interval Δf and the channel coherence bandwidth.

Spatial samples

The spatial samples for the correlation validation measurement are on the circumference of the quiet zone, as illustrated in Figure 7.4.1.3-2. The test zone is a circle with 20 cm diameter in the horizontal plane. The reference point (denoted by a red marker) is in AoA 270°. The mean AoAs of the CDL-A and CDL-C models are slightly different, but the underlying geometry for the CDL model indicates that the mean AoA (or assumed LoS direction) of the model is 180°. The reference point orientation of the validation measurement is proposed to be with 90° offset to the channel model reference AoA to enable accurate sampling of the main lobe of the spatial correlation curve. The reference point orientation must be defined in the channel model coordinate system instead of the chamber/probe coordinate system to enable optimization of OTA model implementation to achieve better alignment with the cluster AoAs and probe directions. In order to have spatial samples that yield reasonable measurement times and adequately capture the main lobe of the correlation curve, a non-uniform sampling is used where the first quadrant i.e., 270°-180°, is sampled with

dense sampling compared to the rest of the circle. The spacing of the spatial samples is summarized in Table 7.4.1.3-1 for test frequencies less than 1800 MHz and equal to or greater than 1800 MHz.

Table 7.4.1.3-1: Spacing of Spatial Samples

Test Frequencies [MHz]	First quadrant of test zone circumference (270°-180°)	Remaining quadrants
617, 722, 836.5 1575.42	$\lambda/15$	$\lambda/4$
1800, 2132.50, 2450, 3600, 4700	$\lambda/10$	$\lambda/2$

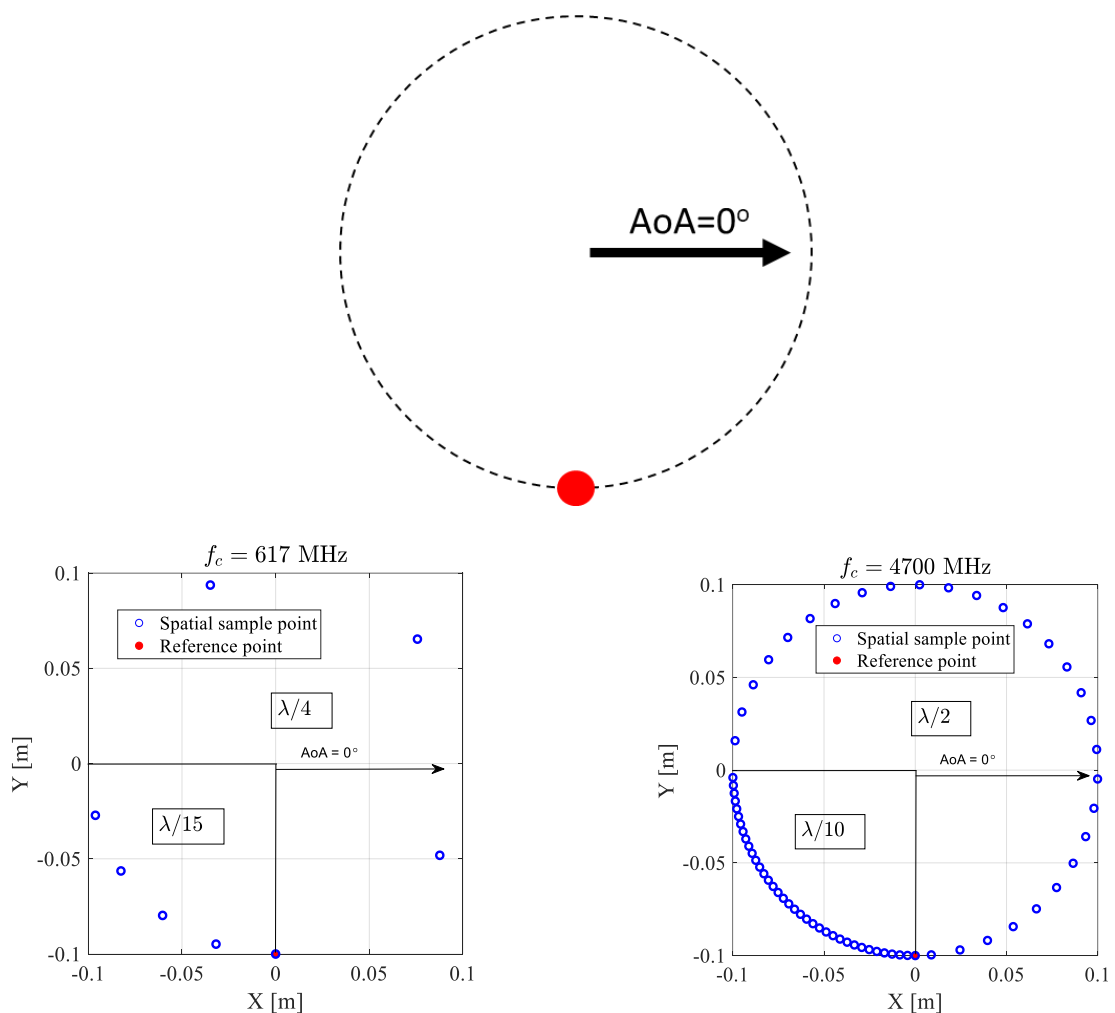


Figure 7.4.1.3-2: Spatial sampling for spatial correlation validation measurement for test frequencies less than and equal to or greater than 1800 MHz: 617 MHz spatial sampling (left) and 4700 MHz spatial sampling (right).

Reference Spatial Correlation Curves

The spatial correlation validation reference curves are tabulated in Tables 7.4.1.3-2 and 7.4.1.3-3 for CDL-A UMi and in Tables 7.4.1.3-4 and 7.4.1.3-5 for CDL-C UMa for a vertically polarized MPAC OTA setup with 16 uniformly spaced probes.

Table 7.4.1.3-2: Spatial correlation reference curves for CDL-A UMi model for a vertically polarized MPAC OTA setup with 16 uniformly spaced probes at FR1 test frequencies below 1800 MHz

617 MHz		722 MHz		836.5 MHz		1575.42 MHz	
Azimuth [°]	ρ_{ref}						
270.0	1.000	270.0	1.000	270.0	1.000	270.0	1.000
251.4	0.999	254.1	0.999	256.3	0.999	262.7	0.999
232.9	0.997	238.3	0.997	242.6	0.996	255.5	0.996
214.3	0.992	222.4	0.993	228.9	0.993	248.2	0.992
195.8	0.981	206.6	0.984	215.2	0.987	240.9	0.987
110.40	0.809	190.7	0.969	201.6	0.975	233.7	0.982
40.80	0.823	120.52	0.778	187.9	0.955	226.4	0.977
331.21	0.96	61.05	0.731	128.66	0.751	219.1	0.971
		1.57	0.88	77.33	0.645	211.9	0.962
		302.09	0.99	25.99	0.762	204.6	0.949
				334.66	0.928	197.3	0.929
				283.32	0.998	190.0	0.903
						182.8	0.868
						152.74	0.620
						125.48	0.363
						98.23	0.299
						70.97	0.364
						43.71	0.460
						16.45	0.58
						349.20	0.71
						321.94	0.86
						294.68	0.97

Table 7.4.1.3-3: Spatial correlation reference curves for CDL-A UMi model for a vertically polarized MPAC OTA setup with 16 uniformly spaced probes at FR1 test frequencies equal to or greater than 1800 MHz

1800 MHz		2132.5 MHz		2450 MHz		3600 MHz		4700 MHz	
Azimuth [°]	ρ_{ref}								
270.0	1.000	270.0	1.000	270.0	1.000	270.0	1.000	270.0	1.000
260.9	0.998	261.9	0.998	263.0	0.997	265.2	0.997	266.3	0.997
251.7	0.991	253.9	0.990	256.0	0.990	260.5	0.990	262.7	0.990
242.6	0.981	245.8	0.980	249.0	0.979	255.7	0.979	259.0	0.979
233.5	0.967	237.8	0.967	242.0	0.966	250.9	0.966	255.4	0.969
224.3	0.951	229.7	0.952	234.9	0.951	246.1	0.950	251.7	0.956
215.2	0.932	221.7	0.933	227.9	0.932	241.4	0.932	248.1	0.942
206.0	0.906	213.6	0.911	220.9	0.913	236.6	0.908	244.4	0.922
196.9	0.877	205.6	0.883	213.9	0.888	231.8	0.881	240.8	0.896
187.8	0.845	197.5	0.854	206.9	0.862	227.1	0.857	237.1	0.872
134.3	0.748	189.5	0.823	199.9	0.833	222.3	0.832	233.5	0.842
88.6	0.729	181.4	0.795	192.9	0.805	217.5	0.815	229.8	0.817
43.0	0.833	139.7	0.737	185.9	0.783	212.7	0.800	226.1	0.792
357.3	0.953	99.5	0.725	144.9	0.742	208.0	0.792	222.5	0.775
311.6	0.978	59.2	0.753	109.9	0.754	203.2	0.785	218.8	0.760

		18.9	0.884	74.8	0.727	198.4	0.782	215.2	0.753
		338.6	0.970	39.8	0.778	193.7	0.781	211.5	0.750
		298.4	0.982	4.7	0.901	188.9	0.786	207.9	0.753
				329.7	0.974	184.1	0.795	204.2	0.760
				294.6	0.980	156.1	0.886	200.6	0.775
						132.3	0.952	196.9	0.792
						108.4	0.949	193.3	0.817
						84.6	0.906	189.6	0.840
						60.7	0.830	185.9	0.865
						36.9	0.741	182.3	0.888
						13.0	0.774	161.7	0.978
						349.1	0.894	143.5	0.945
						325.3	0.966	125.2	0.926
						301.4	0.969	106.9	0.926
						277.6	0.994	88.6	0.948
								70.4	0.948
								52.1	0.896
								33.8	0.747
								15.5	0.682
								357.3	0.799
								339.0	0.912
								320.7	0.956
								302.4	0.968
								284.2	0.973

Table 7.4.1.3-4: Spatial correlation reference curves for CDL-C UMa model for a vertically polarized MPAC OTA setup with 16 uniformly spaced probes at FR1 test frequencies below 1800 MHz

617 MHz		722 MHz		836.5 MHz		1575.42 MHz	
Azimuth [°]	ρ_{ref}						
270.0	1.000	270.0	1.000	270.0	1.000	270.0	1.000
251.4	0.999	254.1	0.999	256.3	0.999	262.7	0.999
232.9	0.997	238.3	0.997	242.6	0.996	255.5	0.996
214.3	0.992	222.4	0.993	228.9	0.993	248.2	0.992
195.8	0.981	206.6	0.984	215.2	0.987	240.9	0.987
110.40	0.809	190.7	0.969	201.6	0.975	233.7	0.982
40.80	0.823	120.52	0.778	187.9	0.955	226.4	0.977
331.21	0.96	61.05	0.731	128.66	0.751	219.1	0.971
		1.57	0.88	77.33	0.645	211.9	0.962
		302.09	0.99	25.99	0.762	204.6	0.949
				334.66	0.928	197.3	0.929
				283.32	0.998	190.0	0.903
						182.8	0.868
						152.74	0.620
						125.48	0.363
						98.23	0.299
						70.97	0.364
						43.71	0.460

						16.45	0.58
						349.20	0.71
						321.94	0.86
						294.68	0.97

Table 7.4.1.3-5: Spatial correlation reference curves for CDL-C UMa model for a vertically polarized MPAC OTA setup with 16 uniformly spaced probes at FR1 test frequencies equal to or greater than 1800 MHz

1800 MHz		2132.5 MHz		2450 MHz		3600 MHz		4700 MHz	
Azimuth [°]	ρ_{ref}								
270.0	1.000	270.0	1.000	270.0	1.000	270.0	1.000	270.0	1.000
260.9	0.998	261.9	0.998	263.0	0.997	265.2	0.997	266.3	0.996
251.7	0.991	253.9	0.991	256.0	0.992	260.5	0.989	262.7	0.988
242.6	0.984	245.8	0.984	249.0	0.983	255.7	0.979	259.0	0.976
233.5	0.976	237.8	0.975	242.0	0.975	250.9	0.969	255.4	0.966
224.3	0.967	229.7	0.966	234.9	0.965	246.1	0.960	251.7	0.957
215.2	0.955	221.7	0.955	227.9	0.953	241.4	0.954	248.1	0.951
206.0	0.936	213.6	0.940	220.9	0.939	236.6	0.947	244.4	0.945
196.9	0.908	205.6	0.918	213.9	0.921	231.8	0.937	240.8	0.940
187.8	0.863	197.5	0.888	206.9	0.898	227.1	0.925	237.1	0.935
134.3	0.309	189.5	0.846	199.9	0.867	222.3	0.903	233.5	0.928
88.6	0.269	181.4	0.793	192.9	0.829	217.5	0.876	229.8	0.918
43.0	0.396	139.7	0.280	185.9	0.786	212.7	0.837	226.1	0.902
357.3	0.619	99.5	0.252	144.9	0.245	208.0	0.798	222.5	0.882
311.6	0.879	59.2	0.257	109.9	0.299	203.2	0.753	218.8	0.851
		18.9	0.471	74.8	0.215	198.4	0.708	215.2	0.816
		338.6	0.661	39.8	0.251	193.7	0.669	211.5	0.767
		298.4	0.937	4.7	0.489	188.9	0.624	207.9	0.708
				329.7	0.652	184.1	0.580	204.2	0.651
				294.6	0.946	156.1	0.175	200.6	0.580
						132.3	0.565	196.9	0.516
						108.4	0.745	193.3	0.444
						84.6	0.820	189.6	0.383
						60.7	0.750	185.9	0.310
						36.9	0.493	182.3	0.229
						13.0	0.120	161.7	0.445
						349.1	0.272	143.5	0.750
						325.3	0.498	125.2	0.879
						301.4	0.843	106.9	0.813
						277.6	0.991	88.6	0.733
								70.4	0.740
								52.1	0.873
								33.8	0.944
								15.5	0.643
								357.3	0.250
								339.0	0.178
								320.7	0.375
								302.4	0.726

								284.2	0.929
--	--	--	--	--	--	--	--	-------	-------

Time Domain Alternative Method:

Time domain techniques can also be used to validate the spatial correlation. The spatial correlation validation measurement setup is illustrated in Figure 7.4.1.3-3. In this case a Signal generator transmits a CW signal through the MIMO test system. The signal is received by a test antenna within the test area. Finally, the signal is collected by a signal analyzer and the measured signal is stored for postprocessing.

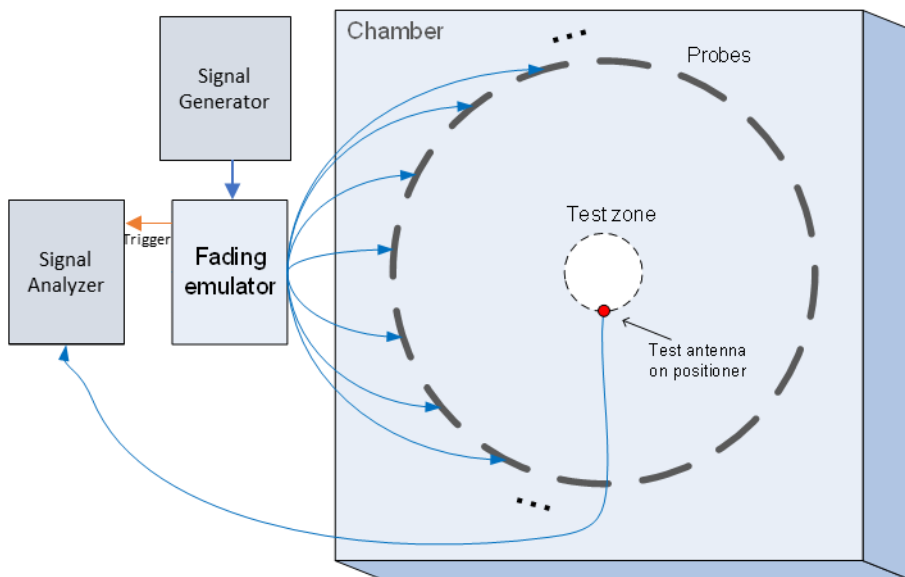


Figure 7.4.1.3-3: Configuration for spatial correlation validation based on time domain techniques

For each spatial point, the channel emulator should issue a trigger signal each time fading is started. For each point collect a time domain trace with the signal analyzer, when done, stop fading. Data recording is synchronized with the channel emulator trigger.

Follow the same procedure to postprocess the data and calculate the spatial correlation by setting m to 1. The settings for the Signal Generator and Signal Analyzer are in Table 7.4.1.3-6 and 7.4.1.3-7 respectively.

Table 7.4.1.3-6: Signal Generator Settings

Item	Unit	Value
Center frequency	MHz	Downlink center frequency in Table 7.4.1-1
Output power	dBm	Function of the CE. Sufficiently above Noise Floor

Table 7.4.1.3-7: Signal Analyzer Settings

Item	Unit	Value
Center frequency	MHz	Downlink center frequency in Table 7.4.1-1
Sampling	Hz	At least 15 times bigger than the max Doppler spread ($f_d=v/\lambda$)
Observation time	s	At least 16s. Channel Model length should be the same or greater than the observation time.

7.4.1.4 Cross-polarization

FR1 Cross polarization validation procedure for MPAC system:

This measurement checks how well the measured vertically or horizontally polarized power levels follow expected values. The test setup for cross-polarization is the same as PDP validation in Figure 7.4.1.1-1.

Method of measurement: Step the emulation and store traces from VNA.

VNA settings:**Table 7.4.1.4-1: VNA settings for cross-polarization**

Item	Unit	Value
Center frequency	MHz	Downlink Center Frequency in Table 7.4.1-1
Span	MHz	40
Number of traces		1000
Number of points		802
Averaging		1

Channel model specification:**Table 7.4.1.4-2: Channel model specification for cross-polarization.**

Item	Unit	Value
Center frequency	MHz	Downlink center frequency in Table 7.4.1-1
Distance between traces in channel model	wavelength (Note)	> 2
Channel model		As specified in Clause 7.2
Mobile speed	km/h	30
NOTE: Time [s] = distance [λ] / MS speed [λ /s] MS speed [λ /s] = MS speed [m/s] / Speed of light [m/s] * Center frequency [Hz]		

Measurement Procedure:

1. Play or step through the channel model listed in clause 7.2.
2. Measure the absolute power received at the center of the test zone, averaged over a statistically significant number of fades.
 - a. Use a vertically polarized sleeve dipole to measure the V component.
 - b. Use a horizontally polarized (vertically oriented) magnetic loop dipole, or a horizontally polarized sleeve dipole measured in four orthogonal horizontal positions and summed to measure the H component.
3. Calculate the V/H ratio.
4. Compare it with the theory value.

FR2 Cross polarization validation procedure for 3D-MPAC system:

This measurement checks how well the measured vertically or horizontally polarized power levels follow expected values. The test setup for cross-polarization is the same as PDP validation in Figure 7.4.1.1-2.

Method of measurement: Step the emulation and store traces from VNA.

VNA settings:

Table 7.4.1.4-1: VNA settings for cross-polarization

Item	Unit	Value
Center frequency	MHz	Downlink Center Frequency in Table 7.4.1-2
Span	MHz	40
Number of traces		1000
Number of points		802
Averaging		1

Channel model specification:

Table 7.4.1.4-2: Channel model specification for cross-polarization.

Item	Unit	Value
Center frequency	MHz	Downlink center frequency in Table 7.4.1-2
Distance between traces in channel model	wavelength (Note)	> 2
Channel model		As specified in Clause 7.2
Mobile speed	km/h	3
NOTE:	Time [s] = distance [λ] / MS speed [λ /s]	
	MS speed [λ /s] = MS speed [m/s] / Speed of light [m/s] * Center frequency [Hz]	

Measurement Procedure:

1. Play or step through the channel model listed in clause 7.2.
2. Measure the absolute power received at the center of the test zone, averaged over a statistically significant number of fades.
 - a. Use a dual polarized horn antenna and by terminating the H branch of antenna to measure the V component.
 - b. Use a dual polarized horn antenna and by terminating the V branch of antenna to measure the H component.
3. Calculate the V/H ratio.
4. Compare it with the theory value.

7.4.1.5 Power validation

FR1 power validation procedure for MPAC system:

This measurement checks the total power in the center of the test zone. The power validation is measured with a spectrum analyzer as shown in Figure 7.4.1.5-1.

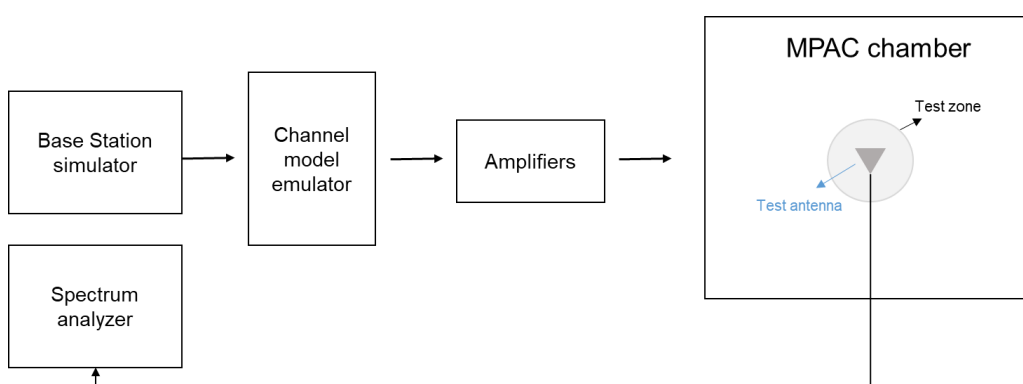


Figure 7.4.1.5-1: Setup for power validation measurements

Spectrum analyzer settings:

Table 7.4.1.5-1: Spectrum analyzer settings for Power validation measurements

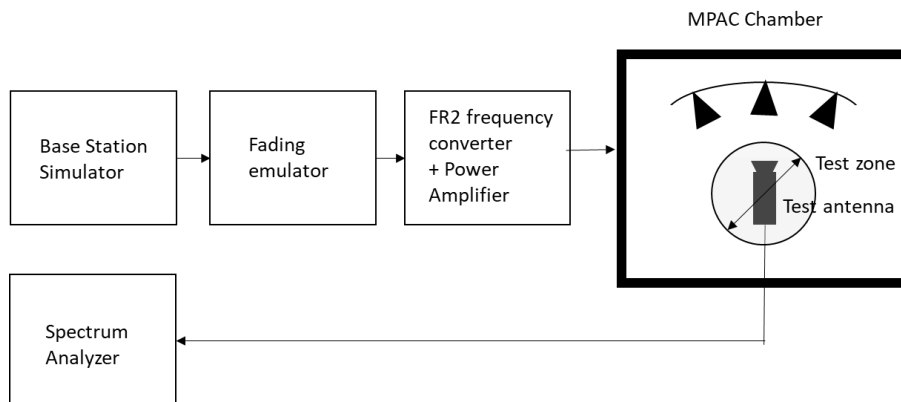
Item	Unit	Value
Center frequency	MHz	Downlink center frequency in Table 7.4.1-1
Integrated Channel Span	Hz	20MHz
RBW	Hz	30 kHz
VBW	Hz	$\geq 10\text{MHz}$
Number of points		≥ 400
Averaging		≥ 100
Detector		RMS

Measurement Procedure:

1. Place a vertical reference dipole in the center of the test zone connected to a spectrum analyzer (or power meter) via a cable.
2. Record the cable and reference dipole gains.
3. Load the target channel model into the channel emulator.
4. Start the NR FR1 signaling in the base station emulator with the required parameter identical to the measurements conditions.
5. Average the power received by the spectrum analyzer for a sufficient amount of time to account for the fading channel – one full channel simulation might be unnecessary.
6. Repeat steps 1 to 4 with a magnetic loop for the horizontal polarization, or a horizontally polarized sleeve dipole measured in four orthogonal horizontal positions and summed to measure the H component.
7. Calculate the total power received at the test area as the sum of the power in the two polarizations.

FR2 power validation procedure for 3D-MPAC system:

This measurement checks the total power in the centre of the test zone. The power validation is measured with a spectrum analyser as shown in Figure 7.4.1.5-2.

**Figure 7.4.1.5-2: Setup for power validation measurements**

Spectrum analyzer settings:

Table 7.4.1.5-2: Spectrum analyzer settings for Power validation measurements

Item	Unit	Value
Center frequency	MHz	Downlink center frequency in Table 7.4.1-2
Integrated Channel Span	Hz	20MHz
RBW	Hz	30 kHz
VBW	Hz	$\geq 10\text{MHz}$
Number of points		≥ 400
Averaging		≥ 100
Detector		RMS

Measurement Procedure:

1. Place a horn antenna with H polarization terminated in the centre of the test zone connected to a spectrum analyzer (or power meter) via a cable.
2. Record the cable and horn antenna gains.
3. Load the target channel model into the channel emulator.
4. Start the NR FR2 signalling in the base station emulator with the required parameter identical to the measurements conditions.
5. Average the power received by the spectrum analyzer for a sufficient amount of time to account for the fading channel – one full channel simulation might be unnecessary.
6. Repeat steps 1 to 4 with a horn antenna V polarization terminated for the horizontal polarization, in four orthogonal horizontal positions and summed to measure the H component.
7. Calculate the total power received at the test area as the sum of the power in the two polarizations.

7.4.1.6 PAS similarity percentage (PSP)

The PSP validation measurements aim at evaluating PAS similarity percentage (PSP), which is one of the validation metrics for characterizing FR2 channel model under test in the quite zone of 3D-MPAC. For PSP validation measurement, only vertical polarization validation is required. The measurement array is essentially a virtual array configuration realized in 3D-MPAC through a ϕ - θ positioning system. The measurement array is a semi-circle and sectored array configuration illustrated in Figure 7.4.1.6-1 where complex channel frequency response is measured at each antenna location 0.5λ apart using a vector network analyser (VNA) setup. The vertical sectors of the measurement array are limited to 60° ($\pm 30^\circ$) and the horizontal sector to 180° ($\pm 90^\circ$) with the broad side direction points towards the probes. Depending of the turntable architecture/implementation, the virtual array configuration for the PSP validation is composed of two alternative semi-circle arrangements (1 x horizontal and either 2 x crossed vertical or 2 x parallel vertical). The radius of the array element locations with respect to the centre of the test zone is 5 cm, which is equivalent to the half of the test zone radius at 28 GHz. For different frequency bands, the radius of the measurement array sectored semi-circles remains fixed at 5 cm while the spatial sampling of the array varies. This measurement validates the proper angular behaviour in the test zone.

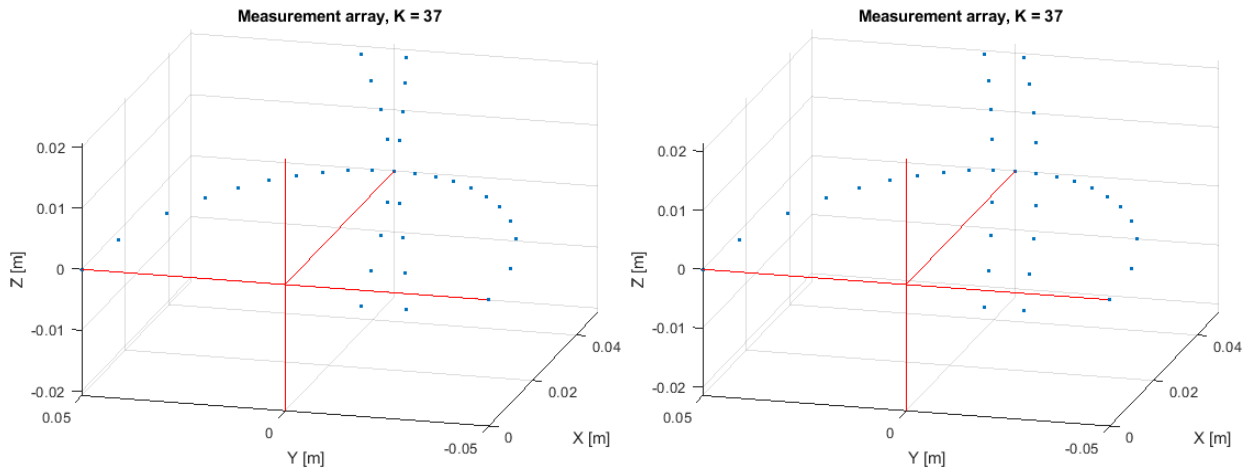


Figure 7.4.1.6-1: Semi-circle measurement array configurations with $K = 37$ elements (at 28 GHz). On the left with two crossed vertical sectors, on the right with two parallel vertical sectors.

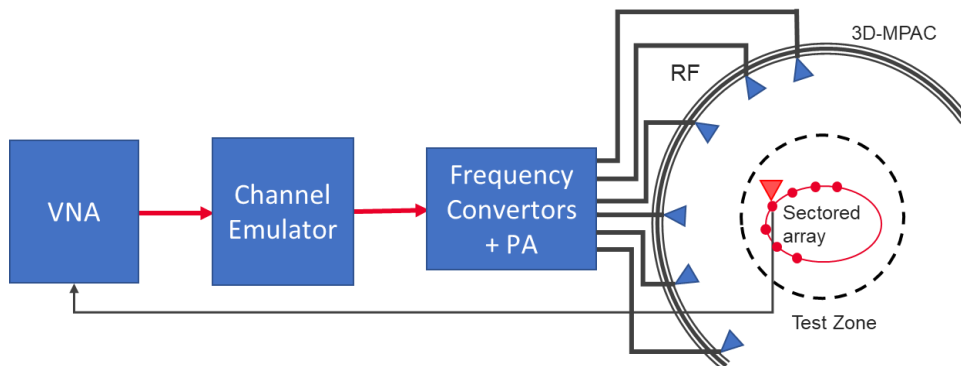


Figure 7.4.1.6-2: Setup for PSP validation measurements

The PSP validation is measured with a vector network analyser as shown in Figure 7.4.1.6-2 illustrating the PSP measurement setup. Port 1 of the VNA transmits signals through the fading emulator and radiate them through L probes within the anechoic chamber. The radiated signals are then received at the test antenna that is positioned inside the test zone. The test antenna is mounted on a ϕ - θ positioner which is capable of moving the antenna to pre-defined spatial locations on a fixed radius from the centre of the quiet zone according the measurement array configuration. Finally, the signal is received at port 2 of the VNA. The most suitable approach for the PSP validation is based on an omnidirectional antenna (omnidirectional pattern in AZ and wide BW in EL) as the test can be automated easily. Alternatively, a directional antenna could be used but requires frequent re-positioning.

The measurement and analysis procedure are given as follows:

1. Set the target channel model in the Channel Emulator.
2. For each position of the test antenna on the measurement array configuration in the test zone, step & pause the emulator to different time instances. Measure the complex frequency responses $H(f, t) = H(m\Delta f, n\Delta T)$, $m = 0, \dots, M - 1$ for all stepped channel snapshots $n = 0, \dots, N - 1$, where the interval between frequency and time samples is Δf and ΔT , respectively. The number of channel snapshots N and frequency samples M .
3. Move the measurement antenna with a positioner to another location k and repeat step 2 to record frequency responses $H_k(m\Delta f, n\Delta T)$ of all stepped channel snapshots.
4. Repeat step 3 to record frequency responses at all $k = 1, \dots, K$ spatial sample points.
5. Estimate the measured PAS through the following two-step processing:

- a) In the first step, calculate the discrete azimuth and elevation angles (DoA) for the measurement array configuration by applying the MUSIC algorithm. Estimate the powers from the DoA and auto-covariance matrix of the received signal acquired through VNA complex frequency response data. A near field to far-field conversion is then applied to the transfer function between probes and measurement array positions.
 - b) In the second step, use the angle and power estimates, i.e. the discrete PAS of N azimuth and elevation directions and power values in conjunction with a 4x4 DUT sampling array for beamforming with the conventional Bartlett beamformer to estimate the “measured PAS seen by DUT” for PSP calculation.
6. Evaluate the reference OTA PAS for the 4x4 DUT array by applying the conventional Bartlett beamformer to the OTA probe weights and the strongest beam from the code book of 128 beam-grid with 4x4 DUT sampling array.
7. Calculate total variation distance (D_p) from the reference and measured PAS. Mathematically,

$$D_p = \frac{1}{2} \int \left| \frac{\hat{P}_r(\beta)}{\int \hat{P}_r(\beta') d\beta'} - \frac{\hat{P}_o(\beta)}{\int \hat{P}_o(\beta') d\beta'} \right| d\beta$$

8. Calculate PSP values as $PSP = (1-D_p) \times 100\%$.

VNA settings:

Table 7.4.1.6-1: VNA settings for FR2 PSP measurements

Item	Unit	Value
Center frequency	MHz	Downlink center frequency in Table 7.4.1-2
Span	MHz	0 (or the minimum)
Number of traces		1000
Number of points		1

Channel model specification:

Table 7.4.1.6-2: Channel model specification for FR2 PSP measurements

Item	Unit	Value
Center frequency	MHz	Downlink center frequency in Table 7.4.1-2
Distance between traces in channel model	wavelength (Note)	> 2
Channel model		As specified in Clause 7.2
NOTE: Time [s] = distance [λ] / MS speed [λ/s] MS speed [λ/s] = MS speed [m/s] / Speed of light [m/s] * Center frequency [Hz]		

Time Domain Alternative Method:

PSP validation can also be implemented using time-domain techniques using the testing setup presented in Figure 7.4.1.6-3. The VNA is substituted by a signal generator, and a signal analyser.

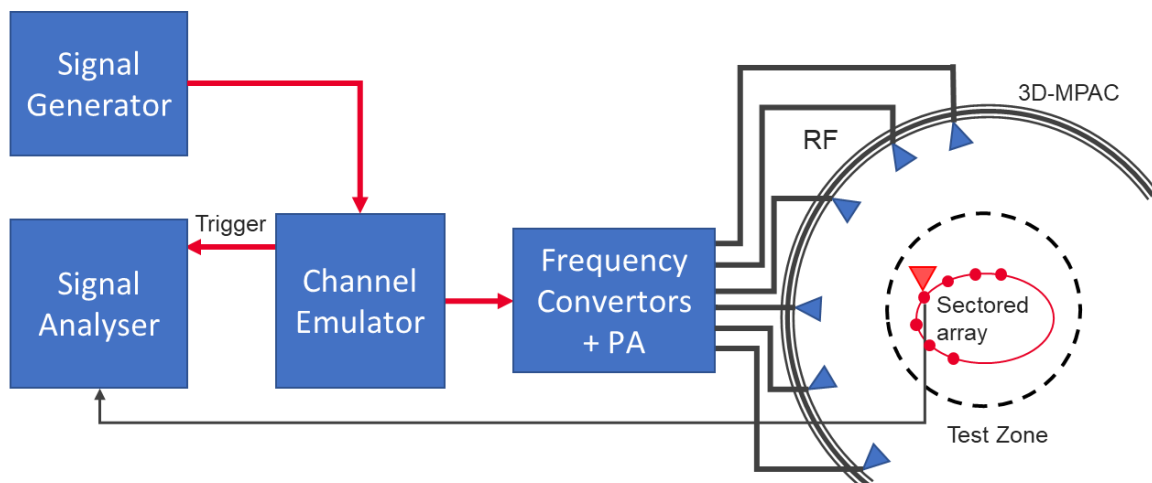


Figure 7.4.1.6-3: Setup for PSP validation measurements based on time domain

Table 7.4.1.6-3: Signal Generator Settings

Item	Unit	Value
Center frequency	MHz	Downlink centre frequency in 3GPP as required per band
Output power	dBm	Function of the CE. Sufficiently above Noise Floor

Table 7.4.1.6-4: Signal Analyzer Settings

Item	Unit	Value
Center frequency	MHz	Downlink centre frequency in 3GPP as required per band
Sampling	Hz	At least 10 times bigger than the max Doppler spread ($f_d=v/\lambda$)
Observation time	s	At least 32s

The measurement and analysis procedure are given as follows:

Follow the same procedure as before, but M is set to 1. The Channel Emulator is not stepped, but it is allowed to play in free run mode for each of the K spatial points.

7.4.2 Pass/Fail Criteria

The Pass/Fail Criteria of channel model validation for FR1 and FR2 is FFS.

8 Base station configuration

8.1 General

In this part, Base station configuration for NR MIMO OTA testing is defined.

8.2 gNodeB emulator settings

< Further down selecting of parameters (FR1 TDD Bandwidth and FR2 DL Modulation) for RMC will be done in WI phase >

The gNodeB emulator parameters shall be set according to Table 8.2-1 for FR1 common parameters, Table 8.2-2 for FR1 FDD 2x2 test parameters, Table 8.2-3 for FR1 TDD 2x2 test parameters, Table 8.2-4 for FR1 FDD 4x4 test parameters, Table 8.2-5 for FR1 TDD 4x4 test parameters, and Table 8.2-6 for FR2 common parameters, Table 8.2-7 and Table 8.2-8 for FR2 TDD 2x2 test parameters.

Table 8.2-1: FR1 Common test parameters

Parameter		Unit	Value
PDSCH transmission scheme			Transmission scheme 1
Carrier configuration	Offset between Point A and the lowest usable subcarrier on this carrier (Note 2)	RBs	0
	Subcarrier spacing	kHz	15 or 30
DL BWP configuration #1	Cyclic prefix		Normal
	RB offset	RBs	0
Common serving cell parameters	Number of contiguous PRB	PRBs	Maximum transmission bandwidth configuration as specified in clause 5.3.2 of TS 38.101-1 for tested channel bandwidth and subcarrier spacing
	Physical Cell ID		0
PDCCH configuration	SSB position in burst		First SSB in Slot #0
	SSB periodicity	ms	20
	First DMRS position for Type A PDSCH mapping		2
	Slots for PDCCH monitoring		Each slot
Cross carrier scheduling	Symbols with PDCCH	Symbols	0, 1
	Number of PRBs in CORESET		Table 5.2-2 of TS 38.101-4 for tested channel bandwidth and subcarrier spacing
	Number of PDCCH candidates and aggregation levels		1/AL8
	CCE-to-REG mapping type		Non-interleaved
	DCI format		1_1
	TCI state		TCI state #1
	Not configured		
CSI-RS for tracking	First subcarrier index in the PRB used for CSI-RS		$k_0=0$ for CSI-RS resource 1,2,3,4
	First OFDM symbol in the PRB used for CSI-RS		$l_0 = 6$ for CSI-RS resource 1 and 3 $l_0 = 10$ for CSI-RS resource 2 and 4
	Number of CSI-RS ports (X)		1 for CSI-RS resource 1,2,3,4
	CDM Type		'No CDM' for CSI-RS resource 1,2,3,4
	Density (ρ)		3 for CSI-RS resource 1,2,3,4
	CSI-RS periodicity	Slots	15 kHz SCS: 20 for CSI-RS resource 1,2,3,4 30 kHz SCS: 40 for CSI-RS resource 1,2,3,4
	CSI-RS offset	Slots	15 kHz SCS: 10 for CSI-RS resource 1 and 2 11 for CSI-RS resource 3 and 4 30 kHz SCS: 20 for CSI-RS resource 1 and 2 21 for CSI-RS resource 3 and 4
	Frequency Occupation		Start PRB 0 Number of PRB = BWP size
	QCL info		TCI state #0
NZP CSI-RS for CSI acquisition	First subcarrier index in the PRB used for CSI-RS		$k_0 = 0$
	First OFDM symbol in the PRB used for CSI-RS		$l_0 = 12$
	Number of CSI-RS ports (X)		Same as number of transmit antenna
	CDM Type		'FD-CDM2'
	Density (ρ)		1
	CSI-RS periodicity	Slots	15 kHz SCS: 20 30 kHz SCS: 40
	CSI-RS offset	Slots	0
	Frequency Occupation		Start PRB 0 Number of PRB = BWP size
	QCL info		TCI state #1
ZP CSI-RS for CSI acquisition	First subcarrier index in the PRB used for CSI-RS		$k_0 = 4$
	First OFDM symbol in the PRB used for CSI-RS		$l_0 = 12$

	Number of CSI-RS ports (X)		4
	CDM Type		'FD-CDM2'
	Density (ρ)		1
	CSI-RS periodicity	Slots	15 kHz SCS: 20 30 kHz SCS: 40
	CSI-RS offset	Slots	0
	Frequency Occupation		Start PRB 0 Number of PRB = BWP size
PDSCH DMRS configuration	Antenna ports indexes		{1000, 1001} for Rank 2 tests {1000-1003} for Rank 4 tests
	Number of PDSCH DMRS CDM group(s) without data		1 for Rank 2 tests 2 for Rank 4 tests
TCI state #0	Type 1 QCL information	SSB index	SSB #0
		QCL Type	Type C
	Type 2 QCL information	SSB index	N/A
		QCL Type	N/A
TCI state #1	Type 1 QCL information	CSI-RS resource	CSI-RS resource 1 from 'CSI-RS for tracking' configuration
		QCL Type	Type A
	Type 2 QCL information	CSI-RS resource	N/A
		QCL Type	N/A
PT-RS configuration			PT-RS is not configured
Maximum number of code block groups for ACK/NACK feedback			1
Maximum number of HARQ transmission			1
HARQ ACK/NACK bundling			Multiplexed
Redundancy version coding sequence			N.A
Precoding configuration			SP Type I, Random per slot with PRB bundling granularity
Symbols for all unused REs			OCNG Annex A.5 of TS 38.101-4
Minimum Number of Slots per Stream			20000 for 15kHz SCS 40000 for 30kHz SCS
Note 1: UE assumes that the TCI state for the PDSCH is identical to the TCI state applied for the PDCCH transmission.			
Note 2: Point A coincides with minimum guard band as specified in Table 5.3.3-1 from TS 38.101-1 for tested channel bandwidth and subcarrier spacing.			

Table 8.2-2: Test parameters for FR1 FDD 2x2

Parameter	Unit	Value
Duplex mode		FDD
Reference channel		R.PDSCH.1-3.1 FDD (Note 1)
Bandwidth	MHz	10
SCS	kHz	15
Modulation DL		64QAM
Modulation UL		QPSK
Active DL BWP index		1
PDSCH configuration	Mapping type	Type A
	k0	0
	Starting symbol (S)	2
	Length (L)	12
	PDSCH aggregation factor	1
	PRB bundling type	Static
	PRB bundling size	2
	Resource allocation type	Type 0
	RBG size	Config2
	VRB-to-PRB mapping type	Non-interleaved
	VRB-to-PRB mapping interleaver bundle size	N/A
	DMRS Type	Type 1
PDSCH DMRS configuration	Number of additional DMRS	1
	Maximum number of OFDM symbols for DL front loaded DMRS	1
	CSI-RS periodicity	Slots
CSI-RS for tracking	CSI-RS offset	Slots
		Table 8.2-1.
Number of HARQ Processes		1
The number of slots between PDSCH and corresponding HARQ-ACK information		2

Note 1: “R.PDSCH.1-3.1 FDD” is defined in Table A.3.2.1.1-3 of TS 38.101-4

Table 8.2-3: Test parameters for FR1 TDD 2x2

Parameter		Unit	Value
Duplex mode			TDD
Reference channel			R.PDSCH.2-3.1 TDD (Note 1)
Bandwidth	MHz		40, [20]
SCS	kHz		30
Modulation DL			64QAM
Modulation UL			QPSK
Active DL BWP index			1
PDSCH configuration	Mapping type		Type A
	k0		0
	Starting symbol (S)		2
	Length (L)		Specific to each Reference channel
	PDSCH aggregation factor		1
	PRB bundling type		Static
	PRB bundling size		2
	Resource allocation type		Type 0
	RBG size		Config2
	VRB-to-PRB mapping type		Non-interleaved
	VRB-to-PRB mapping interleaver bundle size		N/A
	DMRS Type		Type 1
PDSCH DMRS configuration	Number of additional DMRS		1
	Maximum number of OFDM symbols for DL front loaded DMRS		1
	First OFDM symbol in the PRB used for CSI-RS		Table 8.2-1.
CSI-RS for tracking	CSI-RS periodicity	Slots	40
	CSI-RS offset	Slots	Table 8.2-1.
Number of HARQ Processes			1
TDD UL-DL pattern			FR1.30-1 (Note 2)
Note 1: “R.PDSCH.2-3.1 TDD” is defined in Table A.3.2.2.2-3 of TS 38.101-4			
Note 2: “FR1.30-1” is defined in Annex A.1.2 of TS 38.101-4			

Table 8.2-4: Test parameters for FR1 FDD 4x4

Parameter		Unit	Value
Duplex mode			FDD
Reference channel			R.PDSCH.1-2.4 FDD (Note 1)
Bandwidth	MHz		10
SCS	kHz		15
Modulation DL			16QAM
Modulation UL			QPSK
Active DL BWP index			1
PDSCH configuration	Mapping type		Type A
	k0		0
	Starting symbol (S)		2
	Length (L)		12
	PDSCH aggregation factor		1
	PRB bundling type		Static
	PRB bundling size		2
	Resource allocation type		Type 0
	RBG size		Config2
	VRB-to-PRB mapping type		Non-interleaved
	VRB-to-PRB mapping interleaver bundle size		N/A
	DMRS Type		Type 1
PDSCH DMRS configuration	Number of additional DMRS		1
	Maximum number of OFDM symbols for DL front loaded DMRS		1
	CSI-RS periodicity	Slots	20
CSI-RS for tracking	CSI-RS offset	Slots	Table 8.2-1.

Number of HARQ Processes		1
The number of slots between PDSCH and corresponding HARQ-ACK information		2
Note 1: "R.PDSCH.1-2.4 FDD" is defined in Table A.3.2.1.1-2 of TS 38.101-4		

Table 8.2-5: Test parameters for FR1 TDD 4x4

Parameter	Unit	Value
Duplex mode		TDD
Reference channel		R.PDSCH.2-2.4 TDD (Note 1)
Bandwidth	MHz	40, [20]
SCS	kHz	30
Modulation DL		16QAM
Modulation UL		QPSK
Active DL BWP index		1
PDSCH configuration	Mapping type	Type A
	k0	0
	Starting symbol (S)	2
	Length (L)	Specific to each Reference channel
	PDSCH aggregation factor	1
	PRB bundling type	Static
	PRB bundling size	2
	Resource allocation type	Type 0
	RBG size	Config2
	VRB-to-PRB mapping type	Non-interleaved
	VRB-to-PRB mapping interleaver bundle size	N/A
PDSCH DMRS configuration	DMRS Type	Type 1
	Number of additional DMRS	1
	Maximum number of OFDM symbols for DL front loaded DMRS	1
CSI-RS for tracking	First OFDM symbol in the PRB used for CSI-RS	Table 8.2-1.
	CSI-RS periodicity	Slots
		40.
	CSI-RS offset	Slots
		Table 8.2-1.
Number of HARQ Processes		1
TDD UL-DL pattern		FR1.30-1 (Note 2)

Note 1: "R.PDSCH.2-2.4 TDD" is defined in Table A.3.2.2.2-2 of TS 38.101-4
Note 2: "FR1.30-1" is defined in Annex A.1.2 of TS 38.101-4

Table 8.2-6: FR2 Common Parameters

Parameter	Unit	Value
PDSCH transmission scheme		Transmission scheme 1
PTRS epre-Ratio		0
Actual carrier configuration	RBs	0
	Offset between Point A and the lowest usable subcarrier on this carrier (Note 2)	
	Subcarrier spacing	kHz
	Cyclic prefix	Normal
	RB offset	RBs
DL BWP configuration #1	PRBs	Maximum transmission bandwidth configuration as specified in clause 5.3.2 of TS 38.101-2 for tested channel bandwidth and subcarrier spacing
Common serving cell parameters	Physical Cell ID	0
	SSB position in burst	1
	SSB periodicity	ms
	First DMRS position for Type A PDSCH mapping	2

PDCCH configuration	Slots for PDCCH monitoring		Each slot
	Symbols with PDCCH		0
	Number of PRBs in CORESET		Table 7.2-2 of TS 38.101-4 for tested channel bandwidth and subcarrier spacing
	Number of PDCCH candidates and aggregation levels		1/AL8
	CCE-to-REG mapping type		Non-interleaved
	DCI format		1_1
	TCI state		TCI state #1
Cross carrier scheduling			Not configured
CSI-RS for tracking	First subcarrier index in the PRB used for CSI-RS (k_0)		0 for CSI-RS resource 1,2,3,4
	First OFDM symbol in the PRB used for CSI-RS (l_0)		6 for CSI-RS resource 1 and 3 10 for CSI-RS resource 2 and 4
	Number of CSI-RS ports (X)		1 for CSI-RS resource 1,2,3,4
	CDM Type		'No CDM' for CSI-RS resource 1,2,3,4
	Density (ρ)		3 for CSI-RS resource 1,2,3,4
	CSI-RS periodicity	Slots	120 kHz SCS: 160 for CSI-RS resource 1,2,3,4
	CSI-RS offset	Slots	120 kHz SCS: 80 for CSI-RS resource 1 and 2 81 for CSI-RS resource 3 and 4
	Frequency Occupation		Start PRB 0 Number of PRB = BWP size
	QCL info		TCI state #0
NZP CSI-RS for CSI acquisition	First subcarrier index in the PRB used for CSI-RS (k_0)		0
	First OFDM symbol in the PRB used for CSI-RS (l_0)		12
	Number of CSI-RS ports (X)		2
	CDM Type		FD-CDM2
	Density (ρ)		1
	CSI-RS periodicity	Slots	120 kHz SCS: 160
	CSI-RS offset		0
	Frequency Occupation		Start PRB 0 Number of PRB = BWP size
	QCL info		TCI state #1
ZP CSI-RS for CSI acquisition	First subcarrier index in the PRB used for CSI-RS (k_0)		4
	First OFDM symbol in the PRB used for CSI-RS (l_0)		12
	Number of CSI-RS ports (X)		4
	CDM Type		FD-CDM2
	Density (ρ)		1
	CSI-RS periodicity	Slots	120 kHz SCS: 160
	CSI-RS offset		0
	Frequency Occupation		Start PRB 0 Number of PRB = BWP size
CSI-RS for beam refinement	First subcarrier index in the PRB used for CSI-RS		$k_0=0$ for CSI-RS resource 1,2
	First OFDM symbol in the PRB used for CSI-RS		$l_0 = 8$ for CSI-RS resource 1 $l_0 = 9$ for CSI-RS

			resource 2
	Number of CSI-RS ports (X)		1 for CSI-RS resource 1,2
	CDM Type		'No CDM' for CSI-RS resource 1,2
	Density (ρ)		3 for CSI-RS resource 1,2
	CSI-RS periodicity	Slots	60 kHz SCS: 80 for CSI-RS resource 1,2 120 kHz SCS: 160 for CSI-RS resource 1,2
	CSI-RS offset	Slots	0 for CSI-RS resource 1,2
	QCL info		TCI state #1
PDSCH DMRS configuration	Antenna ports indexes		{1000} for Rank 1 tests {1000, 1001} for Rank 2 tests
	Number of PDSCH DMRS CDM group(s) without data		1
TCI state #0	Type 1 QCL information	SSB index	SSB #0
		QCL Type	Type C
	Type 2 QCL information	SSB index	SSB #0
		QCL Type	Type D
TCI state #1	Type 1 QCL information	CSI-RS resource	CSI-RS resource 1 from 'CSI-RS for tracking' configuration
		QCL Type	Type A
	Type 2 QCL information	CSI-RS resource	CSI-RS resource 1 from 'CSI-RS for tracking' configuration
		QCL Type	Type D
PTRS configuration	Frequency density (K_{PT-RS})		2
	Time density (L_{PT-RS})		1
Maximum number of code block groups for ACK/NACK feedback			1
Maximum number of HARQ transmission			1
HARQ ACK/NACK bundling			Multiplexed
Redundancy version coding sequence			{0,2,3,1}
Precoding configuration			SP Type I, Random per slot with PRB bundling granularity
Symbols for all unused Res			OCNG in Annex A.5 of TS 38.101-4
Minimum Number of Slots per Stream			20000 for FR2 UMi models in Tables 7.2.2-1—7.2.2.5 75000 for FR2 InO models in Tables 7.2.2-6—7.2.2.10
Note 1: UE assumes that the TCI state for the PDSCH is identical to the TCI state applied for the PDCCH transmission.			
Note 2: Point A coincides with minimum guard band as specified in Table 5.3.3-1 from TS 38.101-2 for tested channel bandwidth and subcarrier spacing.			

Table 8.2-7: Test Parameters for FR2 TDD 2x2 (16QAM)

Parameter	Unit	Value
Duplex mode		TDD
Reference channel		R.PDSCH.5-2.2 TDD (Note 1)
Bandwidth	MHz	100
SCS	kHz	120
Modulation DL		16QAM
Modulation UL		QPSK
Active DL BWP index		1
CSI-RS for tracking	First OFDM symbol in the PRB used for CSI-RS (l_0)	Table 8.2-6
	CSI-RS offset	Slots
PDCCH configuration	Number of PDCCH candidates and aggregation levels	1/AL8
PDSCH configuration	Mapping type	Type A
	k_0	0
	Starting symbol (S)	1
	Length (L)	Specific to each Reference channel as defined in A.3.2.2 of TS 38.101-4
	PDSCH aggregation factor	1
	PRB bundling type	Static
	PRB bundling size	WB for Test 1-1, 2 for other tests
	Resource allocation type	Type 0
	RBG size	config2
	VRB-to-PRB mapping type	Non-interleaved
	VRB-to-PRB mapping interleaver bundle size	N/A
	DMRS Type	Type 1
PDSCH DMRS configuration	Number of additional DMRS	1
	Maximum number of OFDM symbols for DL front loaded DMRS	1
	Number of HARQ Processes	1
TDD UL-DL pattern		FR2.120-1 (Note2)

Note 1: “R.PDSCH.5-2.2 TDD” is defined in Table A.3.2.2.5-2 of TS 38.101-4

Note 2: “FR2.120-1” is defined in Annex A.1.3 of TS 38.101-4

Table 8.2-8: Test Parameters for FR2 TDD 2x2 (64QAM)

Parameter	Unit	Value
Duplex mode		TDD
Reference channel		R.PDSCH.5-6.1 TDD (Note 1)
Bandwidth	MHz	100
SCS	kHz	120
Modulation DL		64QAM
Modulation UL		QPSK
Active DL BWP index		1
CSI-RS for tracking	First OFDM symbol in the PRB used for CSI-RS (l_0)	Table 8.2-6
	CSI-RS offset	Slots
PDCCH configuration	Number of PDCCH candidates and aggregation levels	1/AL8
PDSCH configuration	Mapping type	Type A
	k_0	0
	Starting symbol (S)	1
	Length (L)	Specific to each Reference channel as defined in A.3.2.2 of TS 38.101-4
	PDSCH aggregation factor	1
	PRB bundling type	Static
	PRB bundling size	2
	Resource allocation type	Type 0
	RBG size	config2
	VRB-to-PRB mapping type	Non-interleaved
PDSCH DMRS configuration	VRB-to-PRB mapping interleaver bundle size	N/A
	DMRS Type	Type 1
	Number of additional DMRS	1
	Maximum number of OFDM symbols for DL front loaded DMRS	1
	Number of HARQ Processes	1
	TDD UL-DL pattern	FR2.120-1 (Note2)

Note 1: “R.PDSCH.5-2.2 TDD” is defined in Table A.3.2.2.5-6 of TS 38.101-4

Note 2: “FR2.120-1” is defined in Annex A.1.3 of TS 38.101-4

Annex A: UE coordinate system

A.1 Reference coordinate system

This annex defines the measurement coordinate system for the NR MIMO OTA. The reference coordinate system, as defined in [5] is provided in Figure A.1-1 below while A.1-2 shows the DUT in the default alignment.

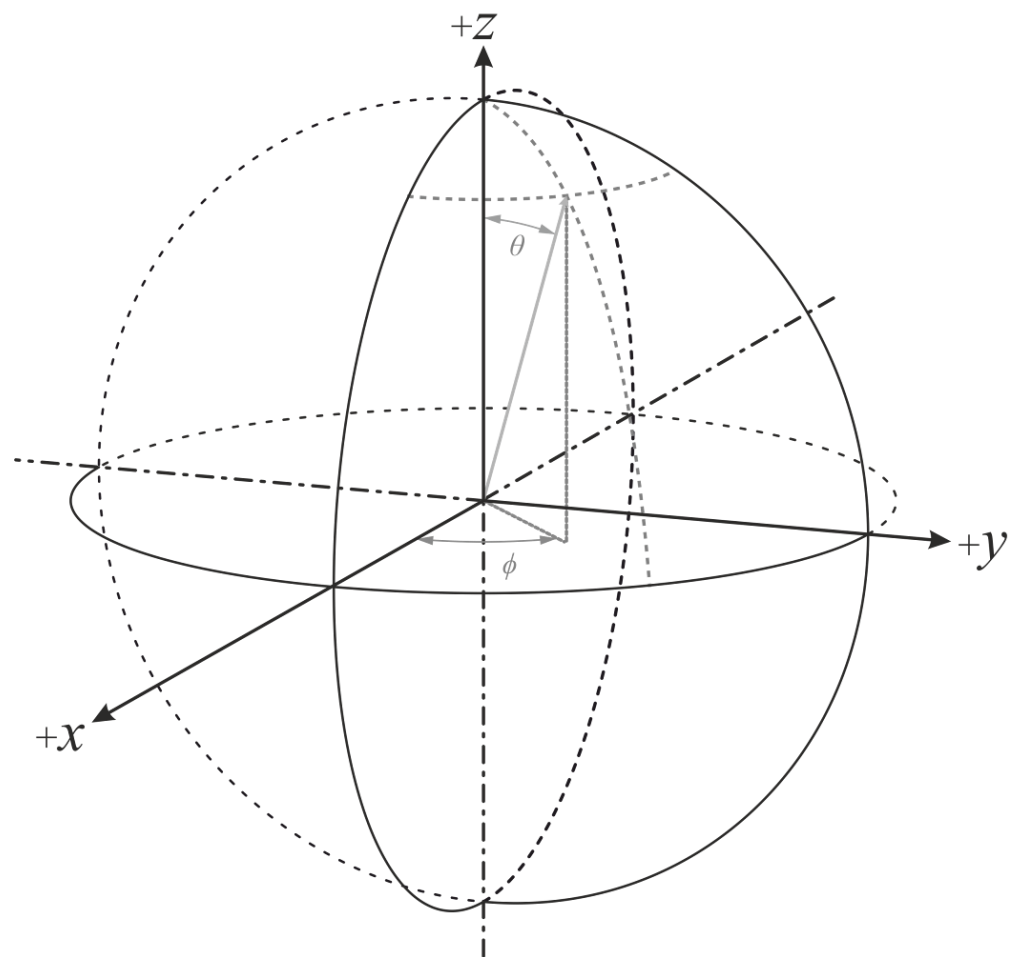


Figure A.1-1: Reference coordinate system

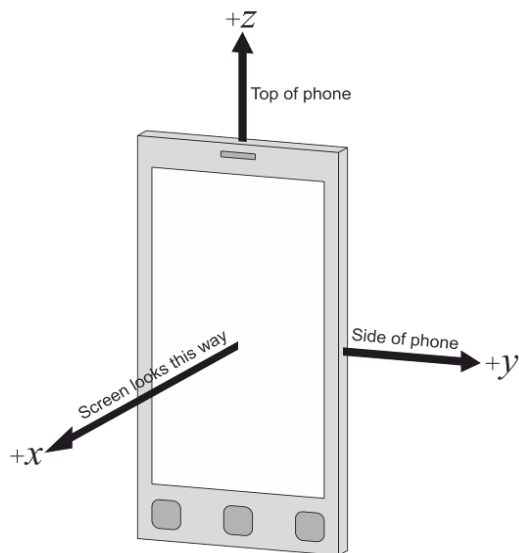


Figure A.1-2: DUT default alignment to coordinate system

The following aspects are necessary:

- A basic understanding of the top and bottom of the device is needed in order to define unambiguous DUT positioning requirements for the test, e.g., in the drawings used in this annex, the three buttons are on the bottom of the device (front) and the camera is on the top of the device (back).
- An understanding of the origin and alignment of the coordinate system inside the test system, i.e. the directions in which the x, y, z axes point inside the test chamber, is needed in order to define unambiguous DUT orientation, DUT beam, signal, interference, and measurement angles.

A.2 Test conditions and angle definitions

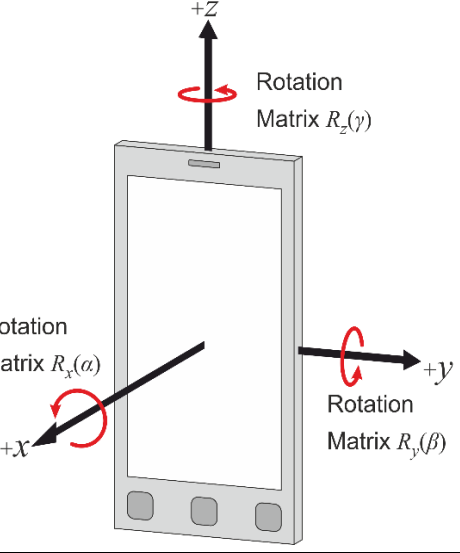
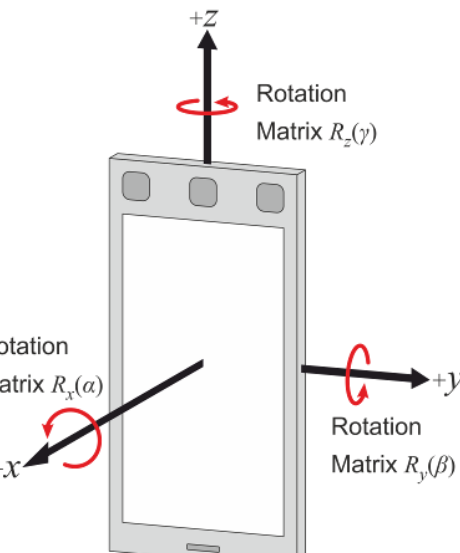
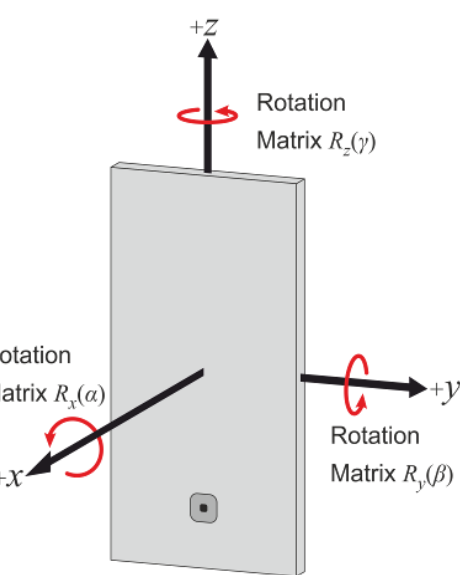
Free space is the test condition for both FR1 and FR2 MIMO OTA testing. The angle definition of the DUT orientation is specified in A.3.

In order to achieve the FR2 test points tabulated in Table 6.2.3.2-1, the UE is rotated so that the test point w.r.t. to the UE coordinate system is aligned with the test system z axis.

A.3 DUT positioning guidelines

Table A.3-1 below lists the DUT positioning conditions along with a diagram. The XY plane or P0 condition is just shown for information as a reference to the coordinate system defined in Annex A.1.

Table A.3-1: Summary of possible DUT positioning options

Testing condition	DUT orientation angles	Diagram
XY plane or P0 Orientation 1 (default)	$\alpha=0;$ $\beta=0;$ $\gamma=0$	
P0 Orientation 2 – Option 1 (based on re-positioning approach)	$\alpha=180^\circ;$ $\beta=0;$ $\gamma=0$	
P0 Orientation 2 – Option 2 (based on re-positioning approach)	$\alpha=0;$ $\beta=180^\circ;$ $\gamma=0$	

Free space data mode screen up (FS DMSU)	$\alpha=0;$ $\beta=-90;$ $\gamma=0$	
Free space data mode portrait (FS DMP)	$\alpha=0;$ $\beta=-45;$ $\gamma=0$	
Free space data mode landscape (FS DML)	$\alpha=90$ (left tilt); $\beta=-45;$ $\gamma=0$	

Note: the repositioning concept is applicable to FR2 only.

Near-field coupling effects between the antenna and the pedestals/positioners/fixtures generally cause increased signal ripples. Re-positioning the DUT by directing the beam peak away from those areas can reduce the effect of signal ripple on TP measurements. The images on the left of Figure A.3-1 illustrate how to reposition the DUT when the near field coupling effects likely originate from the left, while the images on the right Figure A.3-1 illustrate how to reposition the DUT when the near field coupling effects likely originate from the bottom. In either case, Orientation 1 is used for the measurement of one hemisphere while Orientation 2 is used for the measurement of the opposite hemisphere. This re-positioning approach is applicable to FR2 only.

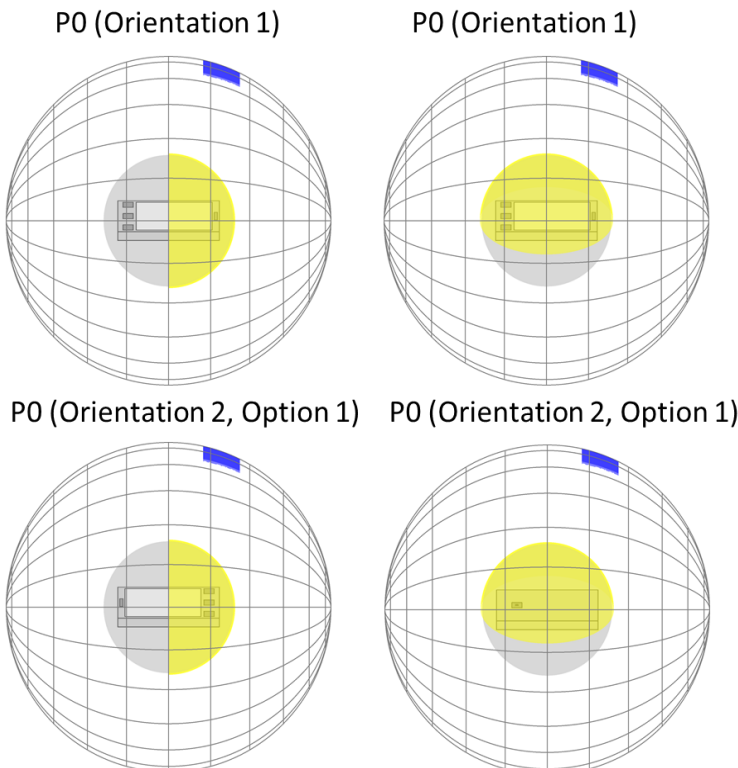


Figure A.3-1: Illustration of DUT re-positioning. The region with reduces signal ripple is illustrated in yellow. The sector which contains the probes is highlighted in blue.

Due to the non-commutative nature of rotations, the order of rotations is important and needs to be defined when multiple DUT orientations are tested.

The rotations around the x, y, and z axes can be defined with the following rotation matrices

$$R_x(\alpha) = \begin{bmatrix} 1 & 0 & 0 & 0 \\ 0 & \cos \alpha & -\sin \alpha & 0 \\ 0 & \sin \alpha & \cos \alpha & 0 \\ 0 & 0 & 0 & 1 \end{bmatrix}$$

$$R_y(\beta) = \begin{bmatrix} \cos \beta & 0 & \sin \beta & 0 \\ 0 & 1 & 0 & 0 \\ -\sin \beta & 0 & \cos \beta & 0 \\ 0 & 0 & 0 & 1 \end{bmatrix}$$

and

$$R_z(\gamma) = \begin{bmatrix} \cos \gamma & -\sin \gamma & 0 & 0 \\ \sin \gamma & \cos \gamma & 0 & 0 \\ 0 & 0 & 1 & 0 \\ 0 & 0 & 0 & 1 \end{bmatrix}.$$

with the respective angles of rotation, α, β, γ and

$$\begin{bmatrix} x' \\ y' \\ z' \\ 1 \end{bmatrix} = R \begin{bmatrix} x \\ y \\ z \\ 1 \end{bmatrix}$$

Additionally, any translation of the DUT can be defined with the translation matrix

$$T(t_x, t_y, t_z) = \begin{bmatrix} 1 & 0 & 0 & t_x \\ 0 & 1 & 0 & t_y \\ 0 & 0 & 1 & t_z \\ 0 & 0 & 0 & 1 \end{bmatrix}$$

with offsets t_x, t_y, t_z in x, y, and z, respectively and with

$$\begin{bmatrix} x' \\ y' \\ z' \\ 1 \end{bmatrix} = T \begin{bmatrix} x \\ y \\ z \\ 1 \end{bmatrix}$$

The combination of rotations and translation is captured by the multiplication of rotation and translation matrices.

For instance, the matrix M

$$M = T(t_x, t_y, t_z) \cdot R_z(\gamma) \cdot R_y(\beta) \cdot R_x(\alpha)$$

describes an initial rotation of the DUT around the x axis with angle α , a subsequent rotation around the y axis with angle β , and a final rotation around the z axis with angle γ . After those rotations, the DUT is translated by t_x, t_y, t_z in x, y, and z, respectively.

A.4 Test Zone dimensions

The test zone size is 20cm for both FR1 and FR2 MIMO OTA testing. Larger test zone size is FFS.

Annex B: Measurement uncertainty

B.1 Measurement uncertainty budget for FR1

B.1.1 Measurement Uncertainty assessment for MPAC

Table B.1.1-1: Measurement uncertainty budget for MPAC

UI D	Description of uncertainty contribution	Example value (410MHz < f ≤ 3GHz)	Example value (3GHz < f ≤ 7.125GHz)	Distribution of the probability	Details in
Stage 2: DUT measurement					
1	Mismatch for measurement process			U-Shaped	B.1.2.1
2	Measure distance uncertainty			Normal	B.1.2.2
3	Quality of quiet zone			Rectangular	B.1.2.3
4	Base Station simulator			Rectangular	B.1.2.4
5	Channel Emulator -absolute value -stability			Normal	B.1.2.5
6	Amplifier uncertainties			Rectangular	B.1.2.6
7	Random uncertainty			Normal	B.1.2.7
8	Throughput measurement: output level step resolution			Rectangular	B.1.2.8
9	DUT sensitivity drift			Rectangular	B.1.2.9
10	Signal flatness			Normal	B.1.2.10
Stage 1: Calibration measurement					
11	Mismatch for calibration process - loopback cable path - system input path - reference antenna			U-Shaped	B.1.2.11
12	Reference antenna positioning misalignment			Normal	B.1.2.12
13	Quality of quiet zone			Rectangular	B.1.2.3
14	Total uncertainty of the Network Analyzer			Rectangular	B.1.2.13
15	Uncertainty of an absolute gain of the calibration antenna			Normal	B.1.2.14
16	Offset of the Phase Center of the Reference Antenna			Normal	B.1.2.15

B.1.2 Measurement error contribution descriptions for MPAC

B.1.2.1 Mismatch for measurement process

This term comes from the mismatch between the system input cables connecting to the base station simulator output port.

B.1.2.2 Measure distance uncertainty

The cause of this uncertainty contributor is due to the reduction of distance between the measurement antenna and the DUT. Given that 1.2m is defined as the minimum range length for FR1 MPAC system, this term could be set as 0 dB.

B.1.2.3 Quality of quiet zone

The quality of the quiet zone procedure characterizes the quiet zone performance of the anechoic chamber, specifically the effect of reflections within the anechoic chamber including any positioners and support structures. For FR1 quality of quiet zone measurement, reference antenna of sleeve dipole or magnetic loop is always used. The standard uncertainty shall be calculated by dividing the maximum ripple by $\sqrt{3}$, as measured in a volume greater than half a wavelength in diameter. This element is considered to be rectangularly distributed.

B.1.2.4 Base Station simulator

gNB emulator is used to drive a signal to the channel emulator and then to the device under test. Generally there occurs uncertainty contribution from absolute level accuracy, non-linearity and frequency characteristic of the gNB emulator.

For practical reasons, in a case that a VNA is used as a calibration equipment, gNB emulator is connected to the system after the calibration measurement is performed by the VNA. Hence, the uncertainty on the absolute level of gNB emulator (transmitter device) cannot be assumed as systematic. This uncertainty should be calculated from the manufacturer's data in logs with a rectangular distribution, unless otherwise informed. Furthermore, the uncertainty of the non-linearity is included in the absolute level uncertainty.

B.1.2.5 Channel Emulator

The channel emulator is also working as a signal source in the NR MIMO OTA system, therefore there occurs uncertainty contribution from absolute level accuracy, non-linearity, frequency characteristic and stability of the channel emulator. These uncertainty contributions shall be taken from the manufacturer's data sheet.

B.1.2.6 Amplifier uncertainties

Any components in the setup can potentially introduce measurement uncertainty. It is then needed to determine the uncertainty contributors associated with the use of such components. For the case of external amplifiers, the following uncertainties should be considered but the applicability is contingent to the measurement implementation and calibration procedure.

- Stability
 - An uncertainty contribution comes from the output level stability of the amplifier. Even if the amplifier is part of the system for both measurement and calibration, the uncertainty due to the stability shall be considered. This uncertainty can be either measured or determined by the manufacturers' data sheet for the operating conditions in which the system will be required to operate.
- Linearity
 - An uncertainty contribution comes from the linearity of the amplifier since in most cases calibration and measurements are performed at two different input/output power levels. This uncertainty can be either measured or determined by the manufacturers' data sheet.
- Noise Figure
 - When the signal goes into an amplifier, noise is added so that the SNR at the output is reduced with regard to the SNR of the signal at the input. This added noise introduces error on the signal which affects the Error Rate of the receiver thus the EVM (Error Vector Magnitude). An uncertainty can be calculated through the following formula:

$$\varepsilon_{EVM} = 20 \log_{10} \left(1 + 10^{\frac{-SNR}{20}} \right)$$

- Where SNR is the signal to noise ratio in dB at the signal level used during the sensitivity measurement.
- Mismatch
 - If the external amplifier is used for both stages, measurement and calibration the uncertainty contribution associated with it can be considered systematic and constant -> 0dB. If it is not the case, the mismatch uncertainty at its input and output shall be either measured or determined by the method described in [7].
- Gain
 - If the external amplifier is used for both stages, measurement and calibration the uncertainty contribution associated with it can be considered systematic and constant -> 0dB. If it is not the case, this uncertainty shall be considered.

B.1.2.7 Random uncertainty

This contribution is used to account for all the unknown, unquantifiable, etc. uncertainties associated with the measurements. Random uncertainty MU contributions are normally distributed. The random uncertainty term, by definition, cannot be measured, or even isolated completely. A value of 0.2dB aligned with LTE is suggested.

B.1.2.8 Throughput measurement: output level step resolution

The cause of this uncertainty contributor is due to the step size in the power level used in the throughput measurement stage. Depending on the system provider implementation, the power level adjustment is based on changing the output power of BS simulator or channel model emulator. Fixed 0.5dB step is defined for NR MIMO OTA testing, an uncertainty contribution of 0.25dB with a rectangular distribution should be reported.

B.1.2.9 DUT sensitivity drift

Due to statistical uncertainty of throughput measurement, drift in the TRMS can not be monitored. An uncertainty value of 0.2dB can be used, or the TRMS drift should be measured, with a setup corresponding to the actual MIMO OTA measurement.

B.1.2.10 Signal flatness

For wireless technologies with wide channel bandwidths, the test system might not have a flat frequency response across the entire channel. While the range calibration corrects for any variation of frequency response as a function of the center frequency of the channel, the broadband radiated power measured or delivered to the test zone will be a function of the entire channel bandwidth as opposed to just the center frequency. Thus, any deviation of the rest of the channel from the signal level at the center frequency will result in an error in the measured result. The determination of the MU element is FFS.

B.1.2.11 Mismatch for calibration process

During calibration stage, there will be impedance mismatch between the various RF cables and components used within the system. Standing waves are created by the reflections between any two components and uncertainty in the signal level will be generated. In general, three mismatch for calibration process should be considered:

- Loopback cable path: This item comes from the mismatch between the reference cable and the loopback cable during the loopback cable measurement step.
- System input path: This item comes from the mismatch between the loopback cable and the system input cable (generally the output cable after BS simulator). The reflectivity of the source output port is measured at the end of the loopback cable connecting to the system input cable.
- Reference antenna: This item comes from the mismatch between the VNA input port and the reference antenna. The reflectivity of the VNA input port is measured at the end of the reference cable connecting to the reference antenna.

B.1.2.12 Reference antenna positioning misalignment

This contribution originates from reference antenna alignment and pointing error. In this measurement if the maximum gain directions of the reference antenna and the receiving antenna are aligned to each other, this contribution can be considered negligible and therefore set to zero.

B.1.2.13 Total Uncertainty of the Network Analyzer

This contribution originates from all uncertainties involved transmission magnitude measurement (including drift and frequency flatness) with a network analyser. The uncertainty value will be indicated in the manufacturer's data sheet. It needs to be ensured that appropriate manufacturer's uncertainty contribution is specified for the absolute levels measured.

B.1.2.14 Uncertainty of an absolute gain of the calibration antenna

The calibration antenna only appears in calibration phase (Stage 1). Therefore, the gain uncertainty has to be taken into account. This uncertainty will come from a calibration report with traceability to a National Metrology Institute with measurement uncertainty budgets generated following the guidelines outlined in internationally accepted standards.

B.1.2.15 Offset of the Phase Center of the Reference Antenna

During range reference measurement, if a directional antenna is used, the uncertainty in the accuracy of positioning its phase center on the axis of rotation will directly generate an uncertainty in this part of the measurement. In practical measurement, sleeve dipoles and loops are used for FR1 calibration, then the uncertainty of this element should be 0 dB, since the phase center offset is negligible.

B.2 Measurement uncertainty budget for FR2

B.2.1 Measurement Uncertainty assessment

Table B.2.1-1: Measurement uncertainty budget for FR2 3D-MPAC

UI D	Description of uncertainty contribution	Example value (26.5GHz ≤ f ≤ 29.5GHz)	Example value (37GHz ≤ f ≤ 40GHz)	Distribution of the probability	Details in
Stage 2: DUT measurement					
1	Mismatch for measurement process			U-Shaped	B.2.2.1
2	Measure distance uncertainty			Normal	B.2.2.2
3	Quality of quiet zone			Rectangular	B.2.2.3
4	Base Station simulator			Rectangular	B.2.2.4
5	Channel Emulator -absolute value -stability -linearity			Normal	B.2.2.5
6	Amplifier uncertainties			Rectangular	B.2.2.6
7	Random uncertainty			Normal	B.2.2.7
8	Throughput measurement: output level step resolution			Rectangular	B.2.2.8
9	DUT sensitivity drift			Rectangular	B.2.2.9
10	Signal flatness			Normal	B.2.2.10
Stage 1: Calibration measurement					
11	Mismatch for calibration process - loopback cable path - system input path - reference antenna			U-Shaped	B.2.2.11
12	Reference antenna positioning misalignment			Normal	B.2.2.12
13	Quality of quiet zone			Rectangular	B.2.2.3
14	Total uncertainty of the Network Analyzer			Rectangular	B.2.2.13
15	Uncertainty of an absolute gain of the calibration antenna			Normal	B.2.2.14
16	Offset of the Phase Center of the Reference Antenna			Normal	B.2.2.16

B.2.2 Measurement error contribution descriptions

B.2.2.1 Mismatch for measurement process

This term comes from the mismatch between the system input cables connecting to the base station simulator output port.

B.2.2.2 Measure distance uncertainty

The cause of this uncertainty contributor is due to the reduction of distance between the measurement antenna and the DUT. Given that 0.75m is defined as the minimum range length for FR2 3D-MPAC system, this term could be set as 0 dB.

B.2.2.3 Quality of quiet zone

The quality of the quiet zone procedure characterizes the quiet zone performance of the anechoic chamber, specifically the effect of reflections within the anechoic chamber including any positioners and support structures.

B.2.2.4 Base Station simulator

gNB emulator is used to drive a signal to the channel emulator and then to the device under test. Generally there occurs uncertainty contribution from absolute level accuracy, non-linearity and frequency characteristic of the gNB emulator.

For practical reasons, in a case that a VNA is used as a calibration equipment, gNB emulator is connected to the system after the calibration measurement is performed by the VNA. Hence, the uncertainty on the absolute level of gNB emulator (transmitter device) cannot be assumed as systematic. This uncertainty should be calculated from the manufacturer's data in logs with a rectangular distribution, unless otherwise informed. Furthermore, the uncertainty of the non-linearity is included in the absolute level uncertainty.

B.2.2.5 Channel Emulator

The channel emulator is also working as a signal source in the FR2 MIMO OTA system, therefore there occurs uncertainty contribution from absolute level accuracy, non-linearity, frequency characteristic and stability of the channel emulator. These uncertainty contributions shall be taken from the manufacturer's data sheet. This uncertainty value shall be the final value after mmWave radio head.

B.2.2.6 Amplifier uncertainties

Any components in the setup can potentially introduce measurement uncertainty. It is then needed to determine the uncertainty contributors associated with the use of such components. For the case of external amplifiers, the following uncertainties should be considered but the applicability is contingent to the measurement implementation and calibration procedure.

- Stability
 - An uncertainty contribution comes from the output level stability of the amplifier. Even if the amplifier is part of the system for both measurement and calibration, the uncertainty due to the stability shall be considered. This uncertainty can be either measured or determined by the manufacturers' data sheet for the operating conditions in which the system will be required to operate.
- Linearity
 - An uncertainty contribution comes from the linearity of the amplifier since in most cases calibration and measurements are performed at two different input/output power levels. This uncertainty can be either measured or determined by the manufacturers' data sheet.
- Noise Figure
 - When the signal goes into an amplifier, noise is added so that the SNR at the output is reduced with regard to the SNR of the signal at the input. This added noise introduces error on the signal which affects the Error Rate of the receiver thus the EVM (Error Vector Magnitude). An uncertainty can be calculated through the following formula:

$$\varepsilon_{EVM} = 20 \log_{10} \left(1 + 10^{\frac{-SNR}{20}} \right)$$

- Where SNR is the signal to noise ratio in dB at the signal level used during the sensitivity measurement.
- Mismatch

- If the external amplifier is used for both stages, measurement and calibration the uncertainty contribution associated with it can be considered systematic and constant -> 0dB. If it is not the case, the mismatch uncertainty at its input and output shall be either measured or determined by the method described in [7].
- Gain
 - If the external amplifier is used for both stages, measurement and calibration the uncertainty contribution associated with it can be considered systematic and constant -> 0dB. If it is not the case, this uncertainty shall be considered.

B.2.2.7 Random uncertainty

This contribution is used to account for all the unknown, unquantifiable, etc. uncertainties associated with the measurements. Random uncertainty MU contributions are normally distributed. The random uncertainty term, by definition, cannot be measured, or even isolated completely. A value of 0.2dB aligned with FR1 is suggested.

B.2.2.8 Throughput measurement: output level step resolution

The cause of this uncertainty contributor is due to the step size in the power level used in the throughput measurement stage. Depending on the system provider implementation, the power level adjustment is based on changing the output power of BS simulator or channel model emulator. Fixed 0.5dB step is defined for NR MIMO OTA testing, an uncertainty contribution of 0.25dB with a rectangular distribution should be reported.

B.2.2.9 DUT sensitivity drift

Due to statistical uncertainty of throughput measurement, drift in the TRMS can not be monitored. An uncertainty value of 0.2dB can be used, or the TRMS drift should be measured, with a setup corresponding to the actual MIMO OTA measurement.

B.2.2.10 Signal flatness

For wireless technologies with wide channel bandwidths, the test system might not have a flat frequency response across the entire channel. While the range calibration corrects for any variation of frequency response as a function of the center frequency of the channel, the broadband radiated power measured or delivered to the test zone will be a function of the entire channel bandwidth as opposed to just the center frequency. Thus, any deviation of the rest of the channel from the signal level at the center frequency will result in an error in the measured result. The determination of the MU element is FFS.

B.2.2.11 Mismatch for calibration process

During calibration stage, there will be impedance mismatch between the various RF cables and components used within the system. Standing waves are created by the reflections between any two components and uncertainty in the signal level will be generated. In general, three mismatch for calibration process should be considered:

- Loopback cable path: This item comes from the mismatch between the reference cable and the loopback cable during the loopback cable measurement step.
- System input path: This item comes from the mismatch between the loopback cable and the system input cable (generally the output cable after BS simulator). The reflectivity of the source output port is measured at the end of the loopback cable connecting to the system input cable.
- Reference antenna: This item comes from the mismatch between the VNA input port and the reference antenna. The reflectivity of the VNA input port is measured at the end of the reference cable connecting to the reference antenna.

B.2.2.12 Reference antenna positioning misalignment

This contribution originates from reference antenna alignment and pointing error. In this measurement if the maximum gain directions of the reference antenna and the receiving antenna are aligned to each other, this contribution can be considered negligible and therefore set to zero.

B.2.2.13 Total Uncertainty of the Network Analyzer

This contribution originates from all uncertainties involved transmission magnitude measurement (including drift and frequency flatness) with a network analyser. The uncertainty value will be indicated in the manufacturer's data sheet. It needs to be ensured that appropriate manufacturer's uncertainty contribution is specified for the absolute levels measured.

B.2.2.14 Uncertainty of an absolute gain of the calibration antenna

The calibration antenna only appears in calibration phase (Stage 1). Therefore, the gain uncertainty has to be taken into account. This uncertainty will come from a calibration report with traceability to a National Metrology Institute with measurement uncertainty budgets generated following the guidelines outlined in internationally accepted standards.

B.2.2.15 Offset of the Phase Center of the Reference Antenna

Gain is defined at the phase centre of the antenna. If the phase centre of the calibration antenna is not aligned at the centre of the set up during the calibration, then there will be uncertainty related to the measurement distance.

Annex C: Environmental requirements

C.1 Scope

The requirements in this clause apply to all types of UE(s) in FR1 and FR2.

C.2 Ambient temperature

All the MIMO OTA requirements are applicable in room temperature e.g. 25°C.

C.3 Operating voltage

For FR1 MIMO OTA, all nominal voltage test cases shall be performed with the DUT operated in stand-alone battery powered mode.

For FR2 MIMO OTA, all nominal voltage test cases shall be performed with the DUT operated in stand-alone battery powered mode or external power source. It shall be demonstrated that the impact of external power source to device performance is negligible comparing to stand-alone battery powered mode.

Annex D: Procedure to characterize the quality of the quiet zone

D.1 FR1 quality of the quiet zone

Unwanted reflections and support structure blockage cause a volumetric ripple to the field magnitude seen from each measurement antenna as shown in Figure D1-1. By rotating an omnidirectional antenna through the test volume as

illustrated by the red line, this volumetric ripple may be probed to obtain an estimate of the measurement uncertainty due to this volumetric error. The quality of the quiet zone test consists of a phi-axis ripple test that covers a cylindrical quiet zone 20 cm in diameter around the phi axis and 20 cm tall. Each reference antenna is oriented with its axis parallel to the phi axis at a total of three positions offset 10 cm perpendicular to the phi with 0 cm and ± 10 cm offsets parallel to the phi axis. At each position, the phi axis is rotated 360° to record the ripple. Each position is labeled by its radial and axial offset from the center position, (R, Z) , using 0, +, or - to represent the appropriate offset in each direction. See [Figure D1-2](#) for additional information.

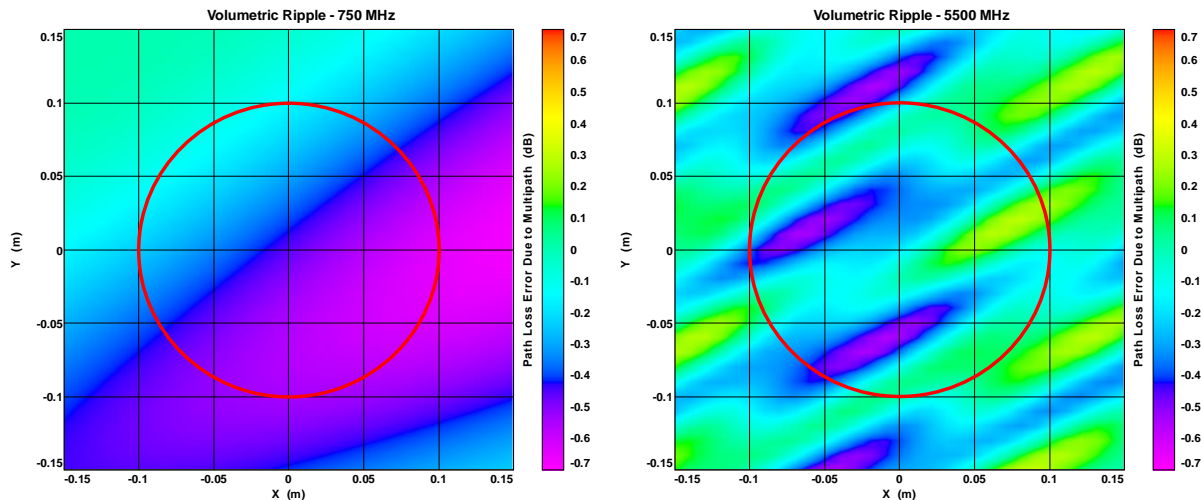


Figure D1-1: Volumetric ripple and 20cm Phi axis cut

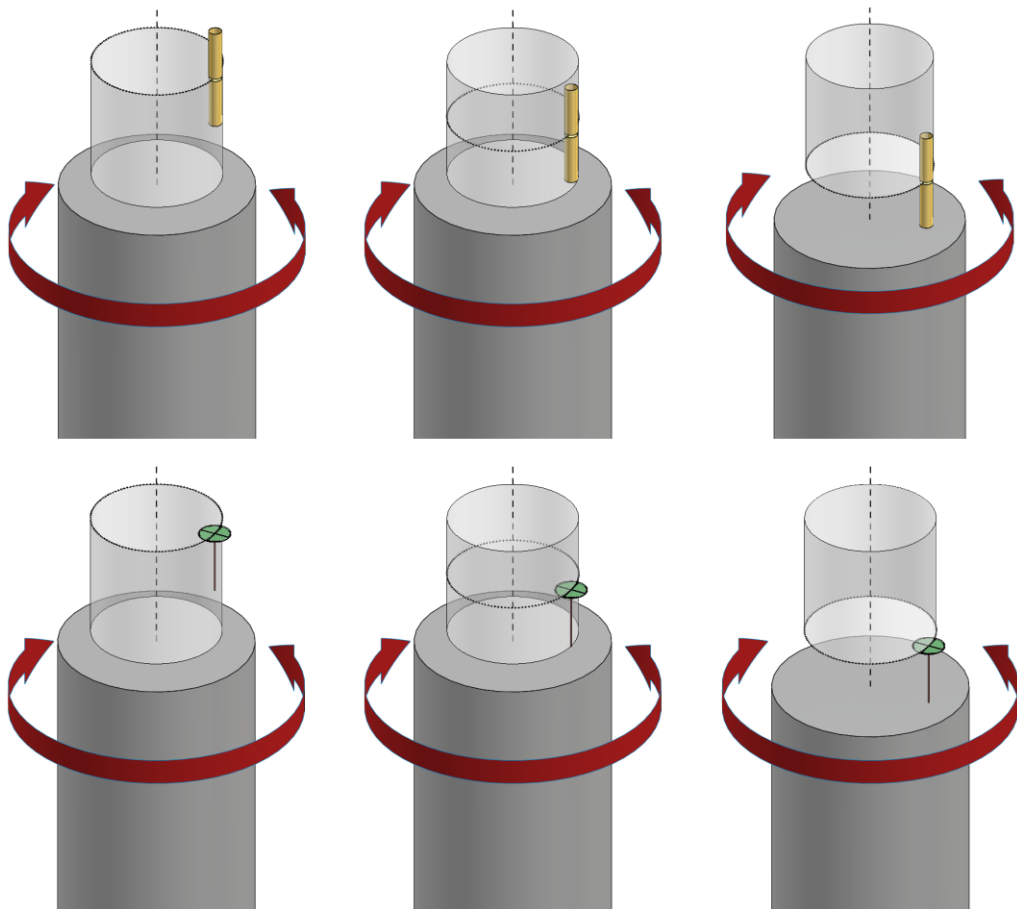


Figure D1-2: Phi-axis test geometry

For each polarization and band, repeat the following steps:

1. Place the Measurement Antenna and any associated theta-axis positioner at theta = 90° such that the Measurement Antenna is boresight with the center of the quiet zone. The Measurement Antenna should be at the same separation distance to be used for actual pattern measurements. This distance must be at least R (the minimum measurement distance is defined in clause 6.6) meters away from the center of the quiet zone. Select the polarization of the Measurement Antenna to correspond to the polarization (V or H) to be tested.
2. Mount the reference antenna to the phi-axis positioner using a low permittivity dielectric support. Use the sleeve dipole for the V polarization and the loop for the H polarization. At each of the six offset positions, ensure that the axis of the reference antenna is parallel to the phi axis of rotation.
3. Attach a signal source to a coaxial cable feeding the Measurement Antenna and set the frequency to the appropriate channel. Set the amplitude to a level appropriate for the measurement receiver. Connect a measurement receiver to the reference antenna. The received signal during the ripple test measurement should be at least 40 dB above the noise floor or noise errors greater than 0.1 dB will result. Ensure that all coaxial cables are dressed to minimize effects upon the measurement results.
4. Rotate the reference antenna about the phi axis and record the signal received by the Measurement Antenna at resolution sufficient to ensure smoothly varying curves for a total of 360°.
5. Record the measurement results to a file that can be imported into a spreadsheet.
6. Record test parameters including: (a) the distance between the measurement and reference antennas, (b) cable losses and other losses associated with the measurement setup, (c) the power of the signal source at the reference antenna connector, and (d) the noise level of the receiver with no signal applied.
7. Repeat steps 1 through 6 above for each reference antenna (polarization and band) for each of the 6 test positions, offsetting 100 mm ±2 mm from the center of the quiet zone in each direction along the phi axis and radially from the center. In order to accommodate reference positioning in the lower portion of the quiet zone, support materials with a dielectric constant less than 1.2 may be removed to a maximum distance of 250 mm outside the quiet zone for the tests that require additional clearance.

D.2 FR2 quality of the quiet zone

The FR2 quality of quiet zone validation test characterizes the quiet zone performance of the anechoic chamber, specifically the effect of reflections within the anechoic chamber including any positioners and support structures. The spherical test zone with 20 cm diameter to be validated with the FR2 quality of quiet zone procedure is illustrated in Figure D.2-1.

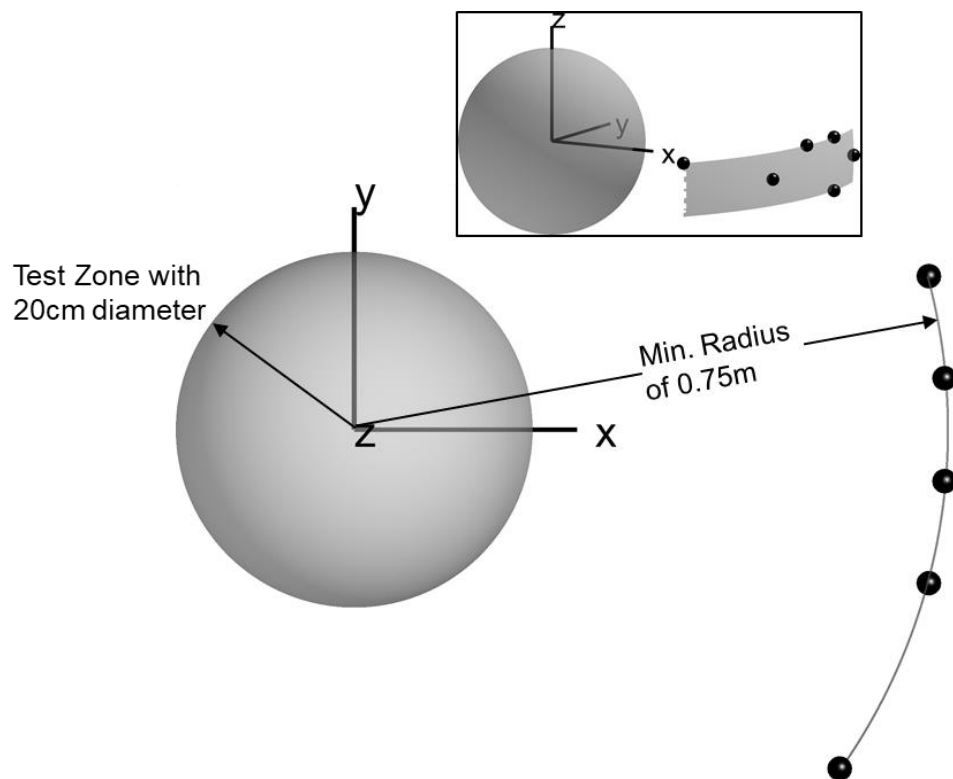


Figure D.2-1: Illustration of spherical 20 cm test zone validated using quality of quiet zone procedure

The quality of quiet zone test procedure, equipment, and test frequencies are defined in Annex O.2 of TS 38.521-2 [9]. For NR FR2 MIMO OTA, only the single-directional EIRP and EIS metrics need to be assessed and the procedure needs to be performed using just a single 3D MPAC probe.

Annex E:

Change history

Change history							
Date	Meeting	TDoc	CR	Rev	Cat	Subject/Comment	New version
2018-10	R4#88bis	R4-1813566				Skeleton of TR38.827 on NR MIMO OTA test methods	0.0.1
2019-02	R4#90	R4-1901362				R4-1815935, R4-1816656 Updated TR scope and FoM	0.1.0
2019-05	R4#91	R4-1906127				R4-1905103 Reference coordinate system	0.2.0
2019-08	R4#92	R4-1909936				R4-1907609 Test methods, EUT orientations, and Channel model validation	0.3.0
2019-10	R4#92bis	R4-1911619				R4-1910396, R4-1909938, R4-1910399 DUT positioning guidelines, Abbreviations, Channel Models	0.4.0
2019-11	R4#93	R4-1913689				R4-1912899, R4-1912900, R4-1912902 Temperature and voltage conditions, RMC for MIMO OTA, Base Station beamforming configuration	0.5.0
2019-11	R4#93	R4-1916173				R4-1916010, R4-1916011, R4-1916012, R4-1916013, R4-1915073, R4-1916176 DoT for FR1; test methods, calibration and channel model validation for FR1; 64QAM RMC	0.6.0
2019-12	RP#86	RP-192415				Submitted for information to RAN	1.0.0
2020-02	R4#94-e	R4-2000894				R4-1916014 RTS system, calibration and test procedure	1.1.0
2020-03	R4#94-e	R4-2002482				R4-2002481, R4-2002472, R4-2002473, R4-2002474, R4-2002475, R4-2002476, R4-2002152, R4-2002480, R4-2002533 spatial sampling points, general part, MU assessment, DoT for FR2, , FR2 channel model validation procedure, calibration and test procedure, EUT orientations for FR2, initial phase of channel model	1.2.0
2020-04	R4#94-e-bis	R4-2003640				R4-2003639, R4-2005559 General part, FR2 3D-MPAC system probes location	1.3.0
2020-06	R4#95-e	R4-2006307				R4-2006308, R4-2006740, R4-2006742, R4-2008273 RMC correction, FR2 QoQZ procedure, FR2 PSP validation procedure, FR2 system correction to avoid ambiguities. Editor's editorial correction.	1.4.0
2020-06	RP#88-e	RP-201068				Submitted to RAN for approval Editorial correction of Figure 7.4.1.6-1.	2.0.0

Change history							
Date	Meeting	TDoc	CR	Rev	Cat	Subject/Comment	New version
2020-06	RAN#88					Approved by plenary – Rel-16 spec under change control	16.0.0
2020-12	RAN#90	RP-202426	0002	2	B	Addition of Time Domain Alternative for Spatial Correlation Validation	16.1.0
2020-12	RAN#90	RP-202426	0003		F	Update of FR2 probe configuration	16.1.0
2020-12	RAN#90	RP-202426	0004	1	F	Number of Slots for NR MIMO OTA testing	16.1.0
2020-12	RAN#90	RP-202426	0007	1	F	CR for 38.827 on corrections	16.1.0